

Vorgelegt an der
Universität Stuttgart



**Universidad
Politécnica
de Cartagena**

**Analysis of stress simulation: a case study for the
evaluation of a homologation test procedure for
the design of rear underrun protection**

MASTER THESIS

Camilo Alejandro Durán Parada

01.10.2020

Director of the paper:

Prof. José Andrés Moreno Nicolás & Antonio González Carpena

Instituto de Ingeniería Mecánica, Materiales y Fabricación

Escuela Técnica Superior de Ingeniería Industrial

Universidad Politécnica de Cartagena

C/ Dr. Fleming s/n

E-30202 Cartagena

Abstract

Accidents between a passenger vehicle and a heavy weight vehicle (HWV) stand out as one of the most dangerous ones. These often result in fatal injuries or the death of the passengers, due to higher dimension and weight differences. One possible accident situation is the underrunning of a smaller vehicle with the rear end of a heavy truck. To avoid these types of accidents important parameters have to be considered when designing the frame of the vehicles or the implementation of safety equipment. Front, side and rear underrun protections (RUP) are all examples of safety equipment that avoid the slippage of smaller vehicles beneath heavy truck frames. In Europe, the legal requirements of these are all fixed in regulations imposed by the United Nations Economic Commission of Europe (UNECE). Within the framework of this work, we will specifically analyse the regulation number R58 (revision 2), which contains all technical specifications for RUPs and all steps to a numerical test. Using a Finite Element (FE) analysis tool like ANSYS Mechanical, we will develop a computer model from scratch to simulate stress distribution of a RUP. The model is to be based on the test procedures specified in the R58 and the design of the RUP will be provided by the company “Laboratorio Técnico de Reformas S.A” (LTR). The main objective of this work is to provide the company with a simulative software which calculates accurate results, comparable to a real physical test. We will also check the strength resistance of the provided RUPs design and if this is capable of withstanding regulative loads. Our results concluded that this was not the case: the utilized screws, which served as union components for the RUP, fail before reaching maximum load. However, after some physical tests performed by the manufacturer, their RUP was also not able to withstand applied forces. The computational and physical results are subsequently similar. In order to verify the accuracy of the simulative program, further ten designs were tested with the same conditions as the first one. After observing promising results, the Entidad Nacional de Acreditación (ENAC) approved the software for further usage and so

the homologation procedure can be started.

Kurzfassung

Unfälle zwischen einem Personenkraftwagen und einem Schwerlastkraftwagen gehören zu den gefährlichsten Unfällen. Diese führen aufgrund der höheren Dimensions- und Gewichtsunterschiede oft zu tödlichen Verletzungen oder zum Tod der Insassen. Eine mögliche Unfallsituation ist das Unterfahren eines kleineren Fahrzeugs mit dem Heck eines schweren Lastkraftwagens. Um diese Art von Unfällen zu vermeiden, müssen bei der Gestaltung des Fahrzeugrahmens oder der Implementierung von Sicherheitsausrüstung wichtige Parameter berücksichtigt werden. Vordere, seitliche und hintere Unterfahrschutze (RUP) sind Beispiele für Sicherheitsausrüstungen, die das Durchrutschen kleinerer Fahrzeuge unter schweren Lkw-Rahmen verhindern. In Europa sind deren gesetzliche Anforderungen alle in Vorschriften der United Nations Economic Commission of Europe (UNECE) festgelegt. Im Rahmen dieser Arbeit werden wir insbesondere die Regelung Nr. R58 (Revision 2) analysieren. Diese enthält alle technischen Spezifikationen für hintere Unterfahrschutzeinrichtungen und alle Schritte zu einer numerischen Prüfung. Unter Verwendung eines Finite-Analyse-Tools wie ANSYS Mechanical werden wir ein Computermodell von Grund auf neu entwickeln, um die Spannungsverteilung eines RUP zu simulieren. Das Modell soll auf den im R58 spezifizierten Testverfahren basieren, und der Entwurf des RUP wird von der Firma "Laboratorio Técnico de Reformas S.A." bereitgestellt. Das Hauptziel dieser Arbeit besteht darin, dem Unternehmen eine Simulationssoftware zur Verfügung zu stellen, die genaue Ergebnisse berechnet, vergleichbar mit einem realen physischen Test. Wir werden auch den Festigkeitswiderstand des bereitgestellten RUPs-Designs prüfen und ob dieses in der Lage ist, regulativen Belastungen standzuhalten. Unsere Ergebnisse kamen zu dem Schluss, dass dies nicht der Fall war: Die verwendeten Schrauben, die als Verbindungselemente für den RUP dienten, versagen vor Erreichen der maximalen Belastung. Nach einigen vom Hersteller durchgeführten physikalischen Tests war ihr RUP jedoch ebenfalls nicht in der Lage, den aufbrachten Kräften zu widerstehen. Die rechnerischen und physikalischen

Ergebnisse sind in der Folge ähnlich. Um die Genauigkeit des Simulationsprogramms zu überprüfen, wurden weitere zehn Konstruktionen unter den gleichen Bedingungen wie die erste getestet. Nach der Beobachtung vielversprechender Ergebnisse gab die Entidad Nacional de Acreditación (ENAC) die Software zur weiteren Verwendung frei, sodass das Homologationsverfahren gestartet werden kann.

Contents

1	Introduction	1
1.1	Introduction	1
1.2	State of the art	2
1.2.1	Introduction to rear underrun protection devices	2
1.2.2	Homologation procedures for vehicles	5
1.2.3	Regulation Number 58	6
1.2.4	Numerical simulation: Finite Elements	19
1.2.5	An overview of friction and its effects on contact elements	26
1.2.6	Study of tensions state for screw connections	31
1.3	Preliminary work	34
1.4	Important literature used as reference	37
2	Nature of the work	39
2.1	Introduction	39
2.2	Aims of the task	39
2.3	Useful effects	40
2.4	Work in the future	40
3	Analysis of literature	43
3.1	Introduction	43
3.2	Analysis of accidents' rates	43
3.3	Analysis of papers from the technical field	48
3.4	Conclusions	58
4	Methods	61
4.1	Introduction	61
4.2	Modelling of parts	62
4.3	Material selection	69

4.4	Contact conditions	72
4.5	Meshing	79
4.6	Transient mechanical analysis	83
4.6.1	Application of loads, fixed supports and time conditions . . .	83
4.6.2	Results of case study one: lack of pretension	89
4.6.3	Results of case study two: inclusion of pretension	94
4.6.4	Calculations with LS-Dyna	102
5	Results and discussion	107
A	Import Solidworks geometry into ANSYS Workbench	111
B	Creating a finer and isolated mesh	113
	Symbols and abbreviations	115
	Table Index	116
	Figure Index	117
	Bibliography	123
	Expression of thanks	129

Chapter 1

Introduction

1.1 Introduction

The constant evolution and development of vehicles has put a stark emphasis on the concerns of passive and active security. Crashes between vehicles are highly expected and thus one of the main concerns regarding users' safety. Due to the high dimension, the structural differences and their weight, heavy goods vehicles (HGV) or trucks pose a higher risk in cases of accidents, mainly with smaller vehicles [1]. In the event of unexpected collision, a rear underrun protection or RUP usually present on heavy vehicles, avoids smaller ones to be pressed underneath the chassis. In Figure 1.1 a crash between a HVG and a passenger vehicle is detailed, where the latter is confined. The device also protects the driver from serious injuries or from being trapped.

The safety and permit of circulation of commercials vehicles is a heavily regulated topic controlled by the European Commission (EC). The Directive made the usage of RUP in HGV obligatory and thus proposing also important requisites that they have to fulfil in order to be installed. Further tests are also presented in the issue, which specify important steps to follow and control or how to interpret the efficacy of results [2].

Based on the regulations imposed by the EC, the objective of this work is to develop a new engineering simulation program to observe the resistances of different instances of RUP usage. It will follow the tests requisites explained in the UN Regulation No. 58 [2], in order to substitute physical tests for a more digital approach.

The design will be constructed in cooperation with the “Laboratorio Técnico de Reformas, SA” in Murcia, Spain. Afterwards, with the aid of the simulation programme ANSYS the design will be physically tested. The results will be presented to the “Laboratorio Técnico de Reformas, SA” in order to observe the efficacy of the simulative programme. If the company deems it capable, the programme will undergo a control performed by the “Entidad Nacional de Acreditación” for its approval and further homologation.



Figure 1.1: Sliding of smaller vehicle under the frame of the heavy weight vehicle [1]

1.2 State of the art

1.2.1 Introduction to rear underrun protection devices

A rear underrun protection consists in its core of two stirrups that support a horizontal beam [3]. The design of the beam can vary depending on the type of protection, but ranges from a circular to a square shape. The stirrup can then be connected

directly to the chassis of the car or to extra elements, such as additional plates, in order to regulate the horizontal distance from the beam to the truck or the vertical one to the surface of the floor. Figure 1.2 shows the two main components of this type of protective device for heavy weight vehicles.

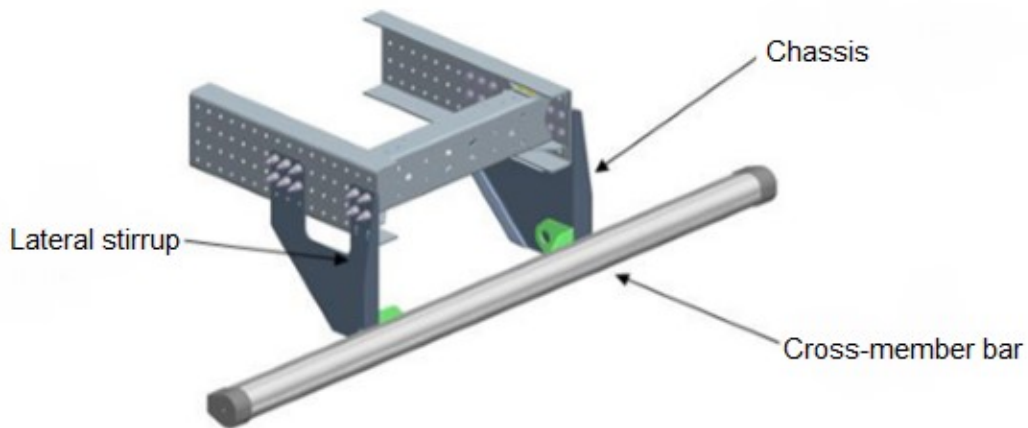


Figure 1.2: Relevant components of a RUP [3]

Mechanisms for RUP regarding their position to the vehicle range from fixed, slidable, foldable and foldable-slidable (Figure 1.3 features an example for each type). Fixed RUP devices are the most popular in the market, due to their lower prices. The adjustable ones offer more flexibility and are used for more specific type of works. However, their prices are higher because of the additional materials and moving parts [3].

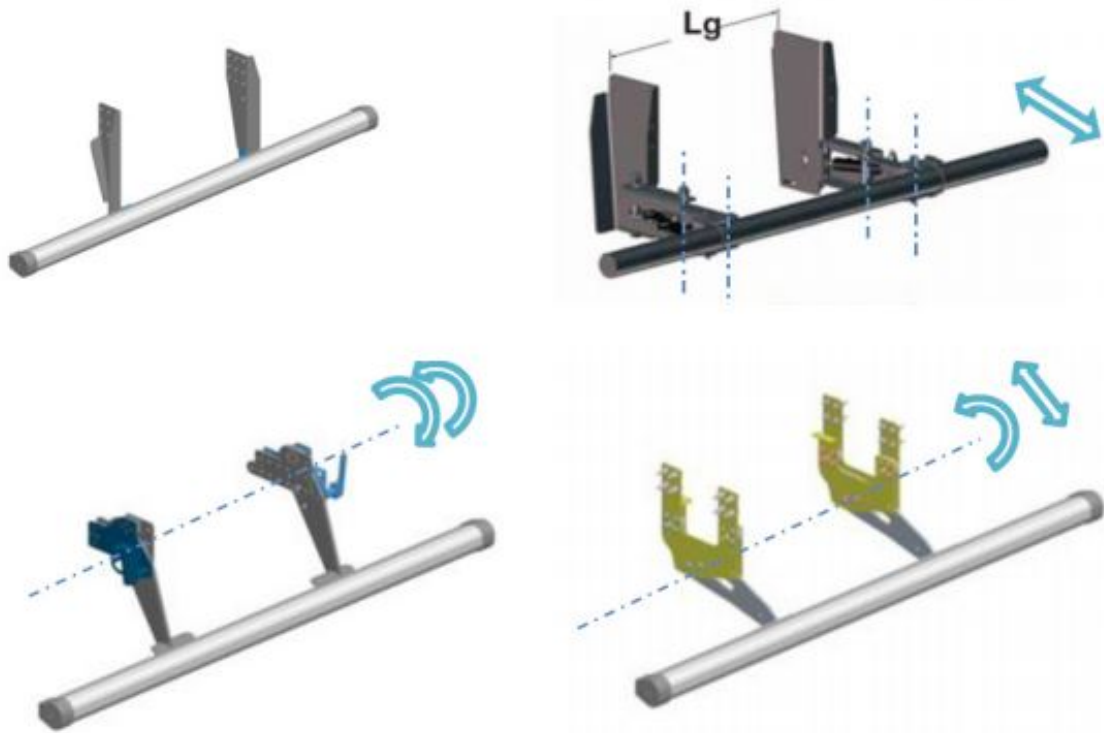


Figure 1.3: Different configurations for RUPs. From upper left to down right: fixed, slidable, foldable and foldable-slidable [3]

During a crash, the kinetic energy of both vehicles dissipates by the bending and crushing of the metal in the outer area. Passengers suffer the effect of the caused energy and the high value of acceleration in a short period of time [4]. The purpose of a rear underrun protection is to absorb the high quantities of energies and reduce acceleration peaks, hence effectively improving the safety of the passenger present in the smaller vehicle. This last one is more prone to serious injuries due to dimension differences. Studies [5] [6] show that the main failure cause of these protective devices lays on the large ground clearance and not allowing the contact of the device with the forepart of the vehicle. The smaller vehicle tends to slide underneath the bigger one causing an extensive passenger compartment intrusion. That is why the RUP has to suffice structural dimension and material specifications in order to withstand demanding forces in the case of accidents. Their usage provides a stable and stiffer surface that restrains the effects caused by the underrun. That is why the regulations have to set the standard for evaluating the capacities of RUP

devices.

1.2.2 Homologation procedures for vehicles

Automotive homologation is defined as the process of certifying singles or groups of components of a vehicle or also a unit as a whole. The statutory regulatory bodies set the procedures and technical requirements that all vehicles have to suffice in order to circulate on open streets. The regulations have to set a minimum standard that correlates to real world conditions [7]. Automobiles then obtain operating permits for their use.

In the European Economic Space (EEE) the Annex IV of the directive 2007/46/EC of the European Parliament and the council of 5 of September of 2007 establish a framework for the approval of motor vehicles and trailers. Additional systems, components and separate technical units intended for such vehicles are also present [8].

Important instances of changes that incur in the removal of vehicles' approval, which include:

1. Change of the vehicle's original type
2. Possible danger to road users is to be expected
3. The environmental or noise behavior is worsened

Other cases of changes such as substitution or implementations of a part must be observed with detail [9].

The homologation procedure for new technical parts of vehicles follow the same patterns in all countries of the European Union. The manufacturer or approval entity has to possess a reliable quality system in its facilities or assembly plants as a first step to start an approval [7]. If this is not the case, both procedures can be carried out in parallel:

1. Design and manufacture of a prototype. This has to be issued with a fulfilled technical sheet with all the respective information.
 2. Carry out necessary tests in accordance with the regulatory acts. During this step a corresponding report with all observation and results has to be written.
-

3. Compile all previous documentation for the issuance of a certificate of homologation [10].

After all these steps are finished, a homologation number can be issued for the new technical part. This is also the case when homologating a new design for a RUP, which we will also follow for our specific study case. This paper will serve as the needed documentation for the finite element software, while the technical reports will be written by the LTR. As a summary, in the following Figure 1.4 we can identify the different elements that can be affected by regulatory acts:



Figure 1.4: Vehicle components susceptible to homologation procedures [10]

1.2.3 Regulation Number 58

Foreword of the United Nations Economic Commission for Europe

The United Nations Economic Commission for Europe (UNECE) was founded in 1947 by the United Nations Economic and Social Council. It is currently made up of 56 countries and since its foundation it has had the objective of promoting economic integration among its member states, the great majority of which are located in Europe [11]. In its beginnings it was founded under the principles of the European

Union: to promote a policy to facilitate actions of improvements in the economic field, to increase initiatives of development and competitiveness, and finally to improve the relationships between countries affected by the war.

The UNECE committees include: environmental policy committee, housing committee, smart city program and of course; an inland transport committee. The transport division provides the secretariat for the World Forum for Harmonization of Vehicle Regulations, and the Transport Innovation and Vehicle Regulations section acts as the secretariat for the Administrative Committee for the coordination of the work. Its mission involves the regulation and control of road transport, as well as designing specific requirements for vehicles and their parts [11]. The focus of the study will lay on the regulation Nr. 58, that states all the requirements for rear underrun protective. Important parts of the regulation will be explained, such as requirements, possible tests, conditions and formats. Their effectiveness will be observed and finally conclusions will be presented that will examine the role of the regulations.

History of the regulation number 58

The first regulatory acts regarding the passive safety of European vehicles were first imposed in the year 1970 with the "Council Directive 70/221/EEC of 20th of March, on the approximation of the laws of the member states relating to liquid fuel tanks and rear protective devices for motor vehicles and their trailers" [12]. Vehicles that didn't fulfil necessary ground clearance were required to be equipped with RUPD. This directive imposed general dimensions without a lot of specifications:

- "11.3.1. The underside of the rear protective device must be less than 70 cm from the ground when the vehicle is unladen."
- "11.3.2. At the place where the rear protective device is fitted its width may not exceed the width of the vehicle or be less than the width of the vehicle by more than 10 cm on either side." [12]

The installations procedures are also described, and an overall bending resistance is expected from the device. The regulatory act is in its core short and non-specific; which lays on the historical necessity of heavy vehicles in the past years. This act served as a base for the more detailed regulatory act of the Economic European

Commission Nr. 58. It's important to highlight that these regulations suffer from constant modifications, based on:

- “The necessity of transportation vehicles in the actuality and thus the numbers of vehicles in circulation.”
- “The evolution of cars, trucks or other vehicles: their masses, dimensions, components and market.”
- “Research and investigations in regard to human safety.” [7]

The first revision entered into force on the 25th of March of 1989. This was replaced in the year 1995 by the second revision, which made some changes to the requirements of rear underrun protections. The final and the revision which is used in the actuality is the Revision 3 which entered into force on the year 2017 [2]. Important advances have been made regarding the safety of passengers in cases of collisions between a heavy truck and a light vehicle. That is why the need for changes to a new revision.

Requirements for the approval rear protective devices

The United Nations (UN) Regulation 58 proposes details for the approval of usage and installation of RUP. This set the standards for RUP by summiting them to simulative forces, based on real life conditions. The intention is to imitate real life situations that substantiate the resistance capabilities of different models. Their scope also encapsulates specifications of vehicles of categories M, N and O. All the important requirements included at [2] will be described in this section and include three important criteria:

- Position of installation (mainly height requirements)
- Dimensions
- Resistances of forces

UNECE Regulation 58, Series 3 makes three important distinctions for the approval of RUP: Part one specifies the rear protective devices intended only for fitting to vehicles of categories M, N and O (emphasis on only the device). Category M vehicles are those designed and constructed for the carriage of persons and their luggage (Regulation EU 678/2011). Category N is designated to motor vehicles

manufactured mainly for the transport of goods; finally, O vehicles are used for the transport of both passengers and goods, as well as for the accommodation of persons. Part two determines the approval of a vehicle with regard to the installation of an RUPD of an approved type. Finally, part three applies to the approval of vehicles with already installed devices. In summary, the regulation number 58 encases:

I Single rear underrun protection devices: from paragraphs 4 to 12

II Approval of vehicles with regard to the installation of an approved protection device: paragraphs 13 to 21

III General vehicles in regard to their RUP: paragraphs 22 to 30

In addition, an introductory scope, containing vocabulary and general requirements is also presented. The regulation also contains information regarding conformity of production and realization of tests simulations, which determine if the rear underrun protection device suffices with the imposed requirements by the commission.

Each approved RUP must be identified by an approval number, if it complies with the requirements explained in the regulations. The first two digits shall indicate the series of amendments corresponding to the most recent technical amendments made to the regulation. The most recent digits, 03, correspond to the third series of amendments, or the most recent series of the regulation, which entered into force on the eighteenth of June of 2016. The approved device must be readily identifiable by means of a visible international approval mark, present in Figure 1.5, which must fulfil the following requirements: first a capital letter 'E' followed by the distinguishing number of the country where the approval was granted (1 for Germany, 2 for France, 3 for Italy, etc.). This is followed by the number of the regulation (in this case 58), followed by the letter "R", a dash and the approval number of the device previously assigned.



Figure 1.5: Example of a homologation mark for a vehicle approved in the Netherlands [2]

Analysis of part I: General requirements for the homologation of a Rear Underrun Protection

As mentioned above, the height of the RUP from the ground is an important criterion to be considered for the respective approval. The regulation states that the height of the profile of the crossbeam to the ground must be at least 120 mm. The ends of the profile or cross member must not have any cutting edges towards the outside. These requirements are met if the side ends have a rounded exterior with a radius of curvature of at least 2.5 mm.

The RUPs intended to be fitted to vehicles of categories M, N1, N2 with a maximum mass of less than 8t, to those of categories O1 and O2, to vehicles of category G and to vehicles with a lifting ramp, must have a profile height of the cross-member of at least 100 mm. The design of the rear protective device may be varied to suit different positions. There must, however, be a secure fixing which does not allow the device to be moved when it is in the respective operating position. A force of less than 40 daN exerted by the operator is required to change the position of the device. In addition, the regulation states that devices with position-adjustable designs must have a mandatory label, with the aim of informing the operator of their service position to ensure protection against entrapment. This label must have a minimum size of 60x120 mm.

Adequate resistance of the device to forces applied parallel to the longitudinal axis of the vehicle is required. This procedure will be discussed in detail in the paragraph

of Annex 5, which will present the values of the testing forces and deformations of the beam. All results shall be recorded and reported in the approval procedure. Of great importance are the requirements in case of vehicles equipped with a lifting platform at the rear, as additional dimensions have to be considered:

- Maximum lateral distance of 2.5 cm between the protective device elements and the elements of the lifting platform, which are responsible for moving the platform and also allow its interruption.
- The elements of the RUP must have an actual area of at least 420 cm.
- If the height of the profile of the RUP is less than 120 mm, each element of the previously mentioned, in addition to those located outside the lifting mechanism, must comply with a minimum area of 350 cm.
- In instances where the width of the vehicles is less than 2000 mm and consequently the above requirements cannot be met, the actual area may be reduced. All these requirements must also comply with the criteria of deformation and resistance.

Analysis of Part II and Part III: Approval of a vehicle with regard to the installation of an RUPD of an approved type and general vehicles with already placed RUPs

For vehicles of category N2 having a mass greater than 8t, other vehicles such as N3, O3 and O4, the ground clearance with respect to the underside of the protective device shall not exceed:

- a) 450 mm for those with trailers with hydraulic, hydro-pneumatic or air suspension. An exit angle of up to 8 degrees, with a maximum ground clearance of 550 mm, shall also be considered acceptable.
- b) 500 mm or an exit angle of 8 degrees, whichever is less, for all other vehicles not mentioned above.

The regulations stipulate that for vehicles of categories M, N1, N2 with a maximum mass of 8t, O1, O2, the distance between the underside of the device and the ground must not exceed 550 mm. In case the corresponding test is carried out, the points of the RUP where the forces are to be applied must not exceed 600 mm above the

ground.

The width of the RUP must not be greater than the width of the rear axle, measured from the lateral extremities of the wheels, and must not be less than 100 mm on each side. If more than half the width of the tires exceeds the width of the bodywork (e.g. O1 and O2 vehicles), and excluding the mudguards, the distance from the end of the RUP to the innermost point of the tires must not be less than 100 mm. The exact points where the test forces are applied must always be entered and reported.

Again, for vehicles of categories M, N1, N2 with maximum mass of 8 t, O1 and O2, a maximum horizontal distance of 400 mm is set between the rear of the crossbar and the rear-most axle elements of the vehicle, which includes any lifting platform system, in addition to subtracting all major deformation (plastic and elastic). Any part that is 2 m above the ground shall be excluded from consideration. Elements with a size of less than 50 mm and non-structural projections, such as rear lamps, are not considered. Vehicles of classification N2 exceeding a maximum mass of 8 t, N3, O3 and O4 must also meet the prerequisite, however with a maximum horizontal distance of 300 mm.

For the test procedure, a maximum distance of 100 mm is required between the foremost and rearmost points of the crossbar, in relation to the longitudinal plane of the vehicle. It must be verified that after the test the height of the device does not exceed at any point more than 60 mm, from its pre-test value. This requirement applies only to vehicles of classification N2 exceeding a maximum mass of 8t, N3, O3 and O4. In the case of vehicles with an exit angle of up to 8 degrees, the height shall not exceed 600 mm. Tables 1.1 and 1.2 allow a general overview of the dimensional requirements and prescription of the regulation 58. All information of the document will be summarized in these tables.

Table 1.1: Contact types and characteristics

NO.	Type of Vehicle	Prescriptions and requirements
7.1	General	<ul style="list-style-type: none"> ●Profile height of the crossbar must be at least 120 mm. ●Ends not curved back, no cutting edges. ●Ends of crossbeams rounded with a minimum curvature of 2.5 mm (also compliant).
	M, N1, N2 < 8 t, O1 and O2, for category G vehicles and for vehicles equipped with a lifting platform	<ul style="list-style-type: none"> ●The height of the profile of the crossbar must be at least 100 mm.
7.2	General for devices with position-adjustable designs	<ul style="list-style-type: none"> ●A force of less than 40 daN exerted by the operator is required to change the position of the device ●Mandatory label, with the aim of informing the operator of the service position. Size: 60x120 mm.
7.4	Vehicles equipped with a lifting platform in the rear frame	<ul style="list-style-type: none"> ●Maximum lateral distance of 2.5 cm between the protective device elements and the lifting platform elements. ●The elements of the RUP must have an actual area of at least 420 cm². ●If the profile height of the RUP is less than 120 mm, each element must have a minimum area of 350 cm². ●In instances where the width of the vehicles is less than 2000 mm the actual area may be reduced.
16.1	N2>8 t, N3, O3 and O4	<ul style="list-style-type: none"> ●Ground clearance of <450 mm for motor vehicles and trailers with hydro pneumatic, hydraulic or air suspension or with an automatic height correction device. ●Maximum ground clearance of 550 mm is also met if there is an exit angle of up to 8.

Table 1.2: Contact types and characteristics

NO.	Type of Vehicle	Prescriptions and requirements
16.1	Other vehicles, other than those previously expressed	<ul style="list-style-type: none"> •Ground clearance of 500 mm or an exit angle of 8, whichever is less.
16.2	Vehicles of the categories M, N1, N2<8 t, O1 and O2	<ul style="list-style-type: none"> •Ground clearance of <550 mm from the lowest point of the device (even empty). •In case of the corresponding test, the points where the forces will be applied must not exceed 600 mm in height from the ground.
16.4	Vehicles of the categories M, N1, N2<8 t, O1 and O2	<ul style="list-style-type: none"> •Maximum horizontal distance of 400 mm between the rear of the crossbar and the elements of the rear axle of the vehicle. •Any part that is 2 m above the ground shall be excluded from consideration. •Items smaller than 50 mm will not be considered.
	N2>8 t, N3, O3 and O4 with lifting platform	<ul style="list-style-type: none"> •Maximum horizontal distance of 300 mm between the rear of the crossbar and the elements of the rearmost axle of the vehicle
	O3 and O4 with lifting platform	<ul style="list-style-type: none"> •Maximum horizontal distance of 200 mm between the rear of the crossbar and the elements of the rearmost axle of the vehicle.
16.5	N2>8 t, N3, O3 and O4	<ul style="list-style-type: none"> •(Test) Maximum distance of 100 mm between the foremost and rearmost point of the crossbar, in relation to the longitudinal plane of the vehicle. •Check that after the test the height of the device does not exceed at any point more than 60 mm from its value before the test.
	Vehicles with an exit angle of up to 8 degrees	<ul style="list-style-type: none"> •The height should not exceed 600 mm.
25.8	General	<ul style="list-style-type: none"> •Verification of device conformity by mathematical calculations.

Test development and conditions

Depending on the manufacturer's requests, the test can be performed on a complete vehicle or on a part of the chassis only (Figure 1.6). In the latter case, the conditions of fastening must be similar to those used for installing the device on a complete vehicle. According to the regulations, the chassis must be placed on a rigid test bench. There must be a minimum distance of 500 mm between the most forward fastening point of the device and the rigid test bench. In addition, the fixing point must be separated from the rearmost point of the rigid test bench by a distance of at least 1 000 mm. All structures used in the test must have similarities to the original vehicle chassis.

The nature of the test may be mathematical-computational or physical, at the manufacturer's discretion. In the first case the values obtained must be validated by a physical test, so that the similarities of the results can be compared. If the software is altered, the approval authority must be informed immediately for re-checking and reassessment. If the profile of the device does not have a flat vertical surface with a width of at least 50 % of the minimum height mentioned in the analysis of part I, II or III; the application of a device to apply horizontal test loads is allowed. This device must not change the properties of the rear protective device.

The main requirements for the pre-test vehicle are as follow:

- The vehicle must be positioned on a flat, rigid and smooth surface

 - The front wheels must face forward

 - Tires must be inflated to an acceptable pressure

 - If the vehicle is equipped with an air, a hydraulic or a hydro pneumatic suspension or a load-dependent height correction device, the test must be carried out under normal running conditions
-



Figure 1.6: Example of a testing bench for separated parts

Each force shall be applied separately and consecutively to a surface not exceeding 250 mm in height and 200 mm in width, with a radius of curvature of 5 mm at the vertical edges. The order in which the forces are applied shall be chosen by the manufacturer.

In the first instance, a horizontal force of 180 kN or 85 per cent of the force generated by the maximum mass of the vehicle is applied (whichever is the smaller) at two points located symmetrically about the center line of the vehicle or device, separated by a distance of at least 700 mm and not more than 1000 mm. The most unfavorable situation would be with the distance of 1 meter, which causes a higher moment. The value of the force can be reduced to 100 kN or 50 % of the maximum mass for vehicles of category N2 with a maximum mass of less than 8 t.

Secondly, a horizontal force of 100 kN or 50 % of the force generated by the maximum vehicle mass (whichever is the smaller) is applied at two points 300 mm, add or take 25 mm, from the outer edges of the wheels of the rear axle or rear protective device (whichever is the wider).

Finally, one outside the same previously selected value is applied at the center of the rear protective device or frame. Again, for vehicles of category N2 with a mass not exceeding 8t, this value may be reduced to 50 kN or 25 % of the maximum mass. In the case of specific vehicle types such as: vehicles with tilting sections or with rear lifting platform, all force values can be reduced by 80 %. The following Figures 1.7 and 1.8 help to visualize the location and the quantity of the forces.

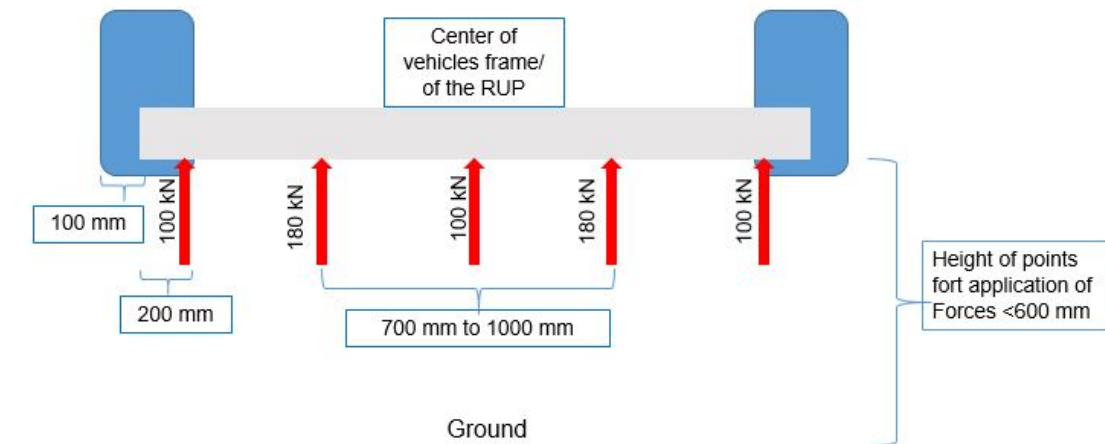


Figure 1.7: Location of forces for a RUP with a width less than the distance between tires

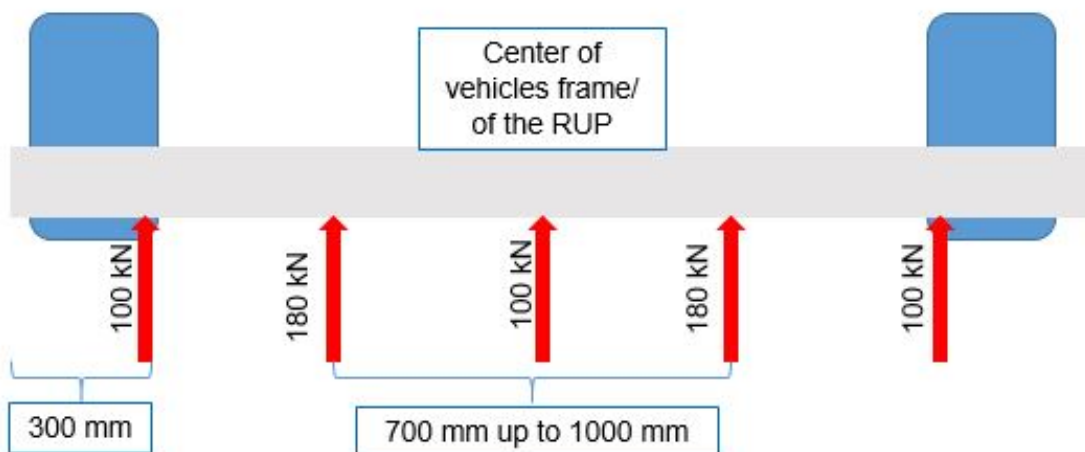


Figure 1.8: Application of forces for a RUP with greater width than the tire distance

Differences between the Revision Nr. 2 and 3 include the dimension of the device (mainly height or area of individual elements). The test procedures have also been adjusted and augmented, since German tests showed that RUPD are submitted to higher forces than those proposed in the Revision Nr. 2. The forces were increased by around 100 %, changing from 100 to 180 kN and also from 50 to 100 kN subordinate to their position. These requirements force changes in RUPD designs with respect to weight and dimensioning. Therefore the construction materials of the RUPs should be chosen with caution. Further revisions with additional considerations are expected to come into force in the next few years, starting from September 1st, 2021.

Conformity of production

The approval of technical parts of vehicles according to the United Nations requires the application of procedures with international standards, such as the quality control of the industrial sector ISO 9001:2008 [2]. The approval can only be authorized by a previously accepted body and involves the use of documentation specifying important information such as: company or group, regional division, vehicle and important dates such as inspection and acceptance. In Spain, the organization that directs these procedures is the ENAC or National Accreditation Entity (Entidad Nacional de Acreditación).

In the specific case of rear protections, it must be ensured that the authority that has allowed the type approval carries out a periodic follow-up control. These will be carried out every two years and will check that the unit still complies with the previously established requirements, as well as those of resistance and deformability. If any requirement is modified and therefore ceases to comply with the regulations, the control entity must be informed automatically. Annex 2 of the regulations is used for this purpose with a request specifying the intention (see Figure 1.9). All modifications must also be informed immediately by submitting Annex 2. The inspection body can then take decisions on the alterations:

- If the modifications do not cause an adverse effect on the device or if the device is not significantly altered; in that case the RUPD still complies with the requirements previously mentioned.
 - An additional test report is required from the technical service responsible for conducting the pre-tests. This will either confirm that the requirements are
-

still met or immediately reject the device approval.

All laboratories or technical services responsible for conducting tests in regards to this regulation must be communicated to the UN secretariat, including their addresses. The control or accreditation body, which issues extensions or rejections of approvals, must also be registered with the UN secretariat.

Communication

(Maximum format: A4 (210 x 297 mm))

issued by:

Name of administration:



Concerning:²

- Approval granted
- Approval extended
- Approval refused
- Approval withdrawn
- Production definitively discontinued

of a type of a vehicle type with regard to the installation of a rear underrun protective device (RUPD) of an approved type pursuant to Part II of UN Regulation No. 58

Approval No.

Extension No.

1. Trade name or mark of vehicle
 2. Vehicle type
 3. Manufacturer's name and address
-

Figure 1.9: Annex 2: communicative paper for the participating parties [2]

1.2.4 Numerical simulation: Finite Elements

Since the introduction of finite element methods in the sixties, this calculative method has been rapidly improved and developed. Finite elements are used as a technique to solve engineering analysis, such as solids or structures and also heat transfer and fluids [13]. The following chapter should give an insight on the usages of this flexible tool and also describe the principles of FE. Furthermore, we will also

present the capabilities of ANSYS as a simulative software for engineering analysis.

Usage and mathematical approach of Finite Elements

Typical application examples of FE calculations are aircraft construction, automotive engineering (like crash test or chassis optimization), pipeline, medicine, geophysics and more. However, the main field of application is the elasto-mechanics. This is due to fact that a lot of problem can arise when simulating some conditions that can only by modelled with the aid of a computer: complex geometries, anisotropy, non-linearity nature of the geometry, inhomogenities and such [13].

The calculation by finite elements follows a base idea: a structure or part that is the main domain of analysis is to be represented with numerous tiny components, named finite elements. Figure 1.10 shows the step known as discretization, where a mesh with all the finite elements is created in order to simplify a bigger object into a form that can be solved [14]. Smaller elements mean easier solvable equations. The solution for the overall geometry equation is obtained with the solutions of the elements.

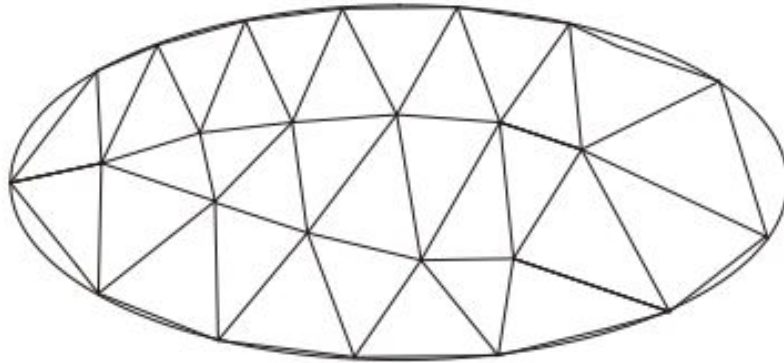


Figure 1.10: Discretization of a subject are with triangular elements [13]

Methodology and precision of Finite Elements

The discretization of the model may lead to possible errors in the FE analysis. The choice of the relative element size together with the selected element type has an important influence on the size of the error that potentially affects similarities to actual conditions. When creating a mesh the choices of precision against resources must be

made: in areas where no large stress gradients can be expected, rough idealization can be performed, so that the system of equations remains as small as possible [13]. The solution time may be decreased significantly. On the other hand, in areas where high stress concentrations are to be expected, correspondingly fine idealization must be performed, so that the actual stress peaks and gradients can be recorded precisely.

When analyzing solid mechanics problems the choice of material and the structural design are two major factors to weight in. Furthermore, the methodology of the FE procedure contains three major phases known as pre-processing, solution and post-processing [14]. In the first phase the mesh is created in order to create sub-domains. It is necessary to specify displacement boundary conditions, temperature conditions, geometry, applied loads and material properties (stress-strain relationship).

During the solution a computer-aided engineering and design (CAE/CAD) or program creates matrix equations for calculating the model and outputs a solution or primary quantities (such as stresses or deformations).

During the post-processing or final steps, all results must be controlled and further additional quantities can be computed. The objective is the examination of the precision of the calculation [15].

Implicit and explicit calculations

For the specific study case of the RUP, a transient structural mechanical analysis has to be performed. This is also denominated as time-history analysis, where a dynamic response and behavior of a structure is observed under conditions of time-dependent loads [16]. All respective reactions can be later measured such as displacements, stresses, forces and more. It is important to mention that in the case of transient structural analysis, bodies can be either rigid or flexible: meaning that more fixture commands are available. A deformation of the structure has to be controlled, since the tests procedures approved by the UNECE depend on varying loads and locations with different time steps [2]. The results will then depend on the damping effects of the calculation [16].

Even though these types of calculation are non-static analysis and there is a rela-

tionship with the loads/physics and time, transient structural analysis problems fall also under the denomination of implicit calculus. In order to understand explicit and implicit finite element methods it is important to distinguish between quasi-static or “time independent” problems and also time dependent ones: In case of the first one the load is applied slowly and with time, so that the effects of the acceleration can be ignored [17].

This is not the case of crash tests or “time dependent” such as explosions, where high forces appear in mere milliseconds. The effects of the deceleration must be accounted in these types of tests. In order to solve both of these cases, an implicit or explicit model can be used. The main difference between both of these lays on the time integration method in order to solve dynamic problems. Through matrix inversion one can solve these last mentioned. When the solution of one step depends highly on the solution of the previous one, this method receives the name of implicit. In other words, the present state but also the future state of the system are both accounted in order to solve the equation. On the other hand, an explicit analysis only the inversion of a diagonal matrix is calculated (less computational time) [18]. The system at a different time is the only state calculated when using an explicit method, not the current state. This makes explicit calculations less time consuming but also less unstable, in comparison to implicit methods [17]. For cases where a high variation of stresses and deformations are expected (for example crashes), the best solution is to apply an explicit calculation, with a program such as LS-Dyna. If the load is applied slowly and more states of the system have to be taken into consideration, an implicit program, such as transient analysis with ANSYS Workbench, is more recommended. However, it is important to note that in this last case more requisites are expected from the specifications: definition of all contacts, time step settings, material failure models and such [19]. In Figure 1.11 the ranges of use of both explicit and implicit calculations can be observed. For the specific study of the rear underrun protection devices an implicit program was applied. If the results show promising calculations, further explicit methods such as with the use of LS-Dyna, will also be executed.

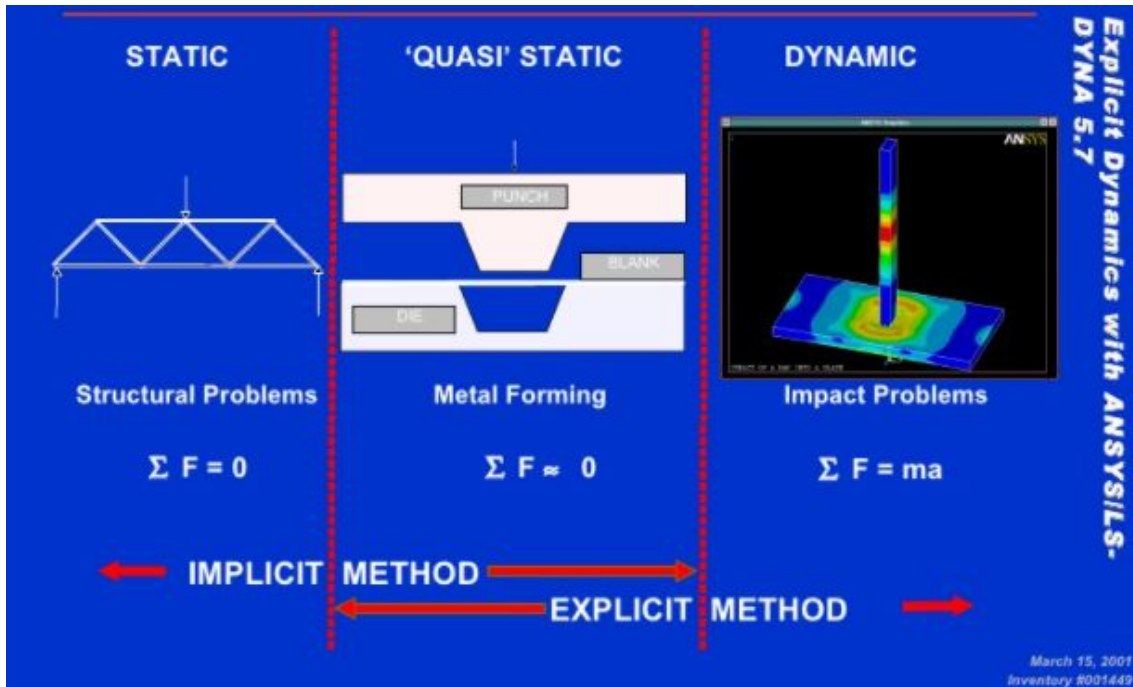


Figure 1.11: Application fields for implicit or explicit analysis [20]

An overview of ANSYS

The widespread FE-programs present in the market allow for a large number of different analysis. The best known and used are for instance ABAQUS, ADINA and of course ANSYS. Since its creation in the 1970, ANSYS has served as one of the most used simulative software for the calculation of linear and non-linear problems present in the thermodynamic, structural mechanics, optic and electric. ANSYS as a company develops and support engineering simulation software used to predict the behavior of new product designs under real-world conditions. Their products range from embedded software such ANSYS SCADE; programs for computer aided design like SpaceClaim; cloud services like ANSYS Cloud and lastly simulative programs for various engineering fields such as LS-DYNA, ANSYS Fluent and CFX [21].

For structural analysis ANSYS offers three main software: Mechanical, LS-DYNA and Workbench. The latter is intended for a simplify usage: the input of calculation problems doesn't require coding and is more intuitive and automatic. The graphical user interface is easier to follow, because of the improved algorithms for contact

finding, networking and interfaces to various CAD systems [22]. The steps are easier explained to the user and projects can be interconnected, reducing constant input of information. ANSYS Workbench can be automated and controlled via the script language Jscript and also supports command input via APDL [19]. Taken all of these advantages in consideration, we decided to use Workbench as our preferred calculating software.

Numerical Simulation: Transient Finite Elements

ANSYS possesses a range of analysis systems that adapt to the needs of the desired calculation. Some uses vary from analysis of fluids, electric devices, thermal systems and of course mechanical problems. The main goal of the analysis is to create a load case similar to the real one and thus simulate in the most exact way the conditions of a system or machine. This way a physical test can be avoided, which may be more expensive in some cases. Destruction of the system is also not necessary, due to the virtual nature of the test. Mechanical problems can be divided into two important categories: static and dynamic. Static Structural is also comprise of two important subcategories, depending on the calculation: linear and non-linear analysis. Dynamic analysis include Modal, Harmonic, Response Spectrum, Random Vibration and Transient (see Figure 1.12) [16]. Modal analysis is normally used to calculate vibration characteristics and mode shapes. When studying a structure's response to steady and harmonic loads (sinus loads) the harmonic analysis yields optimum results. This is the case of forces in rotating machines such as motors and bearings. Response Spectrum is ideal to study reactions to impacts and shocks with expected long duration. These instances can be earthquakes or other seismic events. For cases where the load varies in frequency and its behavior is highly unpredictable; the dynamic structural analysis is ideal. Random vibration is able to calculate the desired reactions of a system under the aforementioned conditions [23].

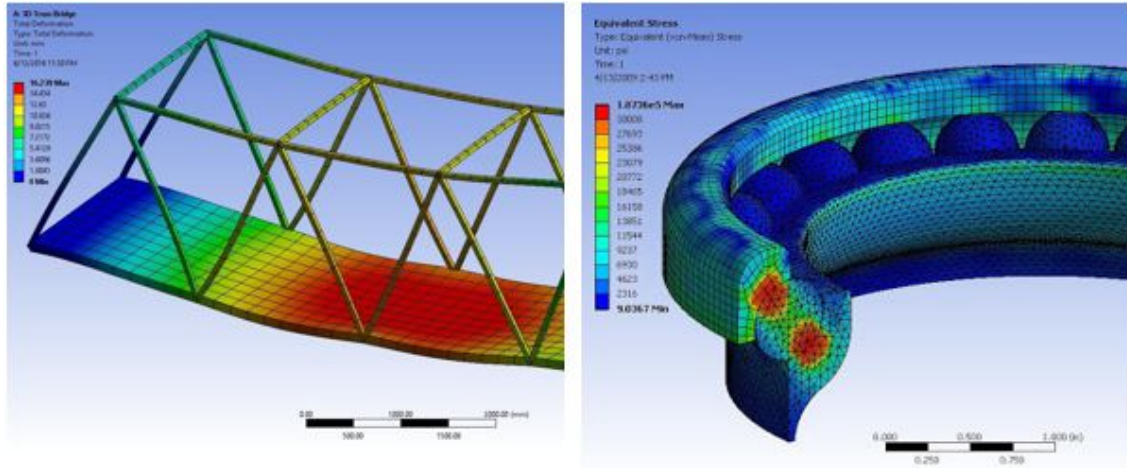


Figure 1.12: Dynamic analysis cases. Left: modal analysis for the resistance of a bridge. Right: harmonic analysis for bearing stresses

Finally, a transient analysis is ideal to calculate a structure's response to time dependent loads. In all dynamics cases the inertial and damping loads are needed. Due to the fact that the period of time for the calculation is inputted by the user, a transient analysis is highly dependent on the size of internal time steps. The complete simulation is defined by "Run Time" and concludes at "Stop Time". Transient simulations are ideal when unsteady states are expected for a system [16], meaning variables can be changed. The time which takes a system to change from a steady state to another steady state is better known as transient. During a transient region all calculations are highly dependent on time (temporary status), serving as the base principle for transient analysis: a bias point analysis is performed first to determine the operating point of the system at time $t = 0$ s. After this calculation, the time is incremented by one user predetermined time step at which the reaction of all the nodes to the loads are calculated based on the previously mentioned values obtained at time $t = 0$ s. This means that for every new time step, the reaction of the nodes (for ex. applied forces or deformations) are calculated and compared to the previous time step solution. ANSYS imposes a requisite for further calculations of time steps: the difference between the two solutions have to fall within a tolerance. The time step is the automatically or manually adjusted until a solution within the tolerance is found. If the tolerance is not respected, the analysis has failed to converge and calculate a solution. That is why estimating the appropriate time steps and skips is

important to reach expected tolerances [23].

When using a transient mechanical analysis, the procedure of setting step sizes is known as scheduling. For periods where a greater accuracy is needed or very high loads are expected for instance, smaller step sizes are recommended. If not the accuracy can be softened. In the case of ANSYS it is important to know all parameters from a transient numerical simulation. These will be presented at Figure 1.13:

- Transient Start Time: Value for the start of the required time interval for the analysis
- Transient Step Time: the nominal time increment used in the analysis
- Transient Max Step Time: Maximal possible variation in size of the time step
- Transient Min Step Time: Minimal variation of the time step, always performed at the start of the step analysis

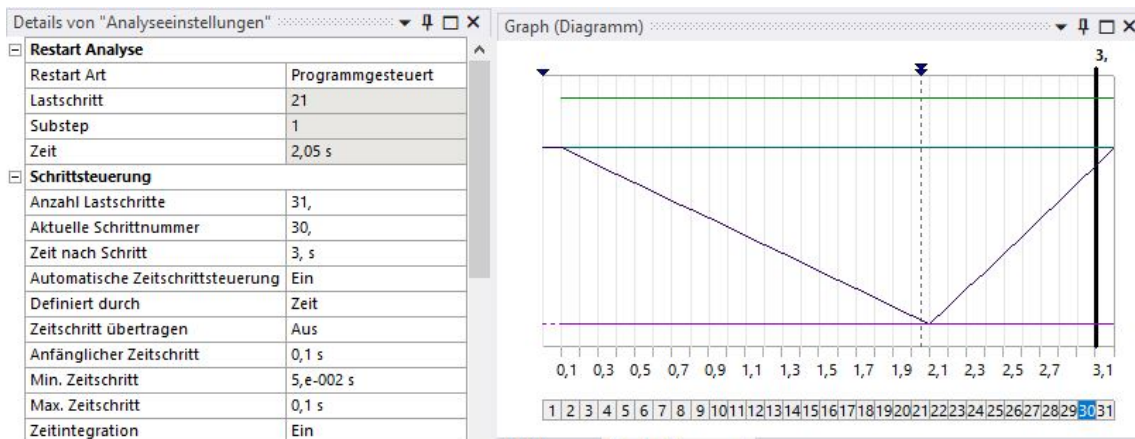


Figure 1.13: Dynamic analysis parameters: quantity of steps, starting and ending time, increments, general overview

1.2.5 An overview of friction and its effects on contact elements

The basis of all systems lays on the relationship of its components. It is important to understand the physics of the parts, mainly the contacts that are created between

them. All simulation programs present high levels of difficulties during the specification of contacts: if these cannot be defined with precision, it is possible that the obtained results vary a lot from the reality or that even the calculations cannot be performed at all. When simulating important contact conditions, the user has to take into account two main factors:

- I Contacts between parts can be abruptly created, disrupted or eliminated depending on their materials, fixtures or applied external loads.
- II Friction between surfaces has to be accounted for [24].

As known, friction acts as a resisting force when two surfaces have relative movement. When observing friction, it is sometimes necessary to study additional field effects such as electrical currents or thermal conductance [25]. For this specific study case, only the mechanical aspects of contacts will be studied.

When applying contacts three key steps have to be followed, as shown in Figure 1.14.



Figure 1.14: Steps and examples of contact definition in ANSYS

Based on these steps, the contact capabilities of Workbench will be examined in depth. When applying contacts in ANSYS, the user has to identify the objects which come into contact and define a contact and a target elements. These last ones depend on the deformability of the objects. Usually, a rigid object with a lower deformability will be assigned as the target, while the more flexible one will be the contact object [24]. In Figure 1.15 the process of selection is better explained with a presented example. The shaft of the screw serves as the contact body; the hole serves

as the target body. If both objects present the same material, an option for a flexible-to-flexible contact also exists, which allows both of them to deform. ANSYS allows multiple choices for both target and contact elements: points, edges, surfaces and nodes. However surface-to-surface contact provides the most advantages; these being the support for more elements (corner-noded or midside-noded elements for example) [26], better results for some typical engineering problems and no restrictions on the shape for target surfaces.

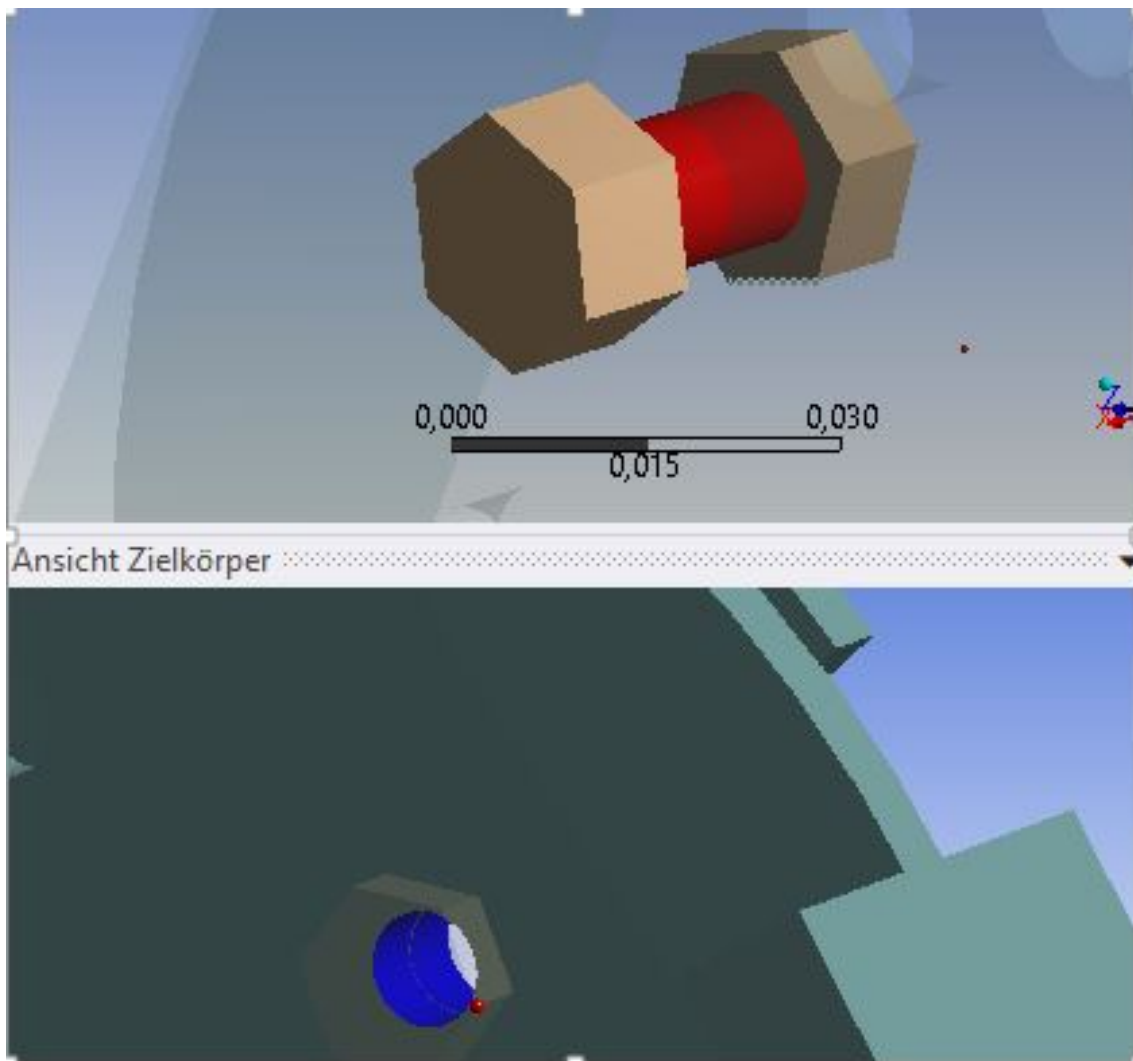


Figure 1.15: Example for contact definition. a) Visualization of contact surface for the shaft of a bolt b) Drilled hole used as target

The behavior between faces is also defined as symmetric or asymmetric. These

can decide the penetrative conditions between faces and will be further explained in chapter 4.4, where all the contacts of the RUP will be defined. Other behaviors can be controlled with the Contact Algorithm, which in its base, it defines the relationship between objects. Further explanation will be provided for the study case also in chapter 4.4. No further real constants were studied in order to simulate the test procedure, which are basically data required for the calculation of the element matrices and load vectors (behavior of contacts). Normal penalty stiffness factor, pinball radius, initial contact closure and more all fall in this category and were left with their default values. Information about these parameters is available at the ANSYS Contact Guide [24].

When specifying the properties of the contact pairs, one must take the effects of friction into consideration. ANSYS follows the Coulomb Law, a simplify model that predicts the effects and movements of two dry and contacting bodies [25]. This model makes a distinction between dry and kinetic friction, which can be represented with the formula:

$$F_{MAX} = F_N \cdot \mu \quad (1.1)$$

Where F_N represents the Normal Load between the two contacting surfaces and μ is the Coulomb friction coefficient. ANSYS applies an additional cohesion sliding resistance [24] which result in the following equation:

$$F_{MAX} = F_N \cdot \mu + S \quad (1.2)$$

When there is lack of movement, the mass experiences a dry friction. This means the product between the friction coefficient and the normal load hasn't surpassed the maximal allowed load. However if the applied load increases so does the friction, until the maximum value of static friction is surpassed, the bodies begin to slide. This state is also defined as slipping and where the kinetic friction occurs [25]. In order to specify the properties of the contact, one must then take into consideration the ability of objects to slide with each other. A brief summary of them will be presented in the Table 1.3 [26] and a further explanation will be provided in chapter 4.4.

Table 1.3: Contact types and characteristics

Name	Gap Open/Close?	Sliding allowed?
<i>Bonded</i>	<i>No</i>	<i>No</i>
<i>Rough</i>	<i>Yes</i>	<i>No, infinite μ</i>
<i>No Separation</i>	<i>No</i>	<i>Yes, $\mu = 0$</i>
<i>Frictionless</i>	<i>Yes</i>	<i>Yes, $\mu = 0$</i>
<i>Frictional</i>	<i>Yes</i>	<i>Yes, if $F_{sliding} > F_{friction}$</i>

To conclude when all contacts are specified, it is recommended to launch a verification on both contact/or target sides. This allows for a better verification of all the regions with a tool called “Contact Tool-Initial Information” (Figure 1.16). There the types of the contacts can be double checked, if there exists a gap between all regions or if an unwanted penetration of the objects is present. With this tool the user can also specify adequate tolerances or ranges of use. The status of the contacts and how the parts deform in relationship to each other, can only however, be checked with an initial run of the simulation. If ANSYS deems there is a possible problem, the program will crash on the first step, so that the possible problems can be identified without long calculation times.

Initial Information							
For additional options, please visit the context menu for this table (right mouse button)							
Name	Contact Side	Type	Status	Number Contacting	Penetration (mm)	Gap (mm)	Geometric Penetration (mm)
Frictional - Glass bottom To Rigid form	Contact	Frictional	Near Open	0.	0.	2.2053e-002	0.
Frictional - Glass bottom To Rigid form	Target	Frictional	Inactive	N/A	N/A	N/A	N/A
Bonded - Multiple To Multiple	Contact	Bonded	Inactive	N/A	N/A	N/A	N/A
Bonded - Multiple To Multiple	Target	Bonded	Closed	270.	8.8818e-016	0.	8.8818e-016
Bonded - Multiple To Multiple	Contact	Bonded	Closed	270.	8.8818e-016	0.	8.8818e-016
Bonded - Multiple To Multiple	Target	Bonded	Inactive	N/A	N/A	N/A	N/A
Color Legend							
Red	The contact status is open but the type of contact is meant to be closed. This applies to bonded and no separation contact types.						
Yellow	The contact status is open. This may be acceptable.						
Orange	The contact status is closed but has a large amount of gap or penetration. Check penetration and gap compared to pinball and depth.						
Gray	Contact is inactive. This can occur for MPC and Normal Lagrange formulations. It can also occur for auto asymmetric behavior.						

Figure 1.16: Information tool for verification of specified contacts

1.2.6 Study of tensions state for screw connections

Screws are widely used in the engineering field as means of connections that are simple and economical for cold-formed steel structural members. Their provided high safety against tension and shear forces, make this fasteners an attractive option in most machines and structures [27]. This is also the case of most rear underrun protections in the actuality: most designs prefer the usage of screws to fasten their materials, due to their simple assembly, their high resistance with relatively low prices, their lack of residual tensions and their low weight. Most fasteners have to provide a high resistance against external forces, as the tensions tend to concentrate in this union regions.

All metals, including bolts, are flexible materials which elongate under the influence of external loads and return to their original shape after the force is removed. However, if the bolt is stretched past a certain point, it will lose its elasticity and enter a plastic zone and suffer from irreversible deformations. This special point or also force is named Yield Point. The usage of bolts under loads superior to their respective yield strengths is not recommended, since they cannot retain their original shape and size. Meanwhile it is also important to mention the proof load as a way to characterize the limit of the elastic range of the bolt. This is the maximum load for a screw and a nut in which they can perform without unexpected permanent elongations. Finally, the tensile strength is defined as the finale maximum load prior to the fracture of the bolt. After this point the load can diminish until an ultimate tensile strength is reached and the bolt fractures (Figure 1.17) [28].

All of the tensions serve to characterize the mechanical and physical properties of joints. Screws, nuts and studs obtain property classes, when they possess a ISO thread, a nominal thread diameter inferior to 39 mm, are made of carbon or alloy steel and were tested at room temperature [29].

In order to fasten two materials together, the bolt and the nut have to work together to apply forces to both sides of the fastened material. This compressing force is known as pretension or pre-load, which is caused by the compression created by the fasteners. After this procedure, the bolt is capable of transferring possible exerted forces through the material [29]. This allows for higher resistance of tensions, mainly because the bolt is not supporting all the loads. In order to calculate the

bolt pretension, the following formula can be employed:

$$F_{PRE} = \frac{M_t}{K d} \quad (1.3)$$

Where M_t equates to the bolt installation torque; K represents the torque coefficient or a simple constant (dependent of thread geometry, thread coefficient of friction and collar coefficient of friction). Finally, d equates to the bolt nominal shank diameter, usually found in the technical data of the bolt if this is standardized [27].

ANSYS is able of modelling a high range of bolted unions: with thread, without thread, complex geometries, bonded or frictional unions and so forth. It is however always recommended to apply a pretension of the bolts, in order to secure the fastened parts and the distribution of the force. This ensures a higher rigidity of the joints, better fatigue performance and less loosening of bolts due to vibrations [30]. In order to simulate this condition, the command PRETS179 is used, so that a pretension section within a meshed structure can be created [31]. This allows for only one degree of freedom, this means that the bolt will be pre-loaded in one direction (usually the normal direction of the selected faces), meanwhile the rest of them will be fixed. Only tensions loads will be simulated, and further requisites include that the elements must have identical meshes with matching nodes. The node ordering during pretension is critical, in order to simulate an adequate displacement of the bolt and assign boundary conditions. That is why it is always recommended to check the meshing in these areas and also observe that the connections between the unions do not present any possible errors. Gaps or penetrations affect a matching mesh. In Figure 1.18 we can observe an example of a bolted union with a present bolt pretension: the force is applied normal to the shaft. The plates will then be forced together, which assures a better distribution of the applying forces.

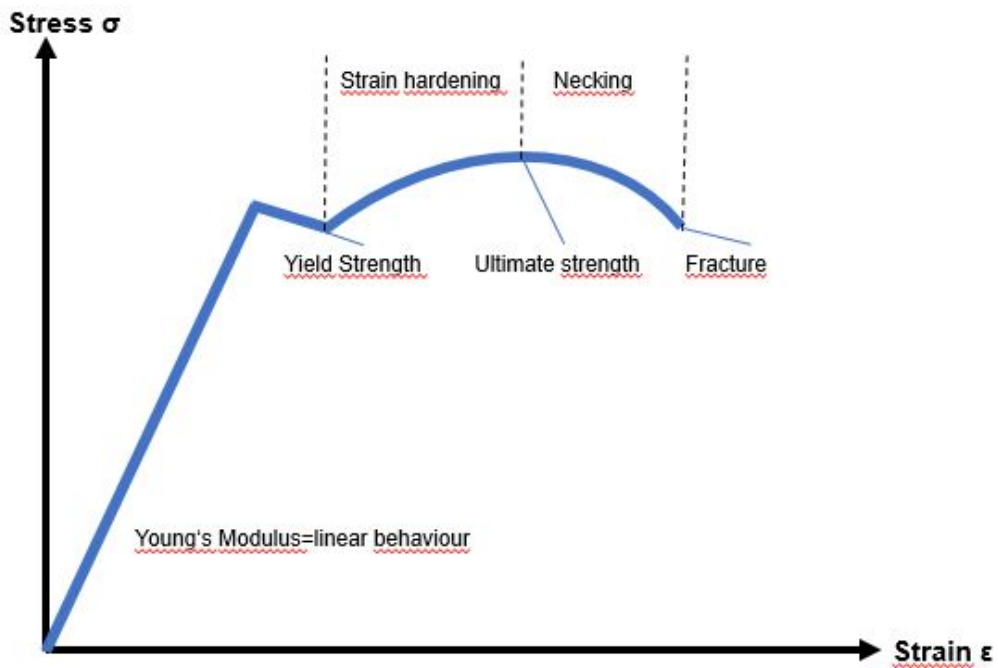


Figure 1.17: Typical low carbon steel stress-strain curve

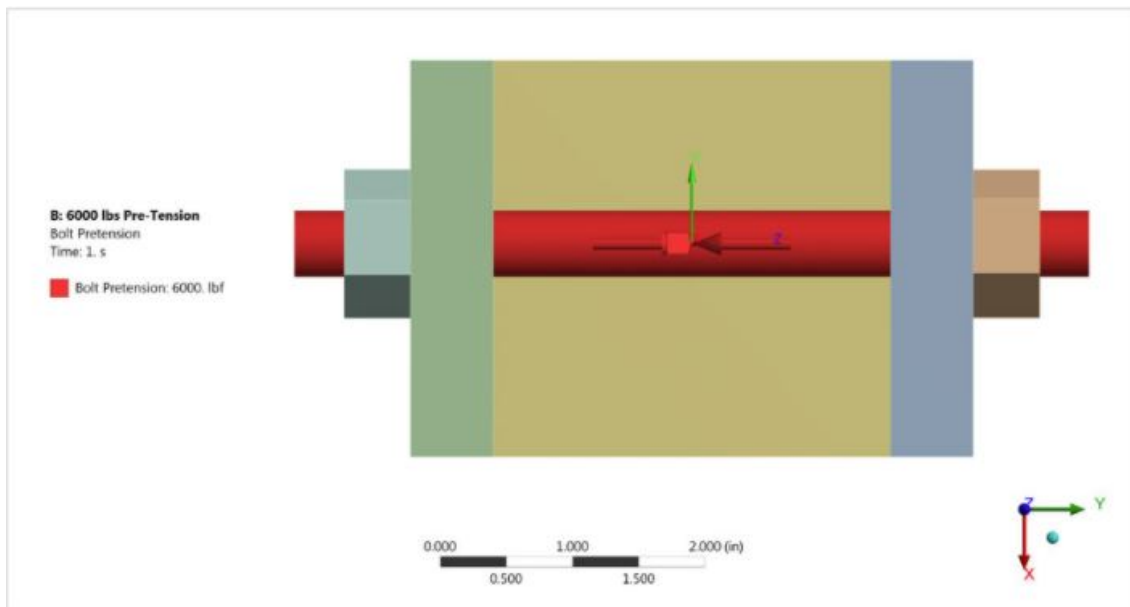


Figure 1.18: Application of pretension in ANSYS for a bolt

In Workbench when designating the respective pretension of bolts, the shaft has

to be selected in order to assign the respective pretension area. It is recommended for the area to be between the head of the bolt and the nut [31]. The normal vector of the global coordinate system respective to the shaft will be selected as the pretension direction. The user is able to change the direction when creating an additional coordinate system. However, for the case study it was not necessary. When utilizing transient mechanics, all seconds belonging to the pretension have to possess a command. The existing ones are:

- Pre-load: Assignment of a specific load for the pretension.
- Deformation: Instead of applying a load, a distance can be inputted in order to represent the behavior of screws under pretension influence.
- Open: The screws will be untightened.
- Lock: Locks the status of the screws after applying a load or performing a deformation

1.3 Preliminary work

By looking at the available and absent information of our case study, we can create a better working plan for all future tasks: The testing design for the RUP was provided by the manufacturer to the LTR and later to us. This was the preferred option, as the manufacturer was also able to perform validating physical tests based on the regulation R58 revision 2. Since the design is a little bit outdated, it was only intended to withstand forces from the second revision. However, this doesn't alter the nature of the expected FE-software. Measurements of the components were also provided. However the information was incomplete; mainly lacking 2-dimensional technical drawings. Just general measurements (Figure 1.19) could be observed on the technical sheets. Solidworks files for all the respective part were also given by the company. Again, some errors could be observed: wrong used lengths caused collision of parts; drills did not possess correct diameters; cross-section was a bar and not a tube. Furthermore, fasteners such as screws and bolts weren't included, subsequently obliging us to search for possible alternatives. A list of materials was also included in the technical data, present in Figure 1.20, but with lacking information with regard to stress-strain relationships. Finally, no yield strength was present, only ultimate strength.

INFORME DE CÁLCULO (Reglamento 58R02)	
Motivo:	Informe de ensayo de acuerdo con el Reglamentos 58R02 en lo que respecta a un tipo de dispositivo de protección trasera contra el empotramiento.
Nombre y dirección del fabricante:	[REDACTED]
Nombre y marca comercial del dispositivo:	Tecno Trailer
Tipo de dispositivo:	CPH1 Var: 1, 2 y 3
Características del dispositivo (dimensiones y fijaciones) y forma de anclaje:	Dispositivo atornillado al bastidor con 8 tornillos M12 8.8. Travesaño soldado al soporte
Longitud máxima del dispositivo	2350 mm
Distancia entre largueros del bastidor en los puntos de fijación del dispositivo.	Entre 750 y 900 mm
Material	Chapa soporte y Tubo de refuerzo acero S355JR. Tubo paragolpes acero S255JR
Masa máxima del vehículo sobre el que puede montarse el dispositivo:	ILIMITADA
CONCLUSIONES:	
La muestra ensayada CUMPLE con las prescripciones descritas en el anexo 5 del Reglamento 58R02.	

Figure 1.20: Spreadsheet with calculations

For the FE-analysis, no testing time was provided by the manufacturer (applying and removing of load) or additional testing factors. Just some general pictures. The installation torque for the pretension of the bolts is also missing. The union between chassis and RUP has also not been specified, but some research data about this can be found online.

All in all this means additional preliminary work before the programming of the FE-analysis. First the components have to be checked for possible errors in their geometry. Afterwards the assembly of the RUP can proceed. Missing parts, such

as bolts, small parts for the chassis of the vehicle and more, must also be designed. We also searched for technical information and stress-strains relationship for all specified materials. After the assembly, we saved technical drawings of the RUP to check for possible discrepancies. In order to contribute to the provided information, additional researches on the topic or case studies with the usage of FE-programs were studied. With all the corrected information and complementing data we can start with the configuration of the simulative program.

1.4 Important literature used as reference

In order to understand the capabilities of ANSYS, we used the guides as introduction to the simulative program. They set specific procedures for performing analyses and provide a guideline for the elements our project needs.

- ANSYS Mechanical APDL guide and ANSYS WORKBENCH guide: Gives an insight on how to create new models or projects. Their schematic provides steps to a new analysis, such as appliance of loads, fixtures and conditions. The guides give an overview to all accessible projects: linear, static, geometries, mesh but just with general information. [22].
 - ANSYS contact technology guide: The manual introduces the specifications of physics of the problem (friction or unions). Includes specification of region of contacts, type of contacts, behaviors and characteristics. Includes some factors for the aid of convergence. [24].
 - ANSYS Mechanical APDL Command Reference: In general a dictionary with explanations about commands used in the ANSYS coding. Doesn't include procedural guidelines just the functionality of commands and their connections with objects [32].
 - ANSYS Modeling and Meshing Guide: Where we obtained the information about meshing capabilities and commands. Modeling guide was not used [33].
 - ANSYS Mechanical APDL Element Reference: Basically explains the usage of commands and their application fields (for example application and conditions of the command for pretension PRET179). Also provides recommendations regarding geometries or elements for a better analysis [31].
-

The data about the Regulation No. 58 is available for the public at the official journal of the European Union [2].

For the methodology of the test based on the imposed UNECE regulation 58, we based our procedure researches on works by Gogte 2014 [3], Barreira 2015 [7] and Smith 2008 [34]. The papers were chosen based on positive results on ANSYS and used empirical data. Furthermore, their designs proved to be conceptual and efficient.

Homologation data is highly dependent on the chosen country, even though many European countries share some similarities. We obtained ours from the “Manual de reforma de vehiculos” [10] from the “Ministerio de Industria, Comercio y Turismo” (Spain) and the “Straßenverkehrs-Zulassungs-Ordnung (StVZO)” [9] made available by the “Bundesministerium der Justiz und für Verbraucherschutz” (Germany).

For the conditions about pretension of bolts, stress-strain behavior and material information, we selected the papers [28], [27] and [29]. Further used literature will be given credit later-on.

Chapter 2

Nature of the work

2.1 Introduction

This chapter will present the motivation behind the process of developing the simulation software. The main objectives of all participating parties will be presented, which is why a distinction between specific and general objectives has to be made. By doing this, future task planning and control of data can be achieved. The former will be based on the flowchart designed by ANSYS Workbench. However it will also be complemented with the European Regulations. Finally, future plans to develop the program will be presented. This will correlate with the evolution of rear underrun protection devices and the implementations of new strict regulations.

2.2 Aims of the task

A distinction between general and specific objectives was made. General objectives were the development of a simulation software for testing the resistance of new RUP designs. This must be capable of imitating conditions stipulated in the regulation 58 with the lowest time consumption possible. Promising results are expected, as the company wanted to proceed with a homologation procedure for the software. Errors or discrepancies to reality had to be avoided. This means accurate meshing, forces, fixtures, unions, parts and technical information. Further requests included minimal possible calculation time and usage of resources, due to the lower CPU capabilities or available computer. However, they weren't obligatory.

Our specific objectives for the study included the comparison between available

literature on the topic in order to observe the main ways of testing automobile parts. We wanted to observe the calculation capabilities of ANSYS: time, precision and difficulty. With these criteria we can assess if this alternative is viable or if other FE-software's are a better option. Moreover, we wanted to analyze the requirements imposed by the new regulation and see if they were too strict or vice versa. In the end, we just want to offer a new testing and accessible method for examining the capabilities of new vehicle's equipment. All in all, we search for a reduction in fatal injuries caused by crashes between HWV and passenger's vehicles. Due to the flexible nature of the software, it can also be used for other parts or even for different conditions (different international regulations). Passenger's safety will be the main priority.

2.3 Useful effects

This work permits the definition of numerical analysis and contributes to simulation methods using finite elements. It covers some concept of dynamic analysis via ANSYS and also its terminology. It reviews works regarding the safety development of mechanical parts. The performed customization of a project schematic in ANSYS Workbench aids by product development mainly on the selection of materials and the quantity of parts. These were the main reasons of failure and should be emphasized in all tests regarding RUP. The placed conditions in the project resemble reality as good as possible, showing promising results. Computational analysis avoids the usage of constant physical proofing as chosen testing methods, thus effectively reducing economical and resource losses.

2.4 Work in the future

Future work includes the analysis of the RUP using explicit time integration. To achieve this, the software must be changed to LS-DYNA, which is more straightforward and the applied forces less time dependent (no ramping of the load). Most works in the field have used LS-DYNA as the preferred simulation software with successful results.

Further RUP with more ergonomic designs must also be tested. The goal is always for less heavy vehicles to be in circulation to avoid fuel consumption and en-

vironmental impact. Different materials, such as alloys, plastics and fiber-reinforced composites should also be considered as alternatives and subsequently tested, with regards to their resistance capabilities. More testing conditions should also be implemented: increase in loads in order to suffice the new regulation's revision 3, additional fixtures and so on. Ways expanding of the software should also be studied in the future and its future implementation in the market will be led by the LTR.

Chapter 3

Analysis of literature

3.1 Introduction

After understanding the capabilities and characteristics of both RUP and Finite-Elements simulation, we still have to emphasize the importance of the obligatory use of rear underrun protection devices. Why is that these safety devices are so important? And why are their requirements constantly changing and becoming stricter? This chapter will provide answers to both of these questions. In the chapter 3.1 we will analyze traffic data that provide an insight on the accident rates and their characteristics. Works and procedures for testing RUP will be presented in chapter 3.2. These will observe the methodologies of testing and level of development of new RUPs' designs, highlighting the actual state of the technology.

3.2 Analysis of accidents' rates

Results at Eurostats, the biggest source for European statistics [35], show a decreasing number of fatalities caused by road accidents over the last 20 years. A number of 23.800 persons were killed in the year 2018 due to road accidents. This number decreases each year, however by a tiny margin only. Around 0.2% from 2017 to 2018, which can be observed in Figure 3.1. The changes hasn't been drastic since the year 2013, however constant efforts are trying to be made in order to halve the number of fatalities. Further statistics [35] show that around 44.8% from all accidents were caused by passenger cars or light weight vehicles, while the other majority, a 20.7%, of fatalities were from pedestrians. Heavy and light goods vehicles account for a 5.4% of all road accidents in the European Union. A graph

in Figure 3.2 presents all important data. The number regarding HWV accidents appears low (only 1 260 fatalities in the year 2018), however while other categories of vehicles show a decreasing trend in number of casualties, the pattern for trucks and HGV remains unchanged or increases within each year (Figure 3.3). This may be explained by the augmenting number of trucks on road each year: Germany observed an increment of 300,000 large good vehicles in a span of 5 years [36]. That is why actions to ensure the safety of the passengers have to be undertaken. 2017 was the year were the modifications to the regulation 58 for RUP were applied. When examining the benefits of the improved evolution and usage of RUPs, the reduction of fatal injuries between years have to be observed. The requirements have become stricter but haven't showed any significant improvements to fatalities reductions. In order to observe a more noticeable trend, we may have to wait some additional years.

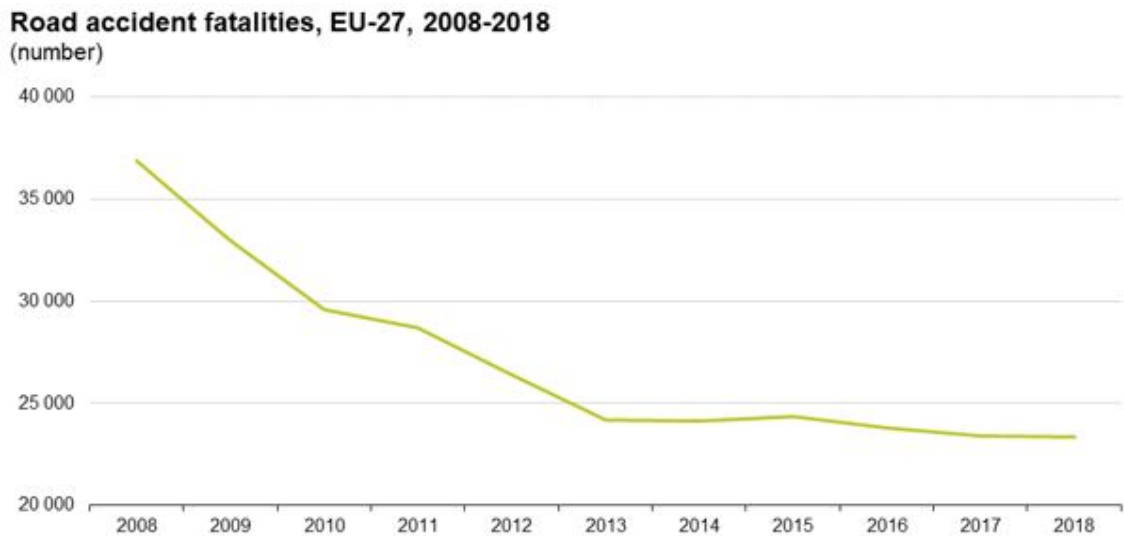


Figure 3.1: Number of road accident fatalities [35]

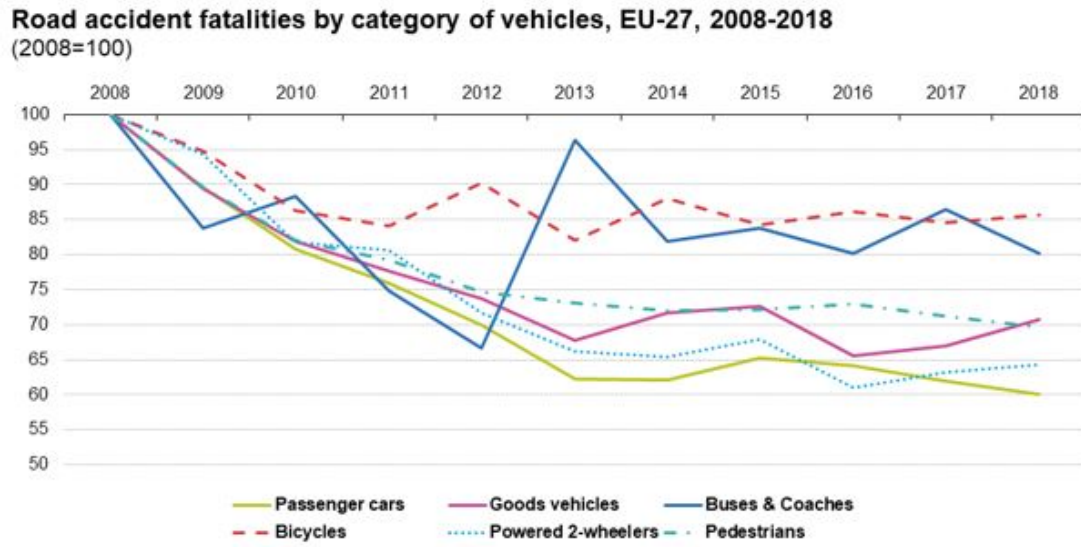


Figure 3.2: Road accident fatalities separated by categories [35]

Road accident fatalities by category of vehicles, EU-27, 2018

(%)

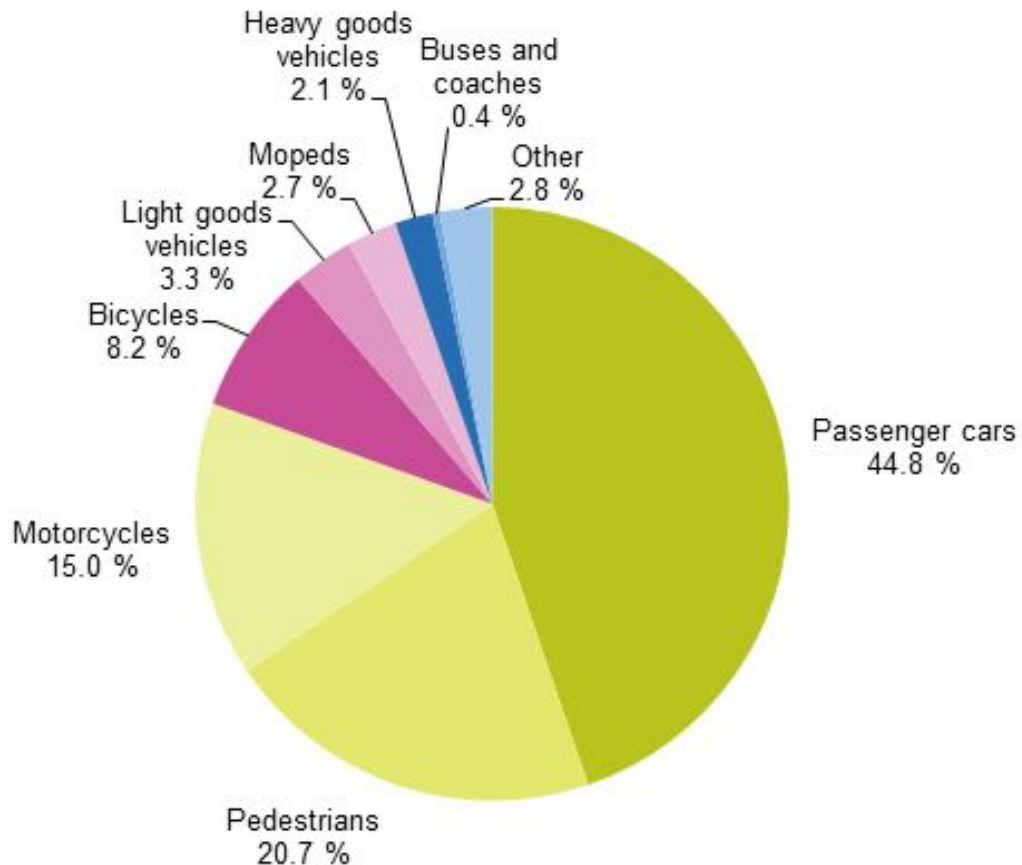


Figure 3.3: Number of road accident fatalities separated by categories 2008-2018 [35]

In order to understand the importance of RUP, a further dissection of accidents with trucks involvement will be presented. Hamacher presents and analyses all possible scenarios of crashes involving trucks. In his work "Unfallgeschehen mit Lkw-Beteiligung unter Berücksichtigung von Leicht-Lkw-Kombinationen" [37] the author provides different accidental statistics for a variety of trucks, divided by their total mass. The collected data were taken from surveys between the years 2010 to 2014 in Germany. His research show that accidents involving HWV, mainly from the class N2 (where the weight can be from 3,5t to 12t), are non-fatal in 72%. However if the vehicle surpasses a maximum mass of 12t this number decreases to 42%, highlighting that the weight of the vehicle influences possible fatalities after a

crash. It is also important to highlight the type of accidents and their probability of occurrence. The results show that crashes between passenger vehicles and a leading truck and also crashes against crossing trucks are more prone to happen, with 27.4% and 17.1% respectively. After that the vehicles tend to collide with the sides of a heavy vehicle (14.3%) or against a forthcoming truck (11.8%) due to lack of visibility of the driver. This results emphasize the importance of RUP, given the fact that most accidents involving trucks are caused by a collision in their most rear part or the back of the vehicle, when taking into account crashes with a leading truck and against crossing trucks. Figure 3.4 shows an overview of all types of accidents involving a truck. The bar chart on the left represents accidents involving a vehicles of the category N2, while the one from the right for vehicles of the category N3. From top to bottom the accidents include: against a stationary vehicle, a crossing vehicle, a forthcoming vehicle in the contrary direction, a leading vehicle in the same direction, against the side of the vehicle, involving a pedestrian, involving an obstacle.

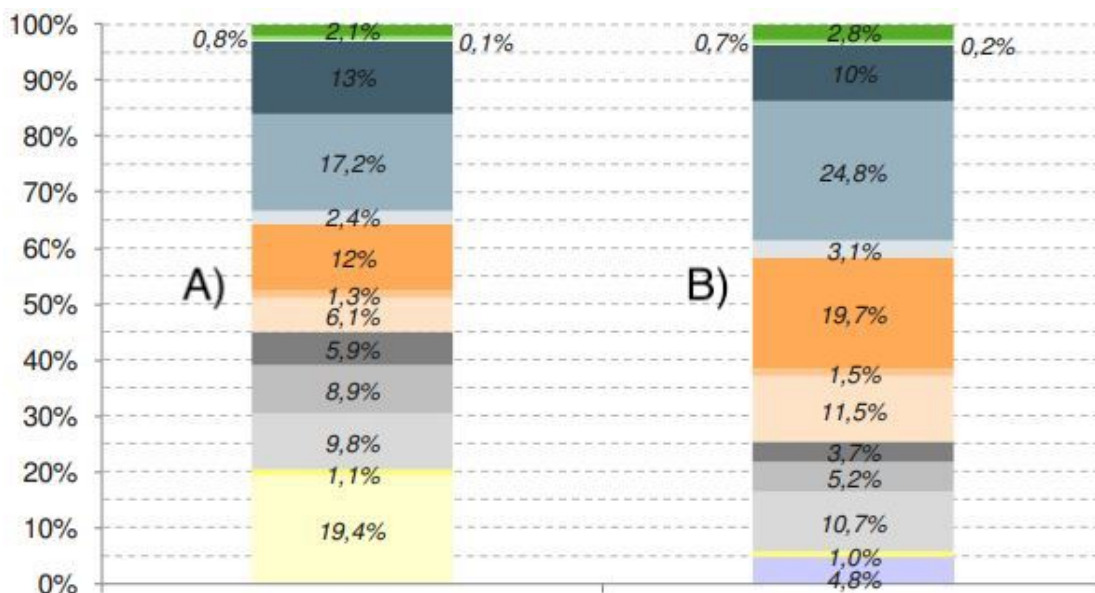


Figure 3.4: Comparison between types of accidents involving a heavy weight vehicle. a) Accidents from N2 category vehicles b) Accidents from N3 category vehicles [37]

It is also shown that more than 50% of all accidents involving a heavy weight vehicle also involve a smaller passenger car. This explains the obligatory use of a

RUP device, in order to avoid fatalities caused by a trapped vehicle.

Reasons for possible accidents include in order of importance: velocity, lack of distance, driving next to the HGV, error in maneuvering, wrong usage of street and overtaking of other vehicle [37]. The reasons may vary, but the safety of the passengers must be guaranteed.

3.3 Analysis of papers from the technical field

Simulation of crash tests for RUP is a constant evolving topic. The evolution of traffic is a very adaptable topic that evolves in dependence of the necessity of people for the transport of passengers or goods. More alternatives regarding the safety of the users, the protection of the environment and the ergonomic of the vehicles are put in the center of importance. Lighter and safer vehicles are more and more desired, which puts an emphasis on the design of RUP. In this section we will observe the historical evolution of RUP and more contemporary works in regard to the testing of these protective devices.

When examining the actual paperwork in regards to the control of RUP, most papers highlight the comparisons between the requirements between countries: mainly India, the United States, Canada and the European Union as a whole. However most papers use old versions of the regulation UNECE R58, where the loads had a lower value. Since the regulation ECE R 58 was developed by a body of the United Nations, almost other countries pertaining to this group (such as Brazil and Japan) follow the same requirements or at least use the European one as reference (India and Australia). So the testing procedures tend to be similar between countries.

Abid et al. [38] highlight the lack of the necessity of European regulations to distribute the loads when performing the rear impact test. The paper also makes distinction of factors contributing to fatalities. The results show that “stiff floor” was the main reason for most fatal injuries. Other reasons also include the crashing position: when the smaller vehicle impact the RUPD not central but offset, the bending of the device was a lot higher than expected, which leads to possible fatalities. The edge of the cross-member could potentially become sharp and serve as a cutting device. This is the main reason why there exists a minimum lateral

distance between the vehicle and the RUP. The constant shift of impact velocity is also debated topic: it is assumed an approximate velocity of 50 km/h for most impacts [38]. However numerous studies suggest that vehicles tend to collide at higher velocities [34] [1], making the requirements partially obsolete. Further physical studies are performed with changing conditions like the weight of the vehicles or the impact velocity. In Figure 3.5 we can observe an experiment with the same RUP and test vehicle, however with varying impact velocities. The first image shows the aftermaths of the vehicle with a driving speed of 48 km/h. In the second image the vehicle had a velocity of 56 km/h, only 8 km/h more. The RUP wasn't able to avoid sliding of the vehicle for the second case and thus the latter suffered from more damages. All of these explained changes may affect the veracity of existing FE-programs that check the resistance of the RUPD.



Figure 3.5: Crash tests for the same vehicle with varying collision speeds: a) 48 km/h b) 56 km/h [38]

In their work “Design and Development of Truck Rear Underrun Protection Device” S. Pooudom et al. [6] focus on different design variation of a RUP and its resistance. Their proposed changes try to investigate the effectiveness of the safety device depending on the angle of installation of the supports and the distance be-

tween supports. These have the task to rigidly connect to the cross bar. Their results reveal that the lower the support angle to the truck chassis, the better are the resistance capabilities of the RUP. A wider separation between supports also lowers resulting moments, which make this option the more useful one. In Figure 3.6 we can observe the results of the simulation for different support angles. Effects of underrunning were avoided in the second vehicle, thanks to a lower support angle. The research was done via LS-DYNA by simulating up to six possible crashes with different percentages of overlapping between the cross bar and the forepart of the smaller vehicle. For this scenario a Toyota Yaris 2010 was used as a test subject.

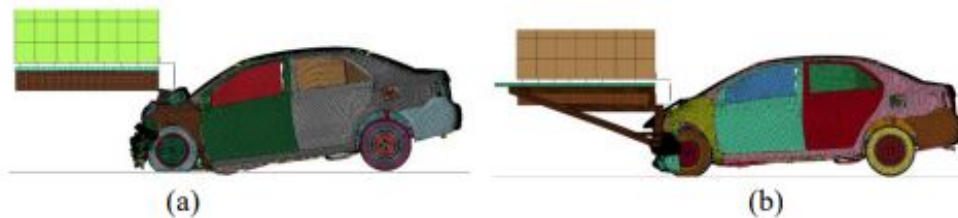


Figure 3.6: Results of full width tests for a standard RUP and for the new proposed design. a) Lower angle for the RUP b) Higher angle for the RUP [6]

In the paper presented by V.S. Gogate et al. [39] a new load case to simulate typical crashes is also developed. Here accident data for the country of India is also presented, which reveals that 16% of all the crashes in the year 2012 were underrun in nature. In half of them the crash happened at full-width underrun and the other one at the offset underrun. Furthermore a combination of both LS-DYNA and MADYMO was used in order to simulate crashing events and possible injuries respectively. All results were validated with a physical test. Their proposed design, present in Figure 3.7, utilizes an additional gusset member to strengthen the RUP and support the cross-member. Other alternatives including augmenting the strength of the device was not beneficial economically and ergonomically. The study shows promising results as a possible design alternative, also applicable to European regulations.

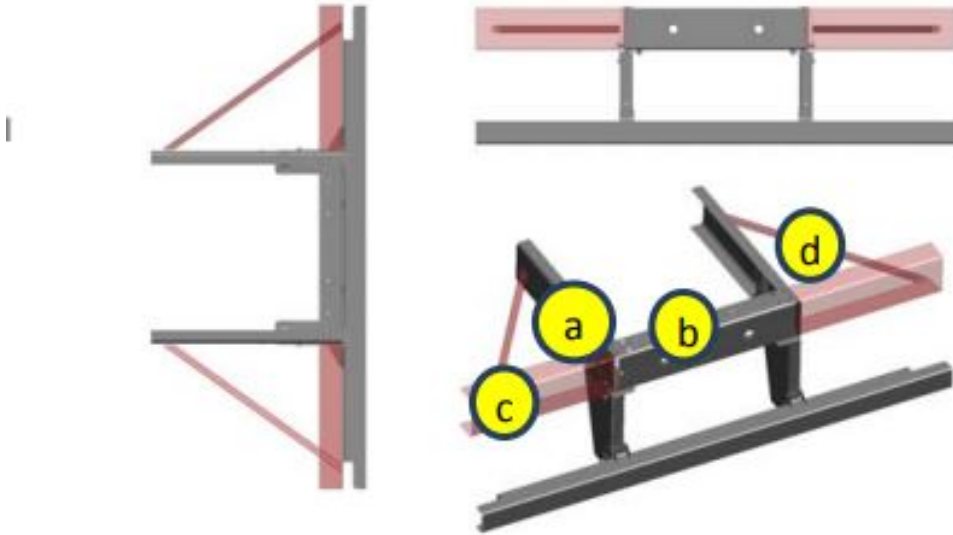


Figure 3.7: Proposed design with an additional gusset member (d) [39]

Another simulation work titled "Optimization Development of Vehicle Rear Under-Run Protection Devices in Heavy Vehicle (RUPD) for Regulative Load Cases" includes the usage of ANSYS and an implicit calculation. P. Sen et al. [40] conducted a design optimization to improve the safety system of RUP by experimenting with a range of materials. When aluminum foam material was employed, good stresses and deformation values were obtained. The dissipation of the energy was successful and not only this; the weight of the vehicle was reduced, improving fuel consumption [40]. A lightweight structure offers also high strengths and resistance against deformation. Gombi et. al [41] also tested a device manufactured with carbon fiber reinforced plastic material. With this material the safety device was able to dissipate 50% of the applied force, in comparison to a steel structure that absorbed up to 90% of the energy. However the plastic device weighted 50 kg less than the steel one.

When observing tests that specifically utilize the European regulation, Jaju and Pandare [42] analyzed a very simple design (observed in Figure 3.8) that showed great results. The focus was on plastic strain and von-Mises stresses. The device was able to withstand the forces from the second revision, however if it wasn't able, additional material implementation was also recommended to achieve the targeted load. In addition in his work "Dispositivos de Protección Trasera. Aportaciones al Reglamento CEPE/ONU 58" Barreira [7] focused on contributions to the regulation

CEPE 58. Here he develops a new physical testing machine to verify the results of his own simulations, where he also employs ANSYS. In his investigation he was able to adapt a mono-cylindrical machine into a new homologated one for testing designs of RUP. He concludes that multi-points testing could potentially be more accurate and can translate to better results. Additionally for symmetrical RUP only 2 forces may be needed in order to check the resistance of the device. His intention was to check the effectiveness of actual requirements for RUP or if these must be modified. Figure 3.9 shows the methodology used his simulations, where he employs transient finite elements in specific multi-points.

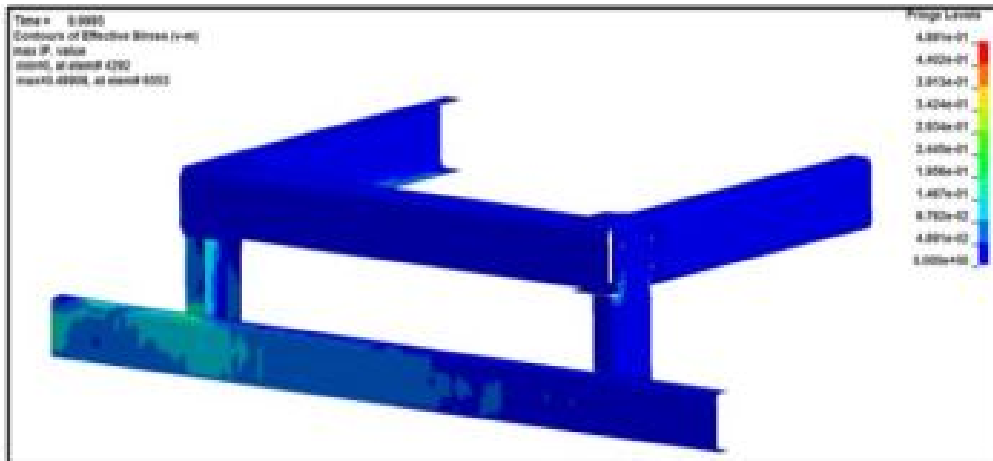


Figure 3.8: Von-Mises stress distribution for a simple RUP [42]

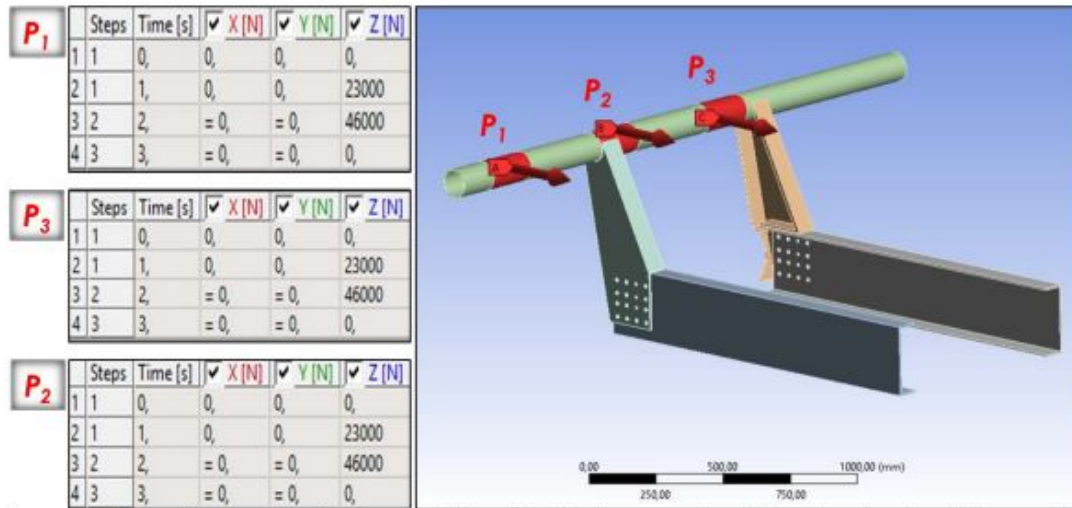


Figure 3.9: Stress application points and load application table on the rear protection device for a multi-point test assuming regulation 58 [7]

Joseph et al. propose a quasi-static test to verify the load bearing capabilities of a proposed RUP design. The analysis was performed with LS-Dyna, as a “dynamic code is able to produce a static result” [43]. All pre-loads of the bolts were also taken into consideration, as this was used to clamp the device to the chassis of the vehicle. The loading device was also constructed, in order to represent the loading conditions in a more precise way. Various design were also modelled: a support bracket was switch in order to check the resistance of the RUPD. The first calculations show that the device was not able to dissipate the forces, as high strains could be observed at the bolts (see Figure 3.10). The authors decided to change the thickness and materials so that the forces could be better withstand. Still with all the modifications the load bearing capacity surpassed the allowed amount specified in the regulation UNECE R58. After further modifications more problems such as buckling were observed, showing that changes are not always positive in regards to the results of the analysis. In the end nearly six designs were observed until the desired effectiveness was achieved, but also respecting constraints and design space. In the end the authors concluded that a good design is “highly dependent of strength factor and energy absorption” [43]. As the screws suffered from the peaks of the von Misses stress, a high quality bolt grade is recommended. Their final work includes recommendations such as: ”augmenting the number of possible bolts, testing for

further dynamic conditions and changes in the design to reduce the weight” [43].

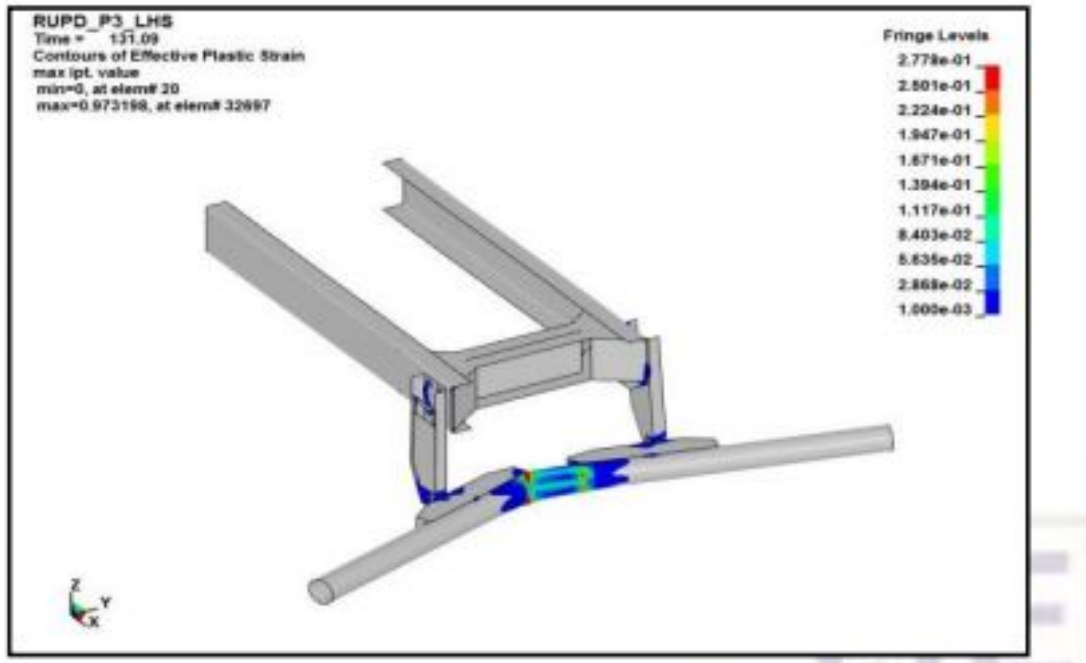


Figure 3.10: Results of the LS-DYNA simulation [43]

Important advances and evolution of the requirements of the RUP have been published by the VC-Compact and the TLR Limited [34], in cooperation with the European Commission. Their focus lays on the improvement of the protection capabilities of the rear underrun protection devices, by reviewing present requirements in regards to:

- Test loads: based on their magnitude direction and application area; rate of application.
- Ground clearance.
- Energy absorption capabilities

Their obtained results based on testing and historical data showed improvements in the following areas:

- Decrease the maximum permitted ground clearance to 400 mm
- Increase the minimum permitted height of the cross-member to 200 mm

- Increase the point loads
 - To 100 kN in point 1: extremes of the cross-member (300 mm apart from outer face)
 - To 180 kN in point 2: 700 to 1000 mm apart, equidistant to centerline
 - To 150 kN in point 3: vehicle longitudinal centerline [34]

A finite model was tested with the aid of the program LS-Dyna and the created design was able to withstand the newly proposed loads, with little displacement. The mechanical strengths were achieved, thus serving as a validation to the newly proposed improvements. A physical test was also directed in order to check the finite element model. The physical results showed even less deformations (see Figure 3.11). A dummy was also placed in order to check the security of the passengers, which suffered little to moderate damages after the impact [34]. If this design showed little deformation, then it is also possible to construct new RUP under this requirements.

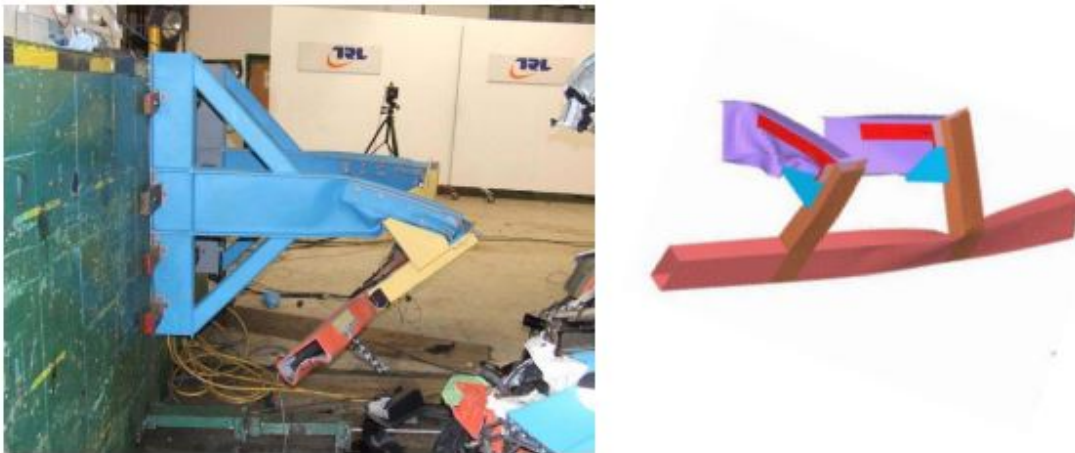


Figure 3.11: Comparison of deformation for the virtual and physical test with the proposed new requirements [34]

The work also makes distinction between quasi-static and dynamics way of testing. It is important to define that sequential vs simultaneous loading was also considered as testing options. The idea behind is to observe which one can be more effective, being that a crash situation has to be simulated. Firstly a distributed load of 270 kN was applied to a model at three different points (P1, P2 and P3 as explained before). So three loads of 90 kN were applied simultaneously at P1,

P2 and P3, revealing conditions similar to a crashing set-up and also to results to the sequential loading condition. In Figure 3.12 we can observe a representation of the the proposed testing method for better understanding. This test proves that sequential loading is not so necessary when performing resistance tests of RUP. The new proposed methods could replace the existing ones in the near future [34], as explained by the authors.

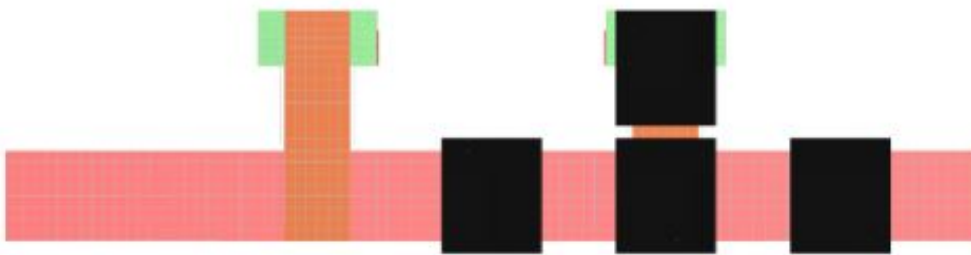


Figure 3.12: Proposed test method with simultaneous loading at three zones represented with black squares [34]

When observing the evolution of the rear underrun protection device, potential operational issues may arise. Changes on the design, such as required height or clearance from the floor, have to also account not only for avoiding under-running, but also for smooth operations. This may be the loading or unloading of trucks from ferries for example. If the design of the RUP is not optimal, damages to the ferry can be made, due to small spaces of bad manoeuvres. The imposed ground clearance from the UNECE R-58 may not be enough to avoid these issues. VC-Compact and LTR [34] believe in a minimum angle from the wheel of the truck up to the lowest part of the device from around 8 degrees in order to avoid these issues (Figure 3.13). This problem [34] could also arise in case of bad terrain or also for construction vehicles.

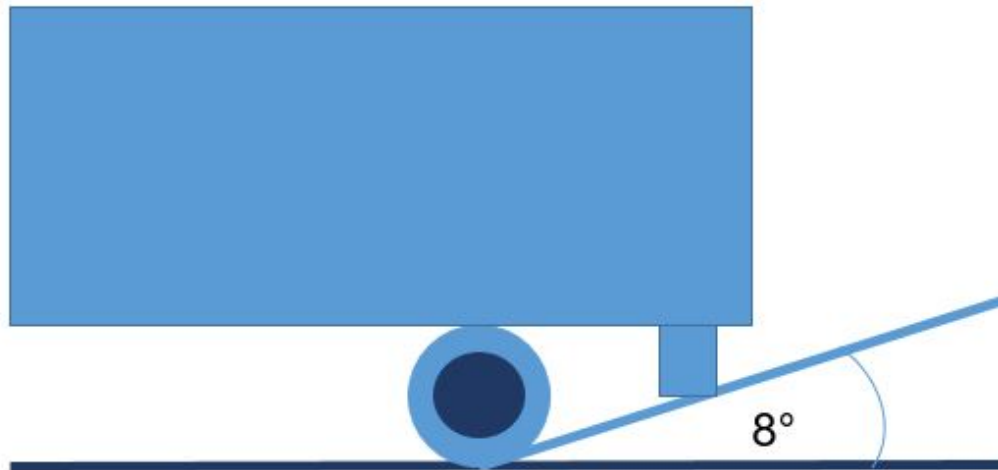


Figure 3.13: Minimum required angle for trucks in specific operations

Results on the cost and benefits of modified RUP lay between a ratio of 0.2 and 15.4, based on the reduced numbers of accidents and the increase prices. Researches show that the added prices of all aspects of the RUP (material, design, construction and installation) have increased within the years due to the increase on mass and the selection of special materials (see [42], [34] and [1]). In the actuality a good device may range from €300 and up to €4200, but their protecting capabilities still have to show significant results. This may be due to the increase number of vehicles in circulation.

3.4 Conclusions

As explained the road security is one of the main concerns for every nation, due to the avoidance of risks of people. A high number of designs of RUP are launched each year as means of passive protection and thus have to be regulated carefully. That is why more numerical techniques are being used within the past year to regulate the respective devices. These have to fulfil all their resisting requirements so that they can absorb most of the energy caused by an unexpected crash. Their use is obligatory as stated by European law, but each country proposes classifications of vehicles that require them. In Germany for example, the StVZO or Straßenverkehrs-Zulassungs-Ordnung determines that “motor vehicles, trailers and vehicles with interchangeable

load carriers with a maximum design speed exceeding 25 km/h, where the distance from the rear limit to the last rear axle exceeds 1000 mm” [9] are obliged to be equipped with a rear underrun protection. Furthermore the chassis of the vehicle or the main parts of the body nearest to the ground, have to exceed a height of more than 550 mm above the road surface. Studies proposed by the ADAC or Allgemeine Deutsche Automobil-Club or Europe’s largest motoring association [1] at the end of the year 2012 reveal that if a small vehicle travelling at a speed of 56 km/h crashes with the rear part of a truck, the RUP according to ECE-R-58 Revision 2 are not able to avoid the smaller vehicle to be trapped underneath the other one. The study presented in this section by the TLR company and VC compact [34] back up these claims, by showing that the velocity in which cars collide against a truck, tends to be in more than 50% of the cases superior than 55 km/h. This is was ultimately prompted the changes between revision 2 and 3: the simulated forces were not similar to the actual forces during crashes. Since the changes are pretty actual, there exists a lack of paperwork that use the revision 3. The developed software part of this master thesis can help as a starting point with new simulations for higher loads.

Studies regarding explicit crash simulations show some trends: sources showed a high pattern on full-scale impact simulations, however offset crashes, where the edges of the rear underrun protection device are impacted, were less studied. Moreover the speed that is usually tested, ranges from 40 km/h to 65 km/h [39] [6] [38]. Higher speeds are less tested, meaning there is a lack of impact tests for this range. Furthermore the tests were limited to compact passenger’s cars of the M1 class, such as Toyota Yaris from 2010 or Chevrolet Malibu [5]. More case studies have to be performed in order to observe a higher variety of vehicles such as sport utility vehicles (SUV), light trucks or multi purpose vehicles (MVPs). Many authors also propose a minimum requirement for energy absorption (see [5] and [6]), which is not specified in the European regulation. Bolted elements are also being more observed, as they tend to suffer the highest stresses during tests. More and more designs are launched to the market with higher focus on the material selection. Cheaper and lighter materials are being additionally tested, as ways for reducing costs and fuel consumption. The presented designs in the papers tend to however still be simple, so that manufacturing costs are maintained as low as possible.

Chapter 4

Methods

4.1 Introduction

The expectations regarding durability and safety of rear underrun protections increases in importance within the years, due to the number of vehicle in use also incrementing as a result of urbanization and economic. The requirements and procedures tests presented in last chapters serve as guidelines to the realization of the simulation program, which is entrusted with the task to proof the durability of rear underrun devices. The work procedure will be organized as followed.

First a design of a new rear underrun protection device must be completed. The geometry requirements must be followed and taken into consideration, when doing the sketches and assigning lengths.

Afterwards the new proposed RUP will be constructed using the computer-aided modelling program Solidworks. This modelling program was selected in favor of the ones installed in ANSYS Workbench, due to its intuitiveness and easier interface. The time for modelling will be cut significantly.

The modelled pieces will then be switched to a format readable by ANSYS and it will be exported to Workbench. There further conditions need to be specified with the following methodology;

- I Materials: elasticity module, tensile strength, yield strength, stress-strain curves etc.
- II Meshing of parts: determination of meshing size based on accuracy, speed of simulation and force peaks.

- III Specification of contacts between parts

- IV Determination of constraints: avoid displacements of parts in the needed directions.

- V Applying of forces: sequential forces based on CEPE 58 revision 2. Pretension of screws will also applied.

- VI Time Steps: input of initial, ending, step-time and also quantity of steps.

- VII Analysis of results: forces by von-Mises, shearing, torsion and displacement.

- VIII Post-process: Graphs with results. Procedures of physical tests in order to validate the computational results. Additional tests with LS-Dyna.

4.2 Modelling of parts

As explained in Chapter 1 a RUPD consists of a cross member with a minimum of one connecting element to the frame or other vehicle structures. Our proposed design possesses a tubular cross member with 100 mm diameter. The whole length of the beam is welded to a L profile reinforcement that increases the resistance of the cross-beam and avoids its deformation. This L profile is also welded to a metal element: connected component or a metal support one shown in Figure 4.1, which it's also fixed to another support piece by means of eight hex screw grade ISO 4018 with 12 mm diameter (Figure 4.2), fixed with a hex nut style ISO 8673 M12x1.5 (Figure 4.3). The height for the cross beam member can be adjusted by folding both metal supports and adjusting them with the respective screws. The support number two is connected to the frame of the vehicle with a bolt and reinforced with a thin metal piece observed in Figure 4.4. This foldable connection between the RUP and the vehicle frame allows for more flexibility in the assembly of the parts.

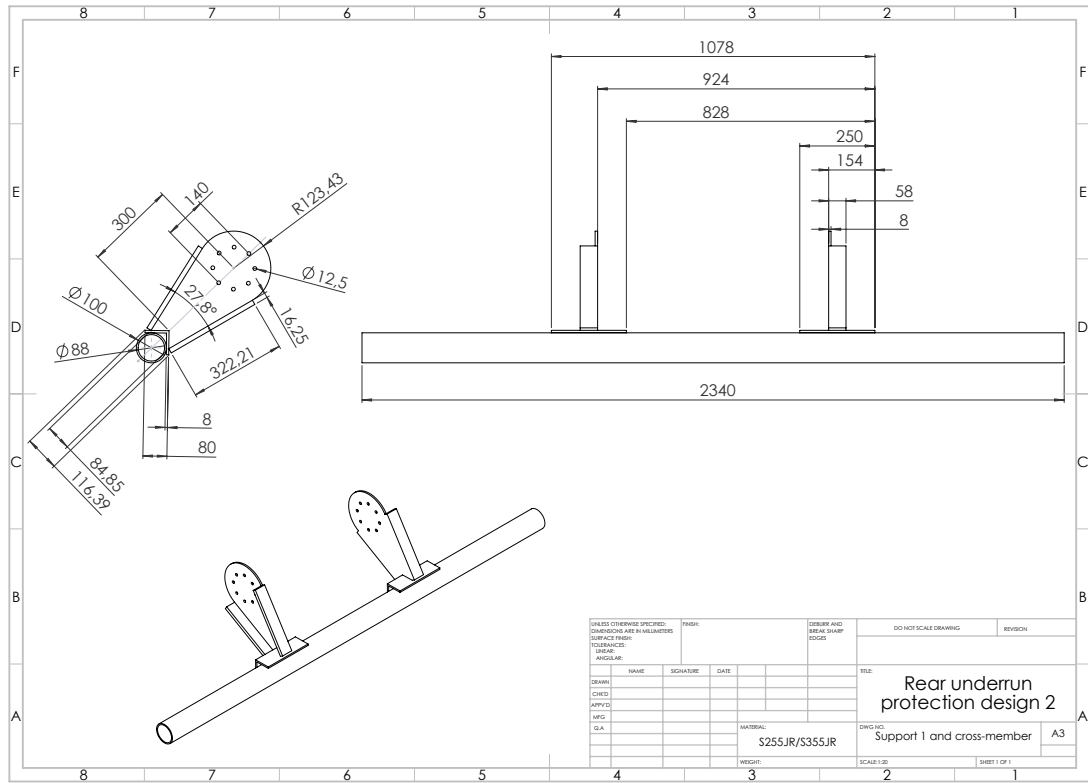


Figure 4.1: Technical drawing of the support 1 and the cross-member, with their respective dimensions

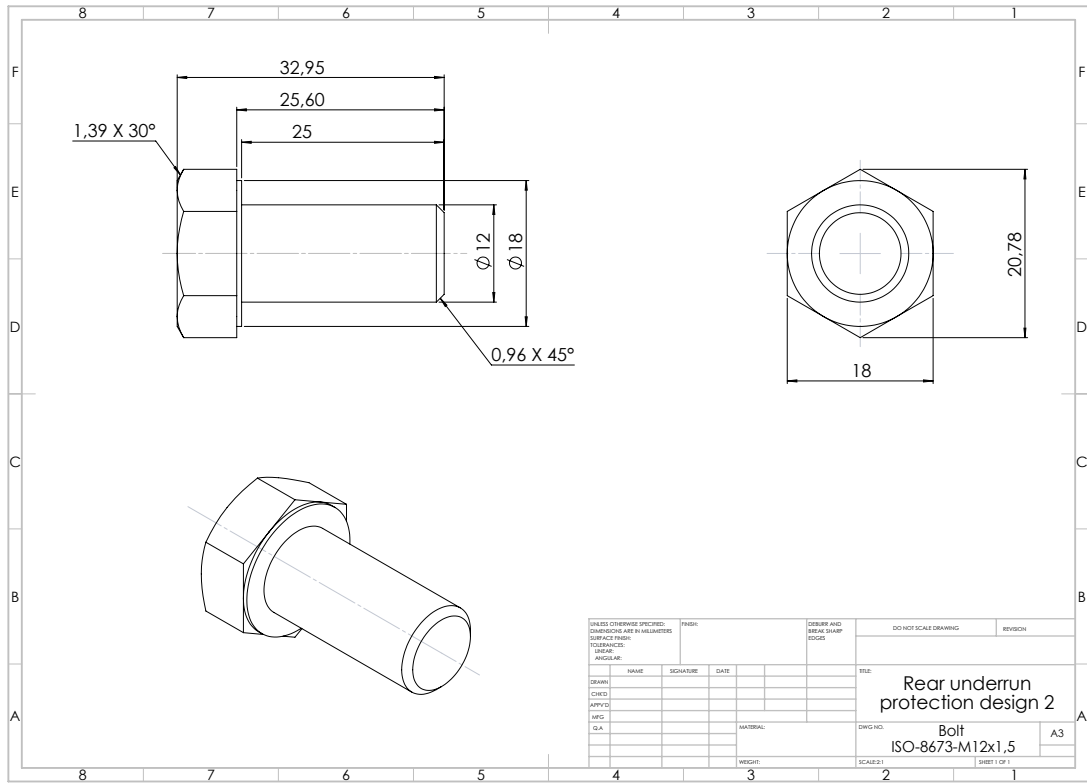


Figure 4.2: Dimensions of the bolt ISO-8673-M12

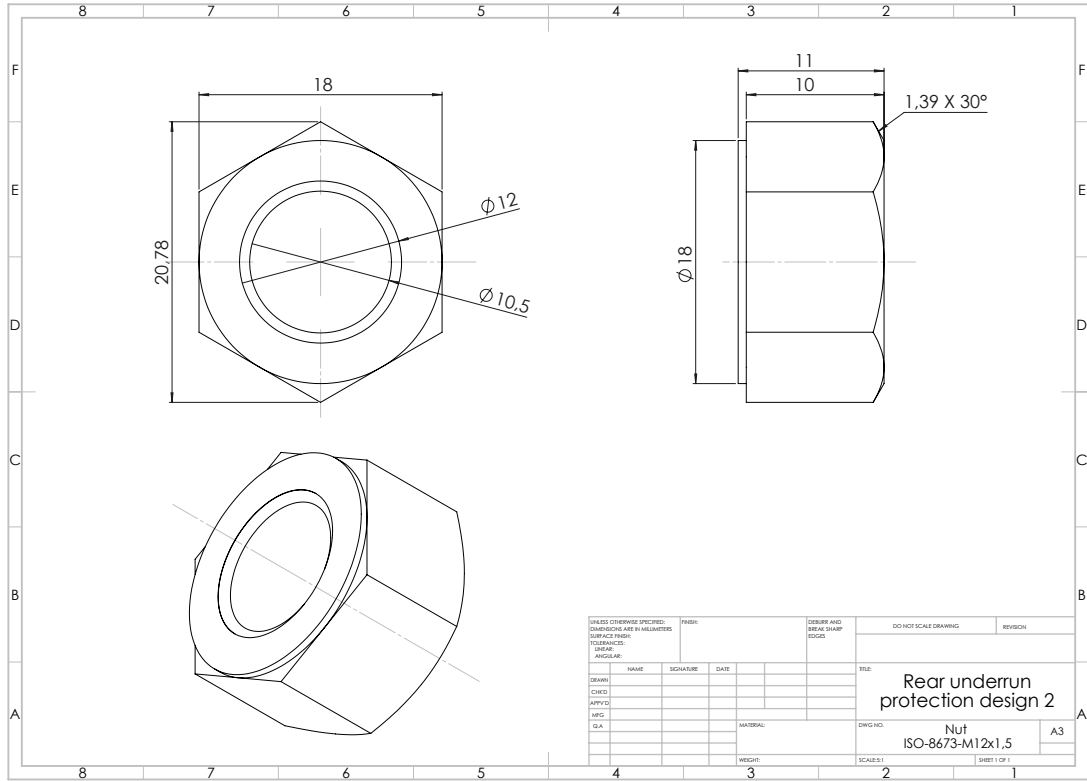


Figure 4.3: Dimensions of the nut ISO-8673-M12

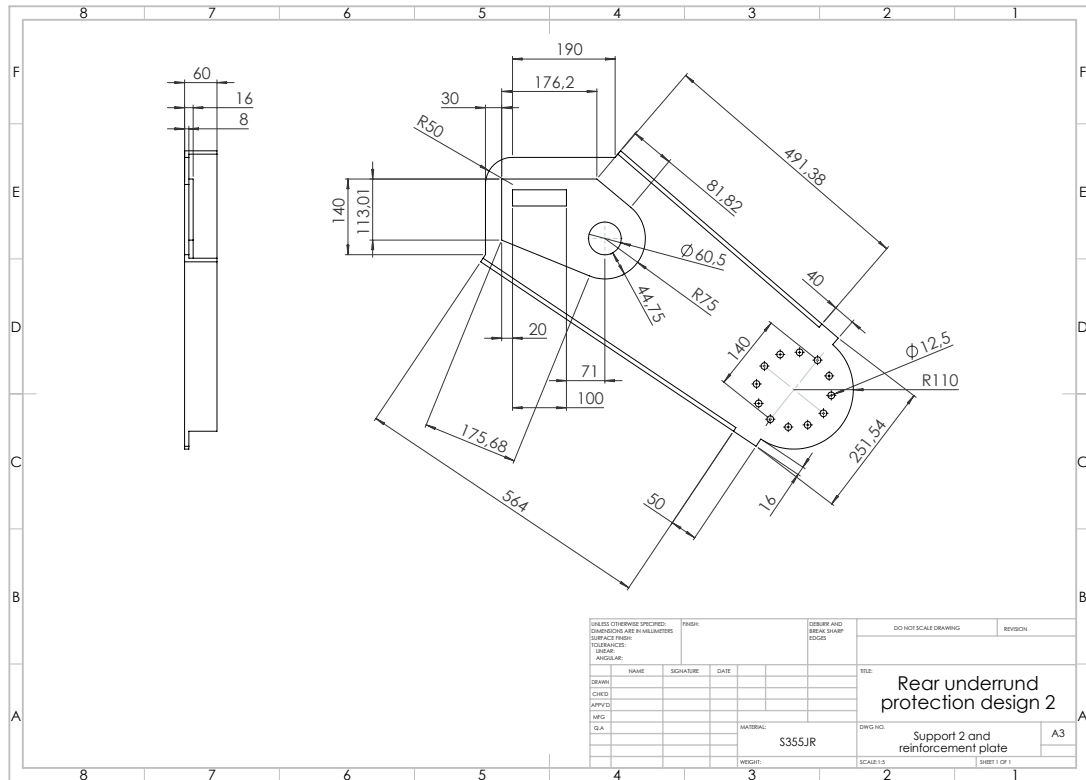


Figure 4.4: Technical drawing of the support 2 and the reinforcement plate, with their respective dimensions

The frame of the vehicle was also represented with two welded U-profile metal rods. Their respective upper and lower surfaces were connected by means of welding and were furthermore attached to a steel plate with 2 orifices, which fixes the bolt to both the frame and the rear underrun protection. In its core the design stays simple but also ensures good safety of the device and also foldable characteristics, which adapt to the type and height of the vehicle. Material bulk is avoided by using a hollow pipe and maintaining the thickness of the parts as low as possible. The fabrication of the supports is characterized by its simple procedures: welding, bending and drilling, which ensure low manufacturing costs. All respective dimensions of the parts and the representation of the vehicle's frame will be presented in the Figure 4.5. For the procedures of the test the support 1 and 2 will form a perfect 180 angle. The model is then saved as an IGES program, compatible with Workbench. It is then exported to ANSYS by simply dropping the file in the geometry box (see Annex A). The RUP can then be modify with two accessible ANSYS programs: De-

signModeler or SpaceClaim. In the following Figure 4.6 we can observe the interface for SpaceClaim specifically.

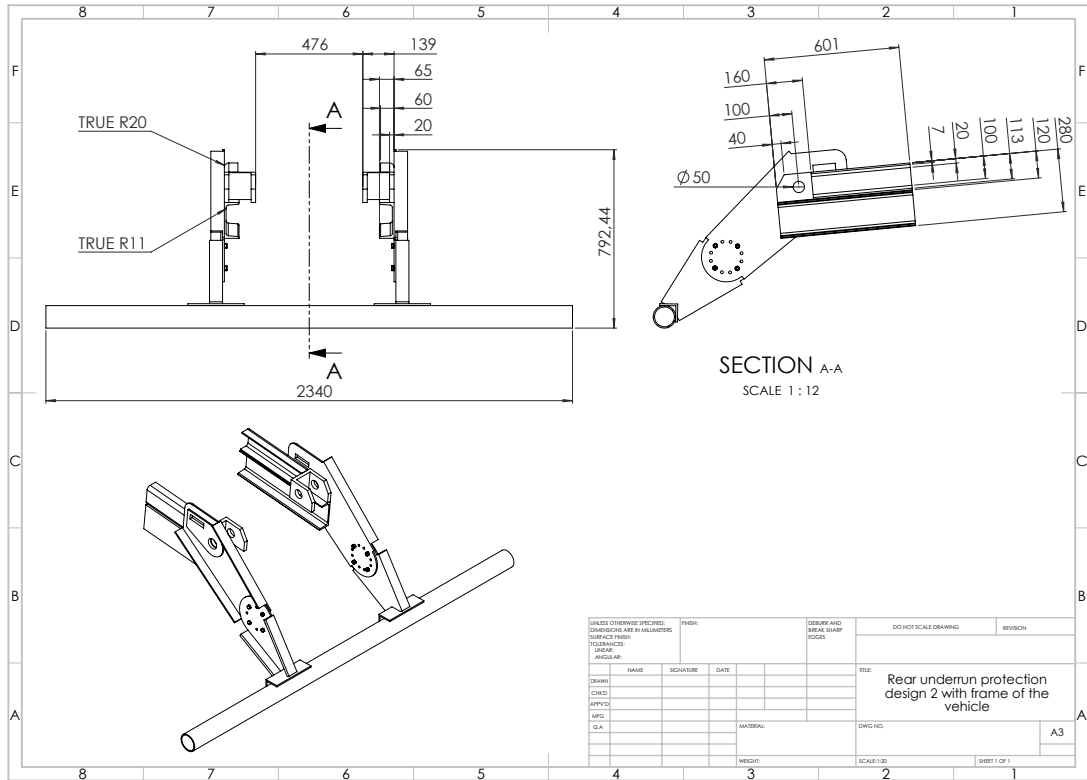


Figure 4.5: Technical drawing for the complete rear underrun protection installed at the frame of the vehicle

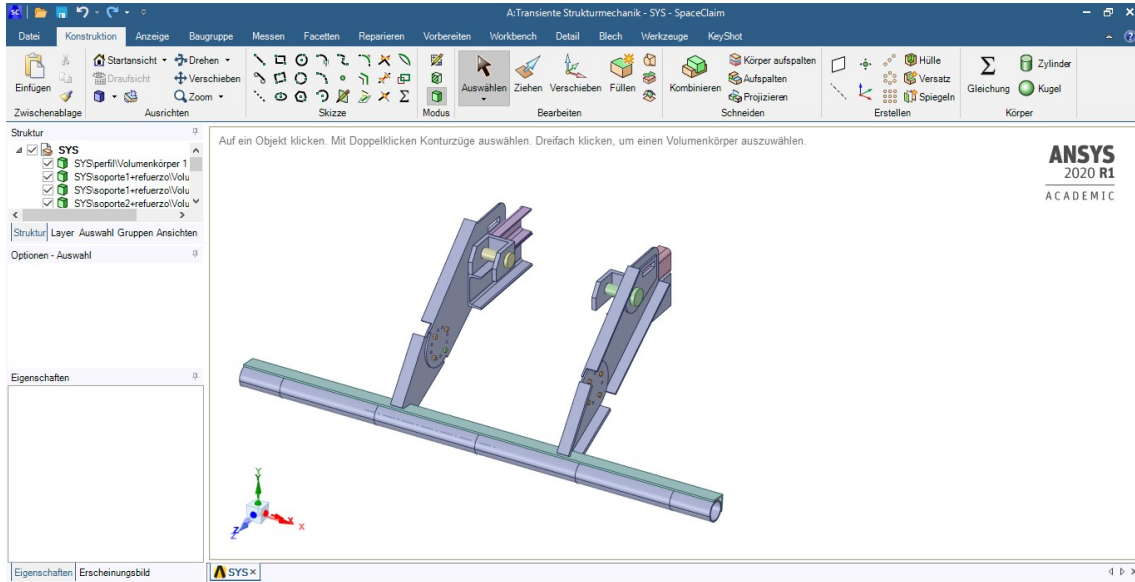


Figure 4.6: Interface and commands of SpaceClaim with our proposed design

The exportation of the file comes with some formatting mistakes: the cross member beam splits and some contacts cannot be exported to the IGES file. Furthermore exported pieces from the parts' bank such as the screw ISO 4018xM12 and the hex nut style ISO 8673xM12 were also modified into an easier design. The thread was eliminated from the screw and just a general grip length was represented in the nominal length, ignoring components such as the pitch, the flank and the crest. The head lacks any clefts and just a simple hexagon was used as default base shape. These changes were also applied to the nut. These all were corrected with simple resolving commands (observed in Figure 4.7) from SpaceClaim. From the list of commands the most used one are the “union of area” and “holes/open edges”, which automatically detect problems in the model and repairs them with ease. The resulting design of the bolt and the nut are presented in Figure 4.8.



Figure 4.7: Reparation commands in SpaceClaim. Translation from German: union of faces, gaps, additional edges, missing faces and so on

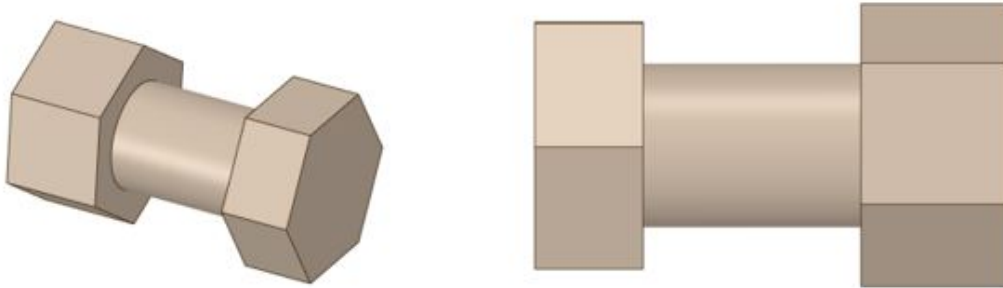


Figure 4.8: Proposed simplified design for the screw and the nut

Due to the difficulty of the use of the ANSYS program, a decision was made to just model with a simpler program such as SolidWorks. The design of the parts results easier, while deciding the contact conditions of the parts tends to be more automatic: all perforations can be aligned with more ease and defining the precision of places for the parts results in less errors. The parts can be assigned as parallel or a special distance can be inputted so that the alignments can be corrected with ease; a feature which SpaceClaim lacks. There all the faces have to be constructed and modelled in their intended positions, so adjustments tend to result in complete elimination of the created features or large unintended modifications.

4.3 Material selection

In general, metal parts of vehicles tend to be manufactured with steel alloys ranging from S250 up to S355. For our stress simulation the forces have to be applied to the cross member area and thus this has to bend in order dissipate the mechanical stress caused by the transmitted forces. For this purpose a more flexible metal has to be assigned to this part, which is why the beam was assigned with the steel S255JR with more flexible properties and a lower tensile stress. The physical properties of this material ensure a controlled bending and a lower probability of a fracture of the metal.

Further parts were assigned with the material S355JR of structural steel. The high tensile strength assures the resistance of the parts and avoids acceptable de-

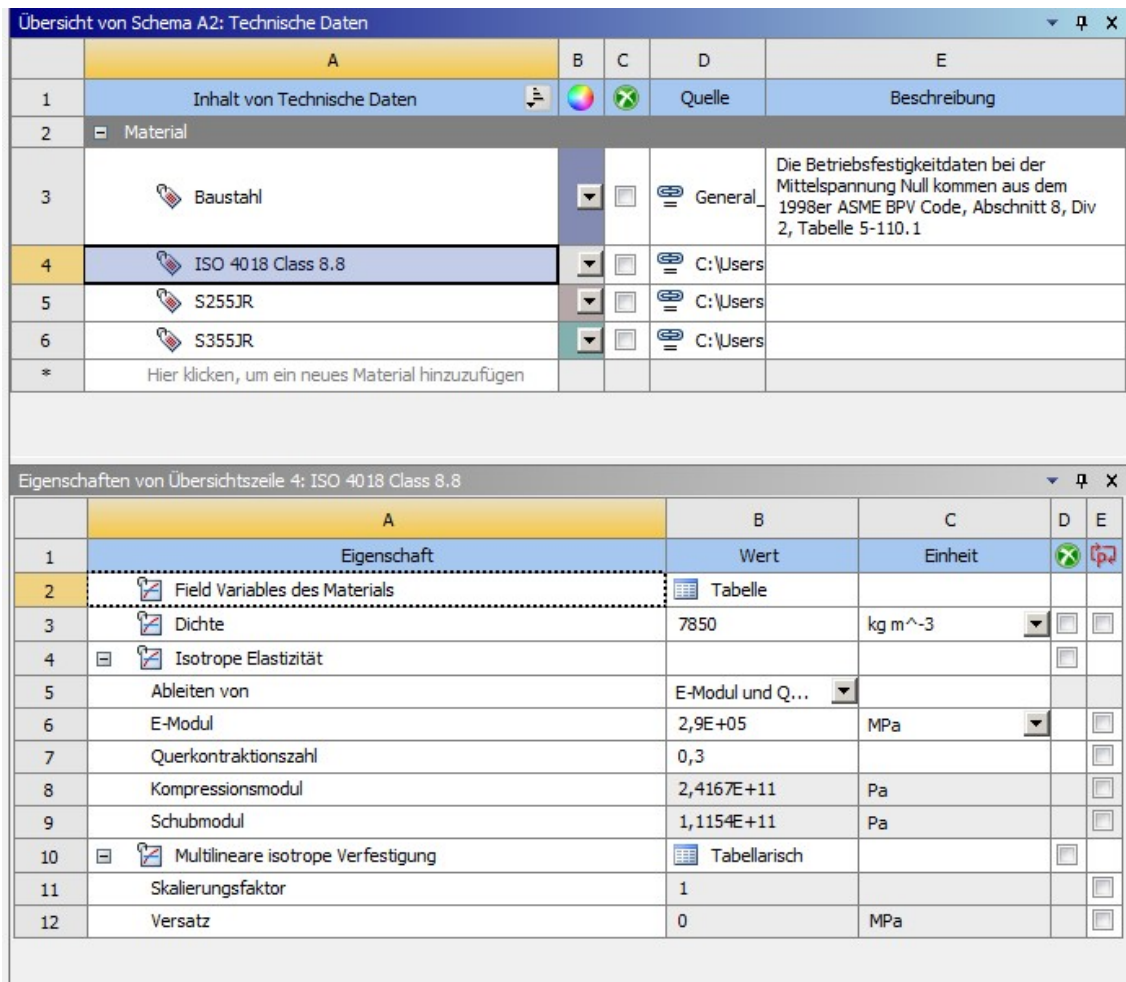
formations of the RUP in case of impacts due to crashes. The Charpy impact value at room temperature was selected due to its accessibility and costs. Higher quality materials were not needed.

Finally the screws and nuts is where the shear strength and the resultant von Mises stress are at their maximum. In order to avoid complete deformation of the device the selected materials for the fastener parts have to possess high tensile strengths. A ISO 4018 class and ISO 8673 class 8.8 nuts were chosen for this purpose. Their mechanical properties allow for a higher elastic elongation proportional to their yield stress of 640 MPa.

All three needed materials and their respective properties were introduced in Workbench, as seen in Figure 4.9. It was assumed a multi-linear isotropic relationship between stress and engineering strain. It is important to specify a room temperature for the materials (the temperature in which the numerical test is performed) and their respective density. For the isotropic elasticity, each material must be assigned with their respective Young's Modulus (constant of proportionality between the normal stress and strain) and the Poisson's ratio. This last parameter describes the contraction or expansion of a material in directions perpendicular to the loading. All the input fields can be observed in Figures 4.9. The Table 4.1 also possesses all the required technical data. In addition a multi-linear isotropic hardening was added. This allows stress-strain input with an undefined number of rows. The user is able to add as many stress and strain points as needed to represent the deformation of the materials under specific loads: only three points were needed for each material (see Figure 4.10). The first two points to represent initial strain until yielding, while the final two define the relationship until fracture. All stress-strain curves of the materials were obtained from physical studies that analyze the mechanical properties of these materials under different conditions: [44], [45], [46], [47], [48] were the used sources.

Table 4.1: Physical properties of the selected materials

Material	ISO 4018 Class 8.8	S255JR	S355JR
<i>Room Temperature</i>	20	20	20
<i>Density</i>	7850 kg/m ³	7850 kg/m ³	7850 kg/m ³
<i>Poisson's Ratio</i>	0,3	0,3	0,3
<i>Yield Stress</i>	580 MPa	245 MPa	405 MPa
<i>Tensile Stress</i>	640 MPa	245 MPa	405 MPa
<i>Fracture Stress</i>	800 MPa	380 MPa	510 MPa



The figure shows two screenshots from a software interface. The top screenshot, titled 'Übersicht von Schema A2: Technische Daten', displays a table with columns A, B, C, D, and E. The 'Material' section is expanded, showing 'Baustahl' and 'ISO 4018 Class 8.8' selected. The bottom screenshot, titled 'Eigenschaften von Übersichtszeile 4: ISO 4018 Class 8.8', shows a table of material properties such as Density (7850 kg m⁻³), E-Modul (2,9E+05 MPa), and Versatz (0 MPa).

	A	B	C	D	E
1	Inhalt von Technische Daten			Quelle	Beschreibung
2	Material				
3	Baustahl		General		Die Betriebsfestigkeitsdaten bei der Mittelspannung Null kommen aus dem 1998er ASME BPV Code, Abschnitt 8, Div 2, Tabelle 5-110.1
4	ISO 4018 Class 8.8		C:\Users		
5	S255JR		C:\Users		
6	S355JR		C:\Users		
*	Hier klicken, um ein neues Material hinzuzufügen				

	A	B	C	D	E
1	Eigenschaft	Wert	Einheit		
2	Field Variables des Materials	Tabelle			
3	Dichte	7850	kg m ⁻³		
4	Isotrope Elastizität				
5	Ableiten von	E-Modul und Q...			
6	E-Modul	2,9E+05	MPa		
7	Querkontraktionszahl	0,3			
8	Kompressionsmodul	2,4167E+11	Pa		
9	Schubmodul	1,1154E+11	Pa		
10	Multilineare isotrope Verfestigung	Tabellarisch			
11	Skalierungsfaktor	1			
12	Versatz	0	MPa		

Figure 4.9: Overview and insertion of material properties in Workbench

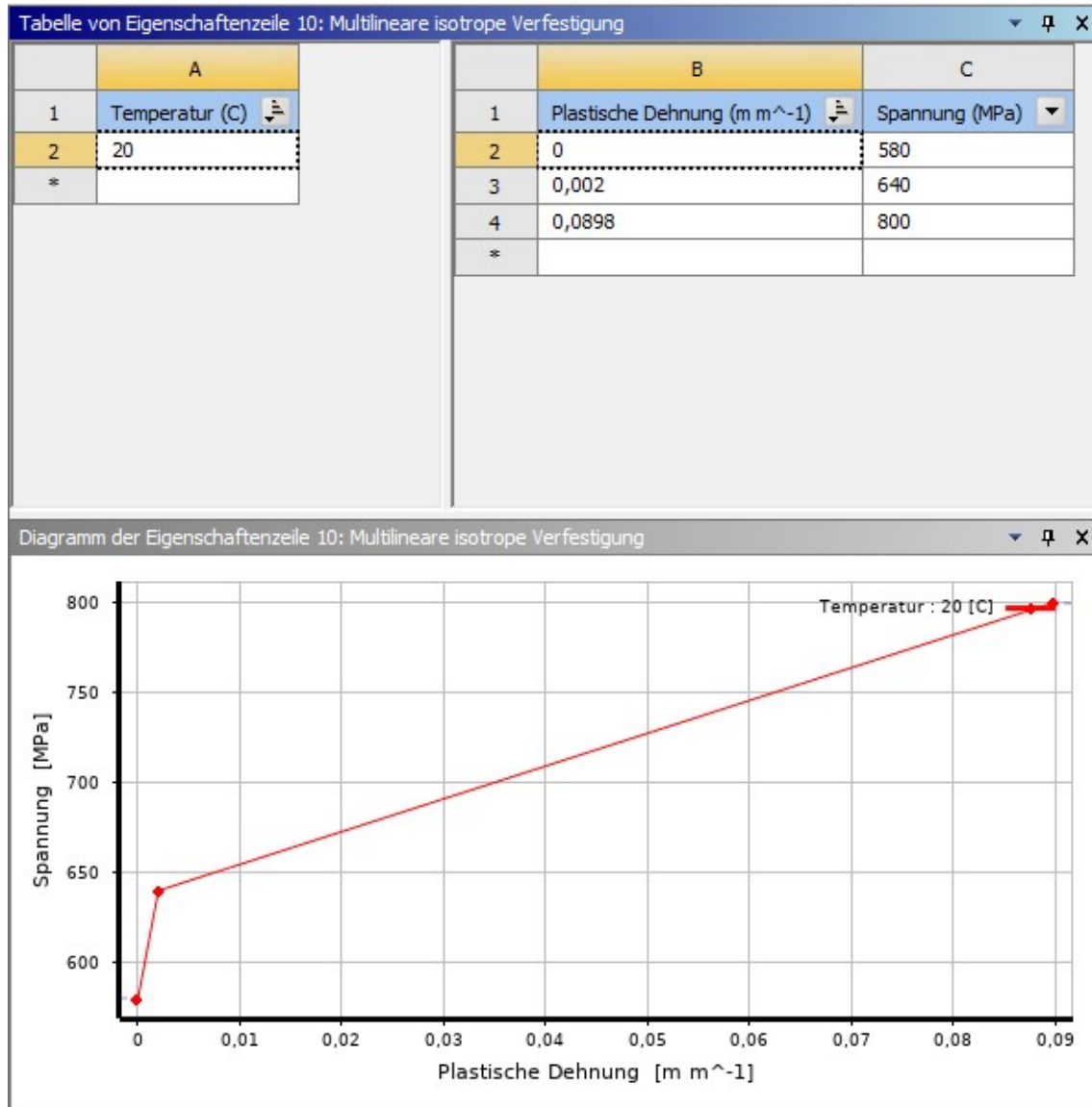


Figure 4.10: Definition of plasticity and fracture behavior. Three points needed representing: proof, yield and tensile load

4.4 Contact conditions

After defining all important technical parameters and verifying the geometry of the design, the model for the simulation can be open through ANSYS Mechanical. Of high importance is the definition of contacts between all parts of the device as a first

step. As default ANSYS is capable of automatically detecting all contacts caused by intersection of parts. Also as default, all contacts are specified as bonded in the beginning, meaning that the surfaces are not able to slide with each other or completely separate. One must think of the regions as a welded or as a glued entity. The program is then able to close any present gaps and ignore any present penetrations of parts: ideal for linear solutions. By applying all bonded contacts it is possible to make prior tests to verify an approximate deformation of the system and check if all specified conditions, be it fixtures or meshing, fulfil all requirements for a FEM calculation. Nevertheless, friction and sliding must also be taken into consideration in order to make the simulation more approximate to reality. Further behaviors include: no separation, frictionless, rough and frictional. The first one functions in an exact fashion as bonded; the targets will be tied. However, it can only be applied to faces or edges, no lines, surfaces or complete bodies. A frictionless contact presents a coefficient of friction equals to zero, hence allowing free sliding between the contacting bodies. Gaps can also form between the two targets, depending on the applied loads. In the case of rough contacts, gaps can also form between the contact bodies. Since the friction's coefficient is set as infinite for this case, the bodies are not allowed to slide. This option is also not available for explicit calculations (further explanation in Chapter 1.2.4). Finally for frictional contacts, the user has to define a coefficient in order to set sliding and sticking conditions. The interfaces carry shear stress up to a certain point [24], where they can start sliding relative to each other. As explained in Chapter 1.2.5 this conditions is referred as sticking. Once a maximum allowed shear stress is exceeded, the two geometries will start to slide [24].

In the case of the test rear underrun protection, the cross member and the supports number 1 from both sides need to be welded with each other, in order to ensure a fixed connection. The L profile serves as a union for these parts. Further welded parts include the U-profile metal rods and the steel plates, that both represent the frame of the vehicle. All of these connections (see Figures 4.11 and 4.12) will be set with the default conditions, meaning bonded. A symmetric behavior will also be applied, as well as a Pure Penalty convergence algorithm [49].

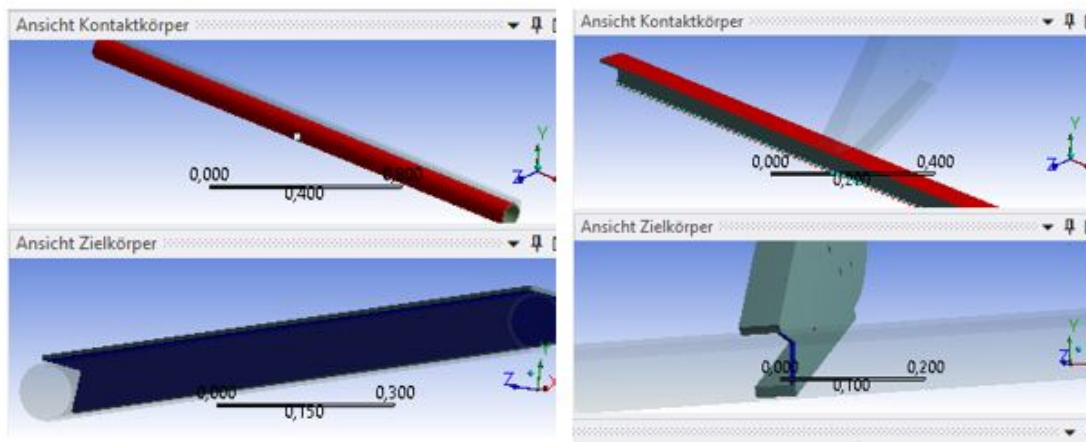


Figure 4.11: Bonded contacts for the RUP: cross member and L profile; L profile and support 1

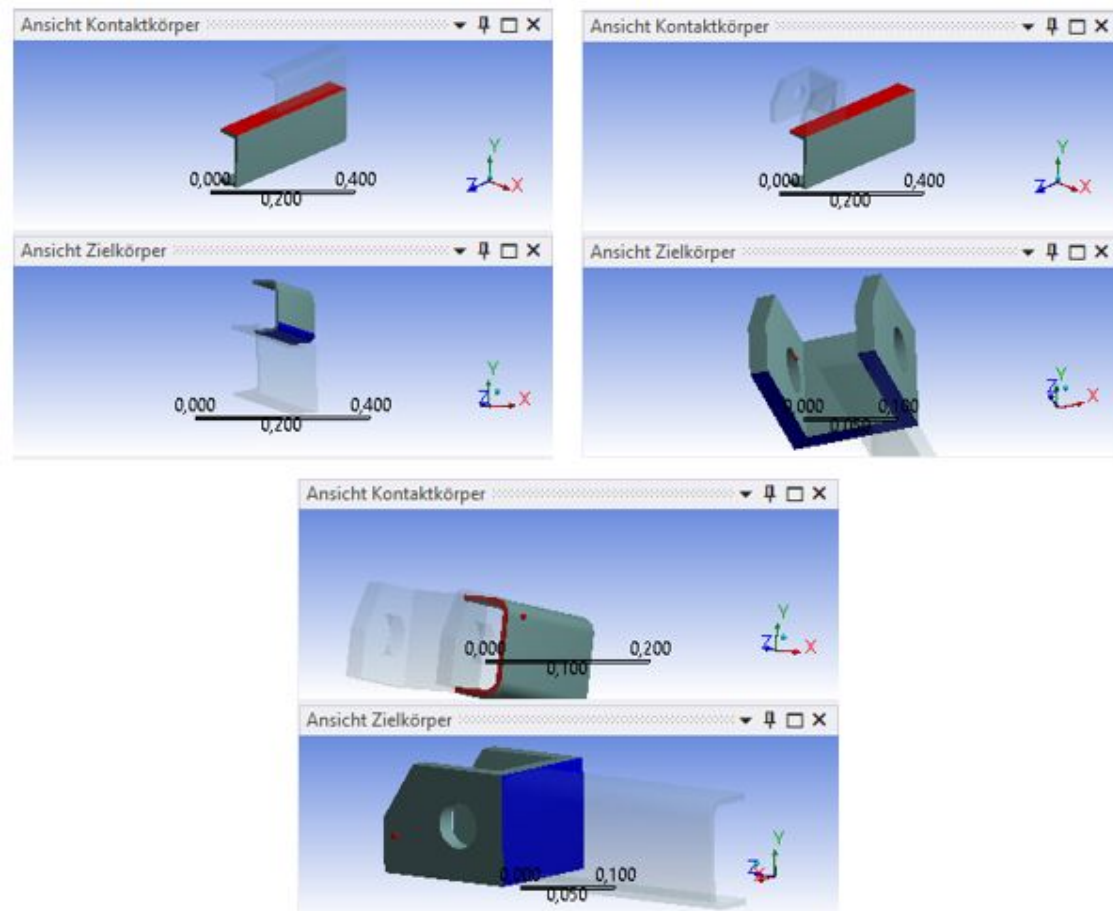


Figure 4.12: Bonded contacts for the vehicle's frame: U profile metal rods and steel plates

In the case of the contacting faces of the support 1 and the support 2, this will be programmed as frictional, with a friction coefficient of 0.2 (see Figure 4.13). The support 2 and the parts of the frame of the vehicle will all be specified as frictional too. Figure 4.14 shows the face of the support 2 as contact (recognizable by the color red), meanwhile the faces of the vehicle's frame will work as targets (blue). All of these mentioned connections were automatically determined by ANSYS and after a general control the contact targets didn't show any signs of errors.

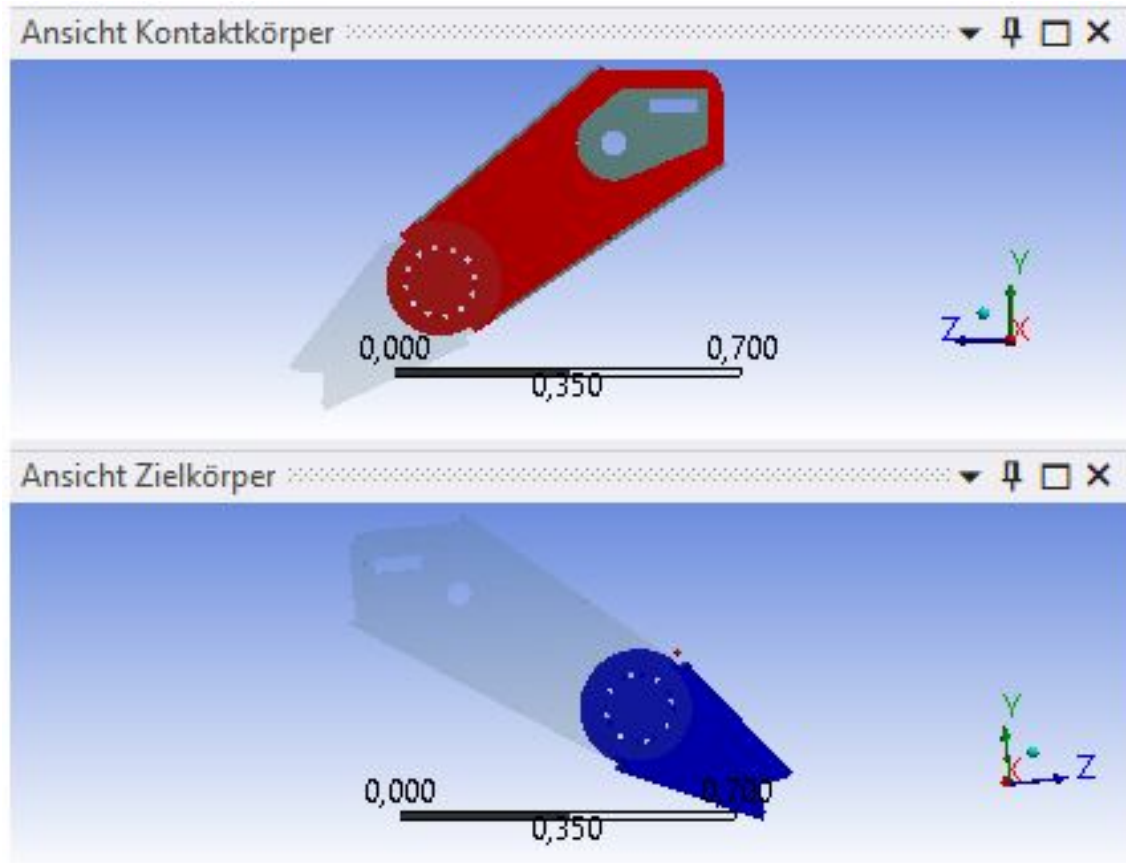


Figure 4.13: Frictional contact between the faces of the support 1 and support 2

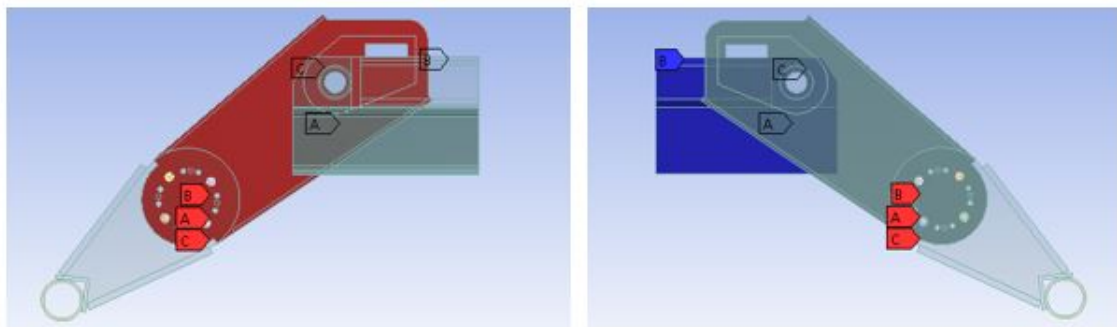


Figure 4.14: Frictional contact between the frame of the vehicle and the support 2

The default connections were not as precise for the bolt and the screws. In order to improve this, manual connections had to be defined: for the connections the

screws were separated in three important sections.

- I The connection between the head of the screw and the lateral face of the support 1
- II The shaft of the screw and the holes of both support 1 and 2
- III The connection between the nut and the lateral face of the support 2

For the bolt a similar procedure was followed, with the exception that the head of the bolt connects to a face of the support 2. The shaft follows the perforations of the steel plate. And finally the nut of the bolt creates an interface with the face of the steel plate. All of the connections of the 8 screws and 2 bolts were set as frictional, with a coefficient of 0.2 (see Figure 4.15 for a better visualization of the joint connections). The behavior was left as symmetric and an Augmented Lagrange algorithm was chosen for the convergence method.

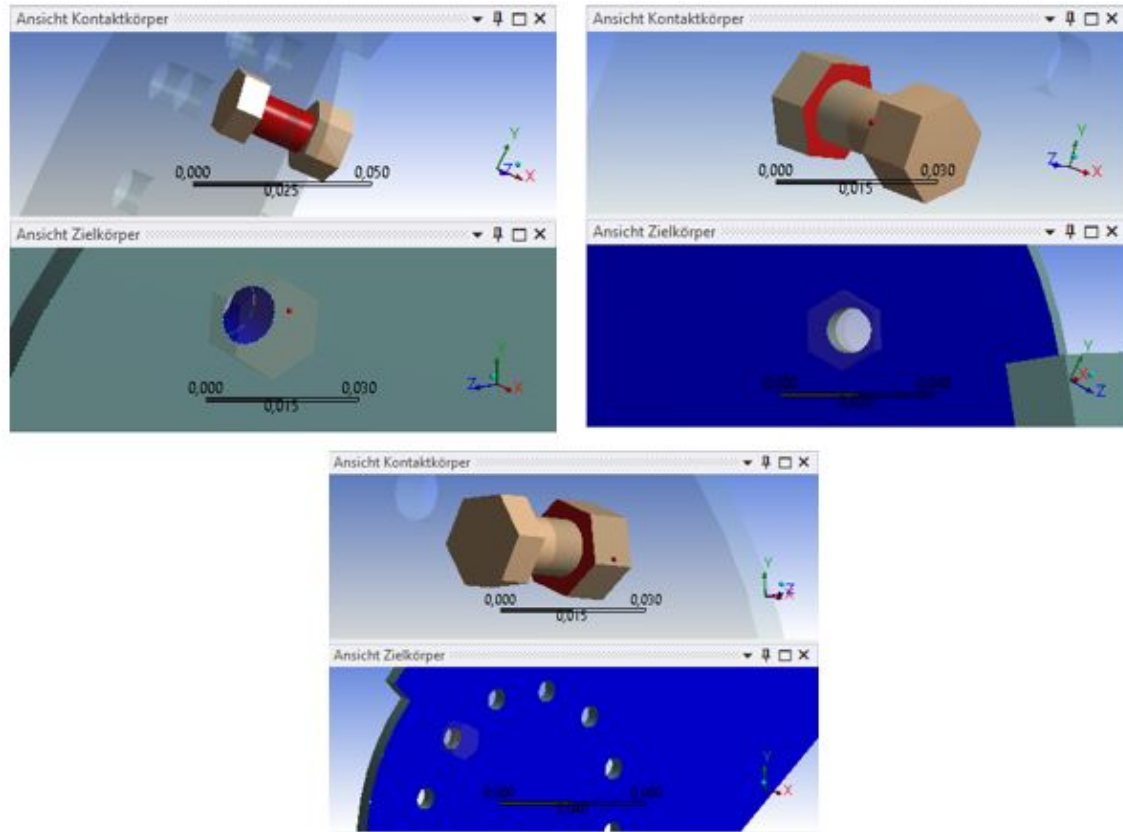


Figure 4.15: Frictional contacts for the screws and nuts. From up left to bottom right: Shaft with drilled holes, head of the screw with support 1, head of the nut with support 2

By choosing a symmetric behavior in all bonded and frictional contacts, the program constrains the contact surfaces from the penetrating surfaces and vice versa. In an asymmetric case only the contact surfaces are blocked from penetrating the target surfaces. The symmetric contact algorithm is recommended when the mesh is not identical in all areas and also not as refined. The objective is then to avoid the penetration of parts such as support 1 against screws or support 2 or other types of contacts. For a convergence algorithm the Pure Penalty Method was selected. When two bodies are in contact, by logic these must not interpenetrate or pass through. ANSYS has to specify this relationship to the specific surfaces named “contact compatibility” [24], in order to avoid unwanted penetrations. Two formulations can be used in order to apply this contact compatibility: Pure Penalty or Augmented Lagrange. For bonded contacts the recommended method is Pure Penalty. This

is compatible with the symmetric behavior and is also recommended for this case, due to its good convergence behavior (fewer equilibrium iterations are needed). The contact stiffness is also high, resulting in a lower or almost negligible penetration. For other contact behaviors such as frictional, the Augmented Lagrange is more recommended due to its high flexibility and features: it is less sensitive to selection of normal contact stiffness[49]. All the other specifications were left at default or were specified by ANSYS automatically. Additionally, the command KBC 0 was added to the APDL code, thus modifying the load to a ramping loading. The loading then increases linearly instead of instantly [32]. All the data is inputted in the detail window (Figure 4.16) present at the bottom left of the ANSYS Mechanical program.

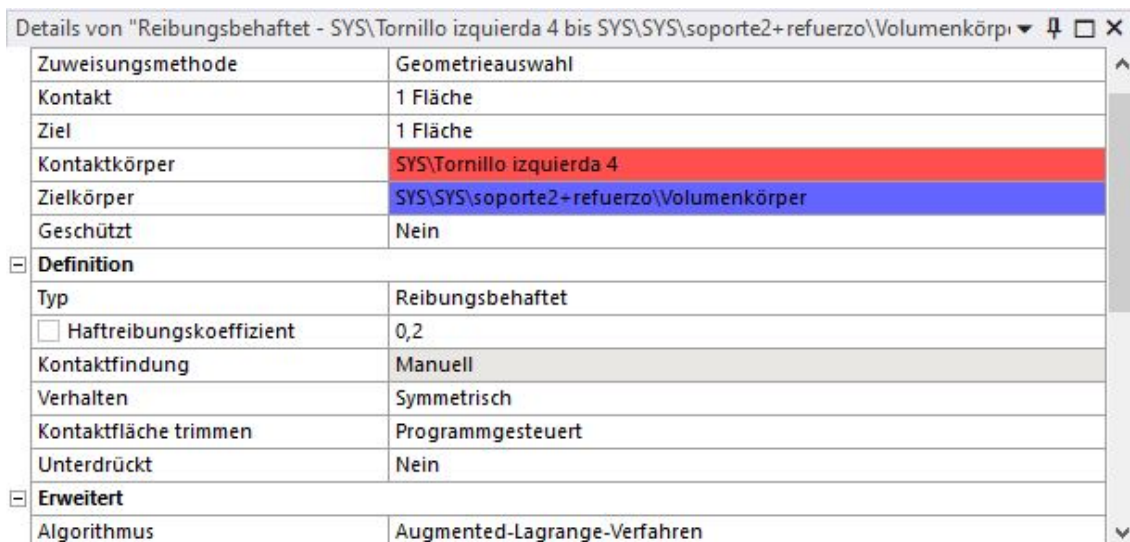


Figure 4.16: Interface window for details and conditions of contacts

4.5 Meshing

Smaller local approximations or representations of parts are utilized in order to simulate more complex and larger objects. This is all obtained by means of meshing or dividing the complex domain in tinier computing grids in form of prisms or pyramids in 3D view or triangles or 2D prisms for 2D representation. More meshing parts or a finer grid typically consumes more calculating and heavily affects the speed of the simulation. A larger mesh solves this problems however the accuracy of the

results can be negatively influenced or a convergence result may not be obtained. The whole purpose of the forces calculation in ANSYS is to find a converging result for the propose case with forces, fixtures and geometries. If the problem doesn't converge a concrete result of the simulation cannot be obtained. That is why choos- ing the appropriate meshing size is an important task by analyzing the RUP. The next Figure 4.17 shows our proposed meshing size for all parts of the rear underrun protection.

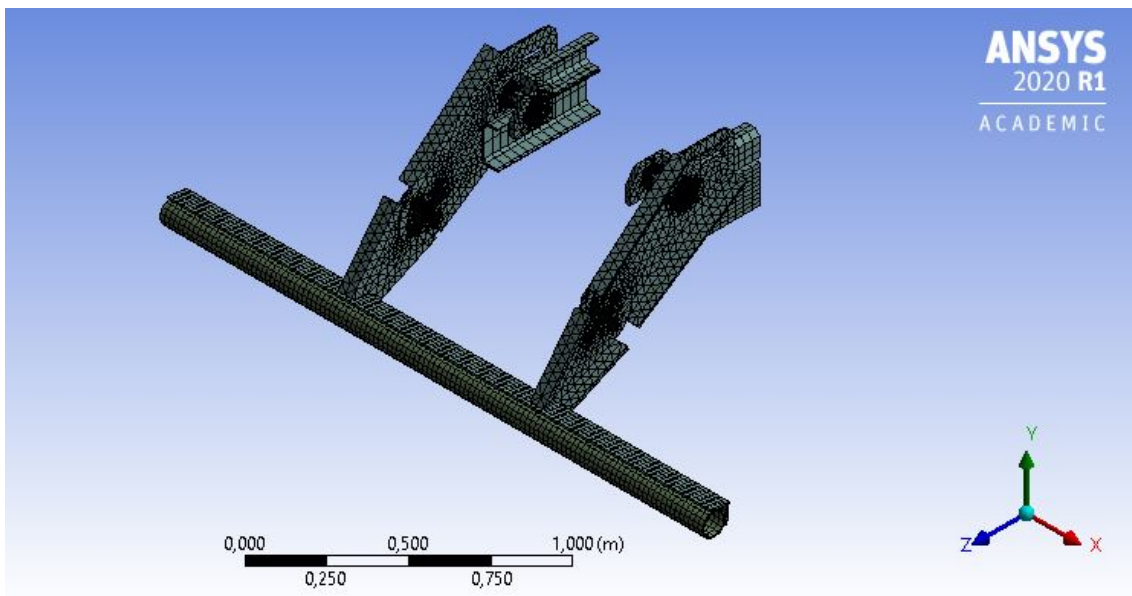


Figure 4.17: Mesh quality for the components of the rear underrun device

For a precise calculation the element size of the meshing parts are maintained at 3 cm. That means the prism possess a side length of 3 cm. That is not the case of the cross member, which has to withstand the applying forces and bend in order to dissipate the kinetic energy caused by the aforementioned. For this component we refined the mesh size to 2 cm (Figure 4.18).

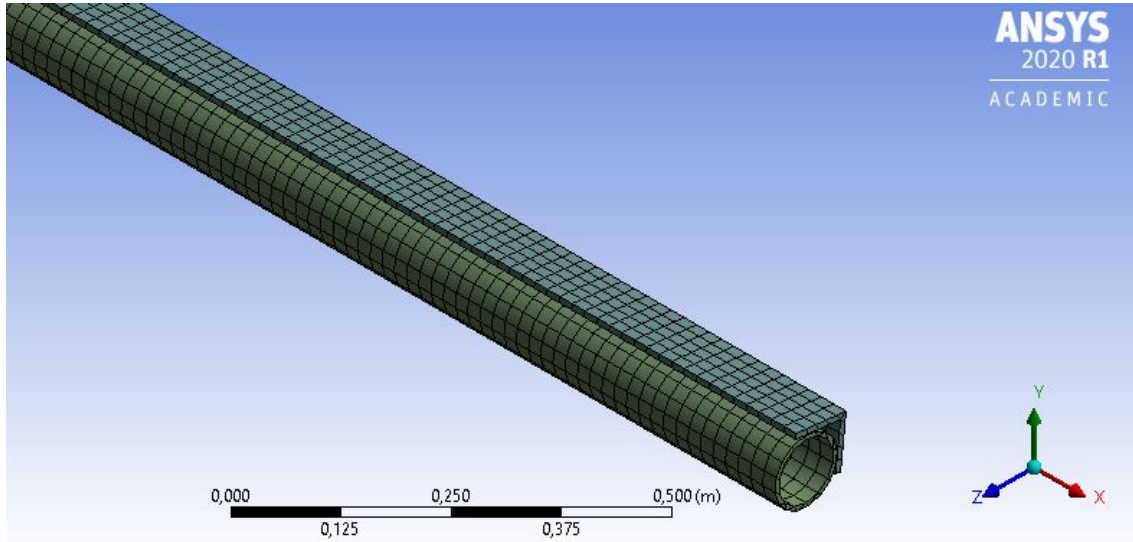


Figure 4.18: Mesh for the cross member and the L union, with 2 cm prisms

Furthermore for additional parts where high deformations are expected or a more precise calculation is needed, the sizing was maintained at 3 mm. These are the case of the screws and nuts, present at Figure 4.19, which are expected to withstand the applying testing forces. Also, the bolt which serves as a fixture to the frame of the vehicle needs a finer mesh of also 3 mm. Not only were these elements refined but their contacts to other parts were also, using a command named “Contact Meshing” [33]. All areas in contact with the screws were meshed with finer prisms. By running some tests, the areas surrounding the bolt, meaning the metal plate, suffered a high deformation. The rotation of the bolt causes the movement of the plate in the Y-direction Axis (see Figure 4.17 for details of the Axis), which is why a finer mesh was needed in order to simulate a precise result and avoid the crashing of the program. These areas also need a Contact Meshing command, which effect is visible in Figure 4.20.

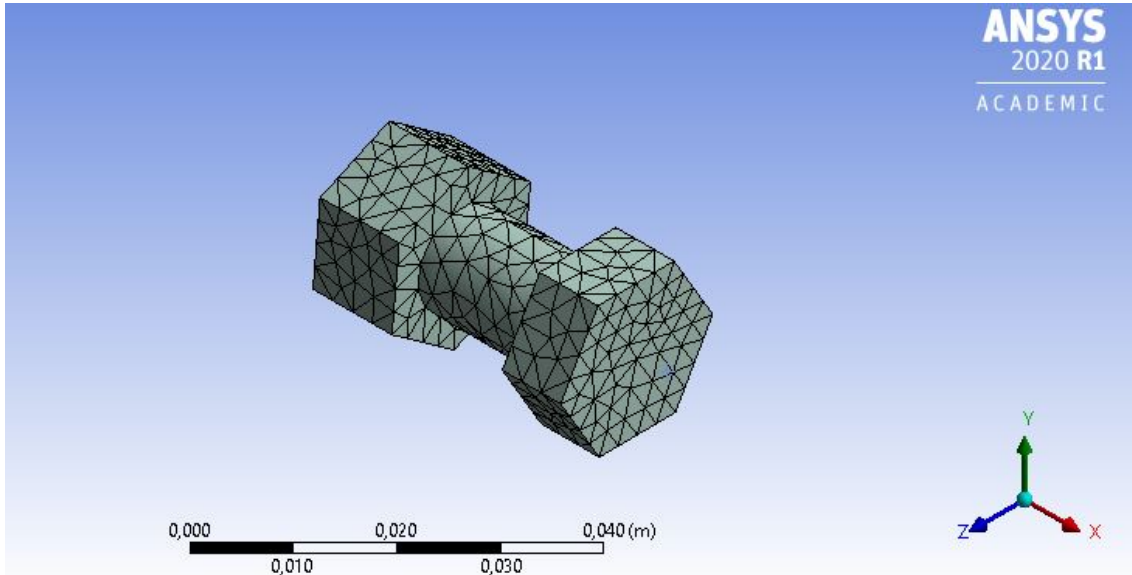


Figure 4.19: Mesh with 3 mm tetrahedrons for the screw and nut

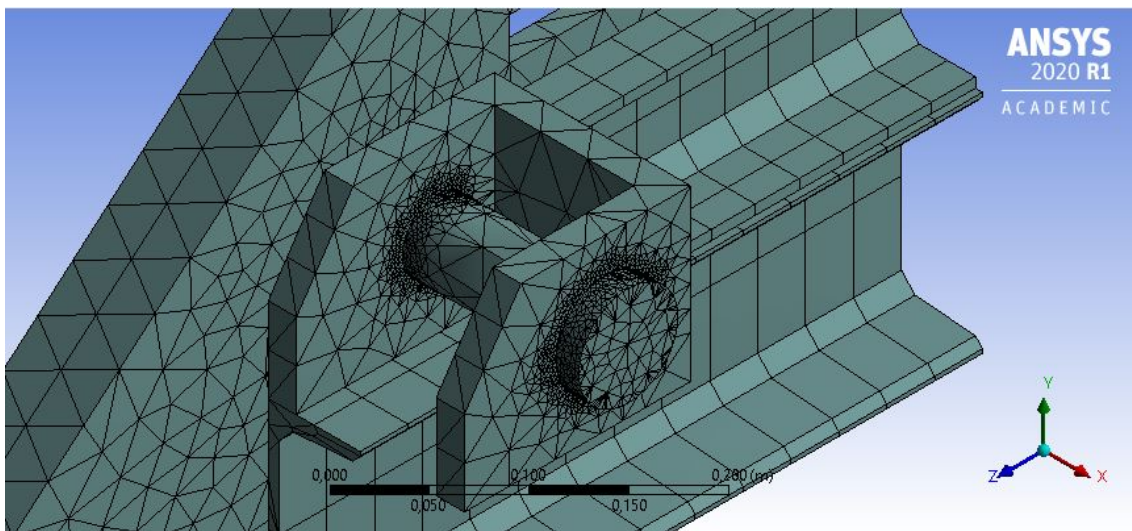


Figure 4.20: Contact meshing of 3 mm for the bolt and its contacting area

After some performed calculations and controls of quality of the mesh, the simulation was not able to reach a convergence, due to the fact that some grids failed at areas near the drilled holes of the support 1 and 2. A finer mesh was needed at this contact areas, so a sphere of influence was used instead of the usual Contact Meshing (Annex B). The latter is limited to an area that is automatically defined by

ANSYS and the refinements are applied. That is why this new method is preferred. This sphere can be augmented in size thus making the process of meshing simpler and more precise.

In order to determine the center of the sphere of influence, an extra coordinate system has to be positioned at the center of the drilled holes, by simply choosing or clicking the desired area. No further problems were observed with the meshing of the parts. Figure 4.21 shows the results of the sphere of influence and the improved mesh.

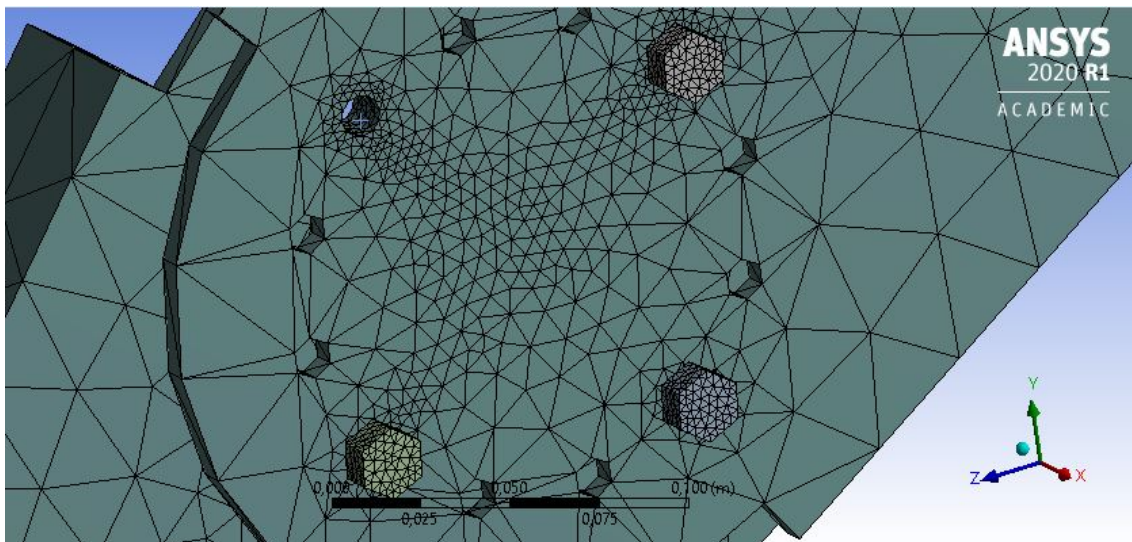


Figure 4.21: Resulting mesh with sphere of influence with a sizing of 3 mm

4.6 Transient mechanical analysis

4.6.1 Application of loads, fixed supports and time conditions

Transient mechanical is applied for a non-static situation where loading conditions are a function of time. The results are then a dynamic response of a structure to forces that vary (increment or diminish) with time steps: these may be then displacements, strains or stresses. Because of its nature the damping and the inertia must also be taken into consideration [18].

As explained each step in time is assigned a force and this can then be augmented or reduced with further introduction of steps. The regulation no. 58 doesn't define specific seconds or minutes during which the load has to be applied or reduced. Based on studies on the topic and further paperwork presented in the chapter 3, each force will be incremented in a span of 2 seconds and removed in 1 second. This was also the recommended test procedure of the manufacturer of the RUP. The developers also directed some additional physical tests to prove the veracity of computational simulation. Starting and ending each step, the beam must be in an idle state where no load is present. Further sub-steps can be assigned in order to ramp up the load more slowly and thus assuring that the simulation can converge more successfully. If the load is applied directly it is possible that the beam deforms and fractures quickly or that the maximum fracture stress of the screws is surpassed.

As stated in Chapter 1.2.3 the regulation number 58 specifies that the forces have to be applied separately and consecutively: two forces of 100 kN each separated by a distance of 1 meter and 500 mm from the center of the beam. Afterwards 2 forces of 50 kN applied 300 mm far away from the outer edges of the wheels of the rear axle or from the rear protective device if this is longer than the edges of the wheels. And finally one force of 50 kN is applied on the center of the beam [2]. Each step will end at 0.1 s and thus the force will see an increment of 1/20th of its total. Decreasing the time step size yields better convergence, allowing the program to run more smoothly. If the load is applied too quickly, the components may deform and destroy at full tilt.

For the decrease of the load in each step a value of 10 kN or 5 kN is suitable in order to reduce computing time. For the analysis the beginning steps were inputted as 0.1 s and the minimal increase between them was set to 0.15 s. The maximum step increment was left at 0.1 s, hence a step possesses 7 total sub steps (the last one sees an increment of only 0,01 s instead of 0.015 in order to exactly arrive to 0.1 s). Figure 4.22 shows the data for the time conditions and in addition a graph, where the five loads are represented.

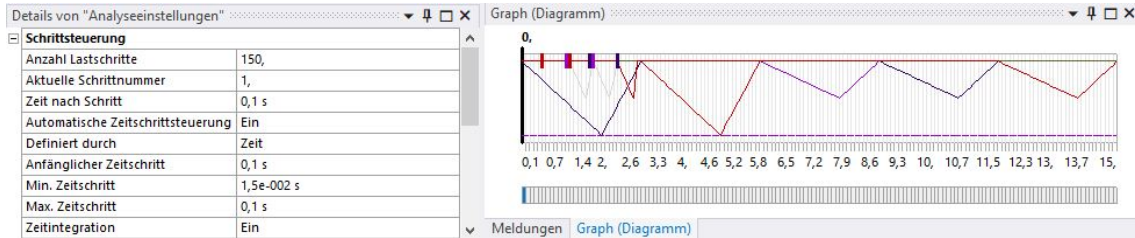


Figure 4.22: Details of time conditions and graph of the forces divided by the respective steps. Translation from German: number of steps, time after steps, initial time step, minimal and maximal time steps between calculations

There are various ways of applying the forces to target objects. Forces can be applied by means of simply selecting a face, point or edge. The first approach of the simulation was to apply the forces to points in the exact places stated in the normative 58. However high amounts of forces were being administered at a simple point of the RUP and thus not being able to extend further this. The simulation wasn't able to run, due to present high deformations of the nodes in near proximity to the point-forces. Picking faces was also not recommendable, as this calculations could potentially be inaccurate: dividing the RUP in 5 faces was not an option and the formed areas surpassed the allowed length of 200 mm. So nodal forces were selected as a compatible option. The nodes of the cross member are characterized by being hexagons with an edge length of each 2 cm. By picking the correct amount of nodes one can select up to a horizontal length of 200 mm and a vertical one of 100 mm, just the accepted amount by the normative. The intersection between nodes will serve as points where the wanted forces will be applied. Since mid-side nodes (characteristic of quadratic elements) can affect the calculation time and will not affect the mesh quality of the device, the element order will be set to linear. This means no mid-side nodes will be placed on the geometry, which effectively reduces the number of degrees of freedom. The "nodal force" command doesn't allow selection of the wanted nodes, instead a specific component has to be chosen. So before applying the loads, a total of five components, each containing the necessary nodes for where the loads have to be applied, have to be created (see Annex for more details). Afterwards all nodal forces can be created and all the load conditions explained in the last paragraph can be inputted (see Figure 4.23 for all the created nodes and the places for load application). The load will be divided by the number of existing nodes, which follow the directions of the global coordinate system. The X

and Y-forces will be deactivated, meanwhile the Z-force follows tabular data entered by the user (Figure 4.24).

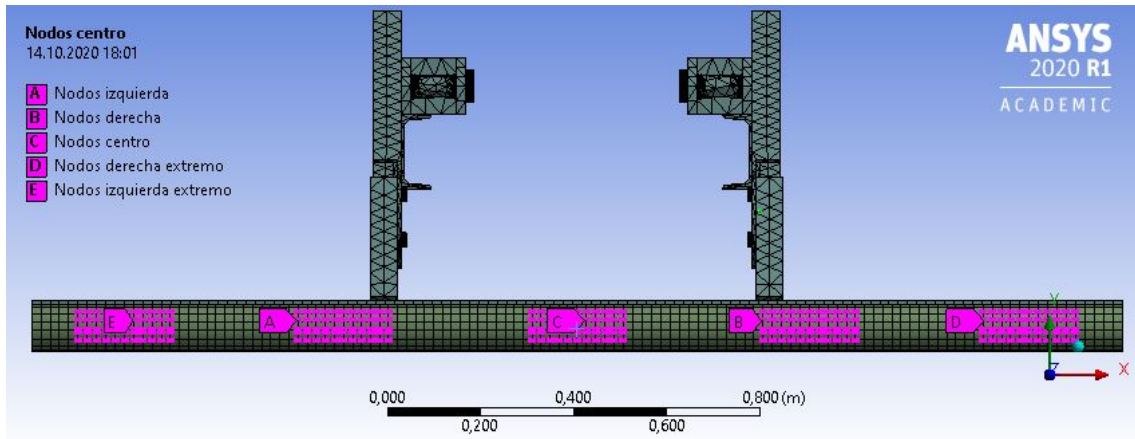


Figure 4.23: Selected nodes representing the area where the load is applied under UNECE 58 requirements

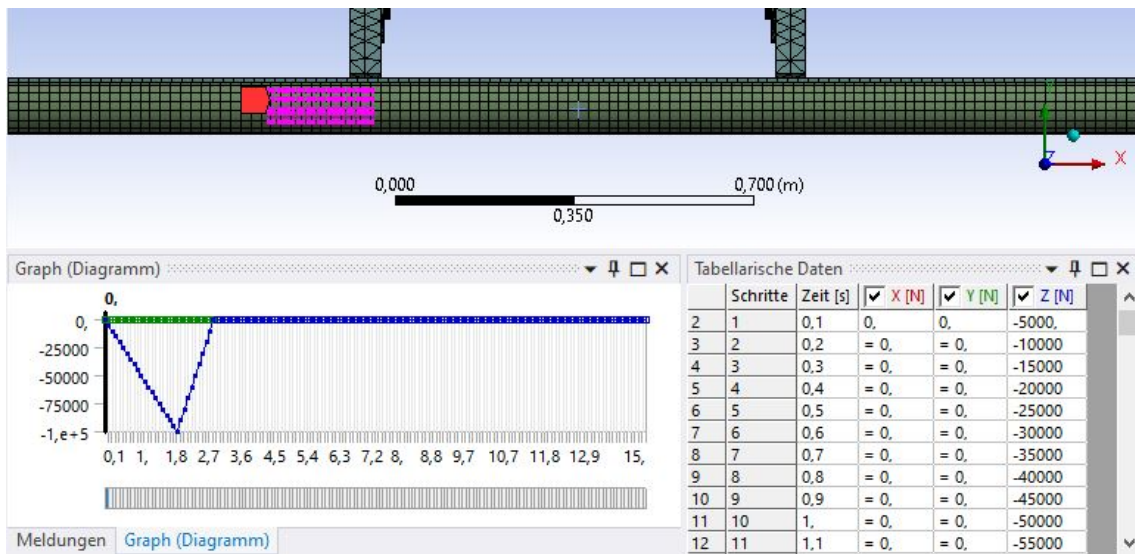


Figure 4.24: Input of loads by means of tabular data

Since not the complete frame of the vehicle was designed just an approximate, a fixed support was assigned at the end of these faces (see Figure 4.25). A fixed support doesn't allow the displacement of the assigned parts in either X, Y or Z axis. Moreover a displacement condition was set at the faces of the steel plate

attached to the support 2 (Figure 4.26): This blocks selected degrees of freedom in a specific direction, for this study case in the Y-Axis. After setting all required forces, supports, mesh sizing and materials for the RUP model, Workbench can run the simulation for the study case with all respective specifications. In Figure 4.27 and 4.28 we can see all the results of the applied commands and conditions for the rear underrun protection and the procedural settings. Workbench also allows code input of APDL Mechanical instead of the previously mentioned automatic techniques. By using the command condition of KBC, 0 the force can be apply linearly instead of directly [32]. The avoidance of a sudden spike in forces ensures a convergent result. After that the program can run the needed calculations.

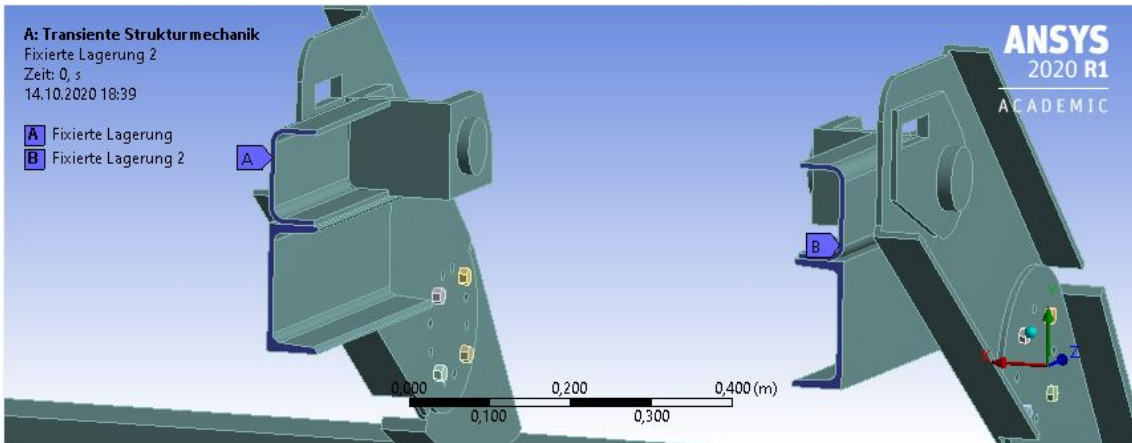


Figure 4.25: Fixed support for the faces of the frame of the vehicle

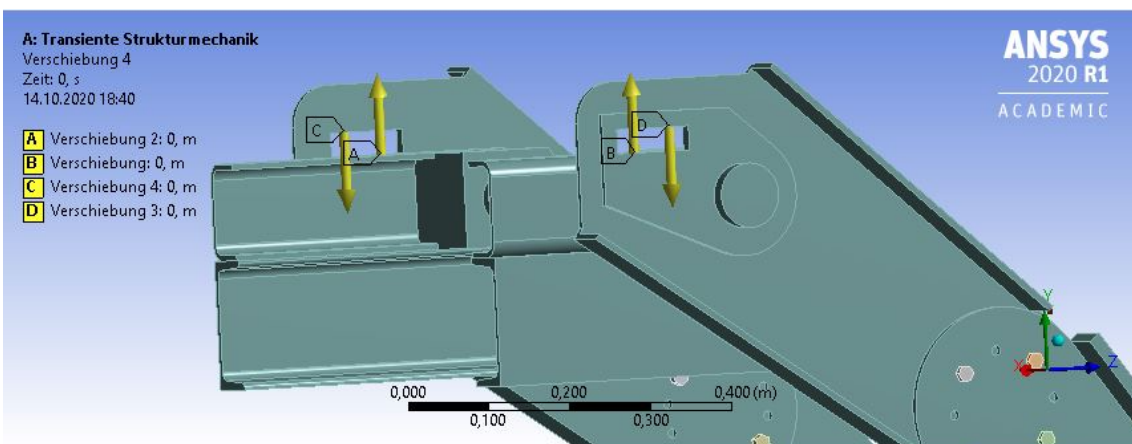


Figure 4.26: Input of displacement of 0 for the vehicle's frame in the Y-axis

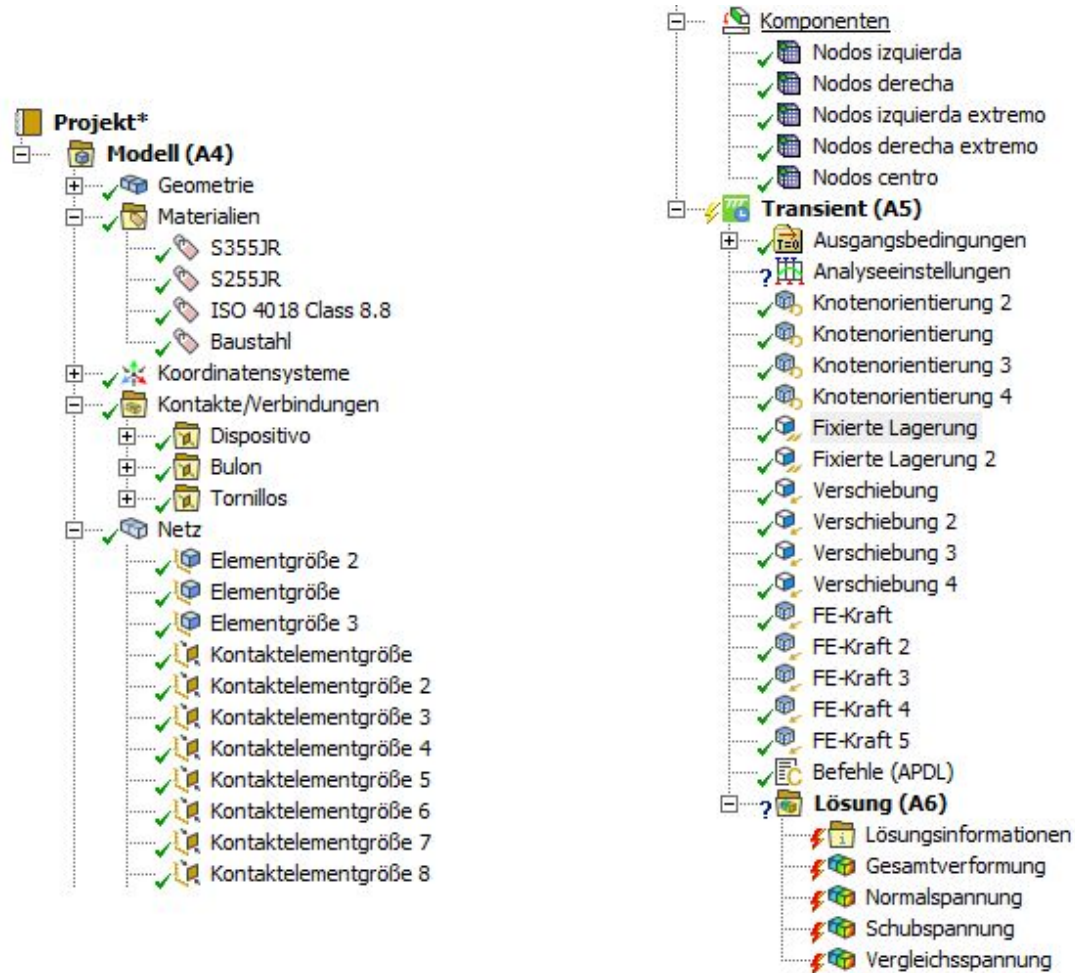


Figure 4.27: Total applied commands for the simulation. From big importance: components, materials, coordinate systems, contacts, mesh, components, transient conditions and results

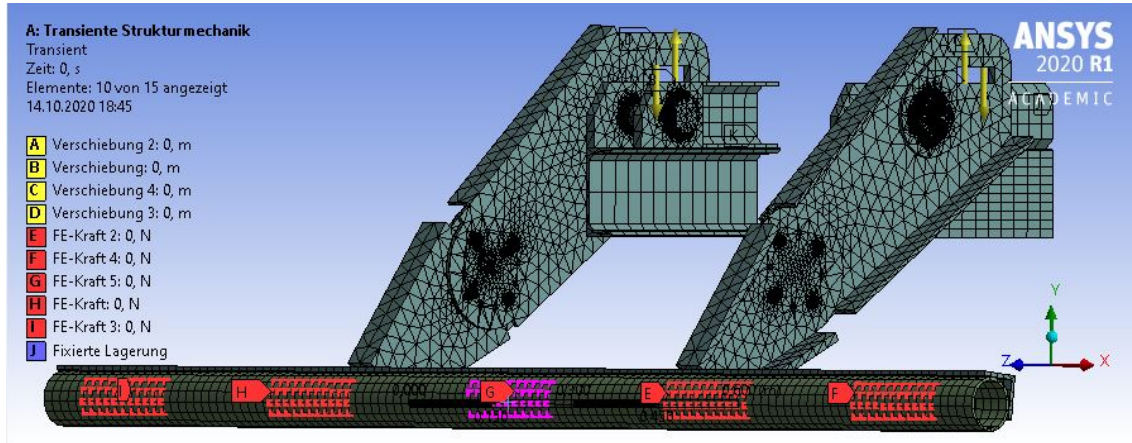


Figure 4.28: Total applied commands for the simulation present at the RUP

4.6.2 Results of case study one: lack of pretension

Two significant simulations were run with varying conditions: for the first, the mesh will include lesser parts (hexagons and tetrahedrons) and the bolts will lack a pretension. A high number of simulations were run as a test and the size of the meshing didn't change the final result: the RUP was not able to withstand the test forces, no matter the sizes of meshing elements. A general mesh was then decided for the RUP that reflected the expected results of the physical tests.

After a total of 25 hours the simulation of the first case crashes due to an “error of deformability”: an element suffers from a high deformation (possibly a total destruction) causing the simulation to be terminated. As part of the results we decided to analyze the total deformation of the RUP, the nominal tension in the X-axis, the shear tension and the von Mises yield criterion or maximum distortion criterion (the results can be seen in Figure 4.27). By further investigation of the destroyed areas, the critical element was identified as a meshed part of the support no. 2, near the drilled holes for the screws (see Figure 4.29). This is to be expected since the screws suffer from the highest shearing forces in the RUP (Figure 4.30). The bolts elongate due to the applying forces before they shear. The plates of the support one and two separate (see Figure 4.31), causing the screws to dissipate the forces by themselves. The supports 2 of both sides also bend (Figure 4.32) because it is fixed on the upper part to the frame of the vehicle, which cannot move because

of the fixed support. Meanwhile the bottom part bends in direction of the load, because of the lack of screw pretension. Because the supports separate there exists excessive hole clearance and the areas are not able to transport the loads to all the device. The bolts are left isolated. Maximum shear strength tends to be 60% of the tensile strength [50], that is why shearing caused by the bearing between opposite plates in the joint is to be expected. Stress distribution spreads as it makes the thread elongate and the head of the screw and nut to compress, due to the union to the support [50]. The maximum axial load is reached at the head of both components (Figure 4.33). As the contact between the shaft of the screw and the drilled holes of the screws is specified as frictional, the holes also deform due to the changes in the screw. The cross member is also pulled in the negative direction of the Y-Axis, coming closer to the ground (Figure 4.34). This makes the support rotate, thus pressuring the screws more. The fixed conditions dont allow for a deformation of the tube in the X-Axis. The maximal force of 100 kN is reached after 20 steps, however the calculation is terminated at the 25th step were a decrease of the load is expected for the device. Diminishing the load doesn't technically means lack of displacements of deformations, which is shown in this case. The design of the device still deforms even when the load is being reduced. The high values of the von Mises' stress indicate a failure of the component after the shape change energy exceeds a limit value. After some verification with the fabricator, he indeed validates the results: the device also gets highly distorted after the physical test, which means the design is not capable of withstanding the regulative forces.

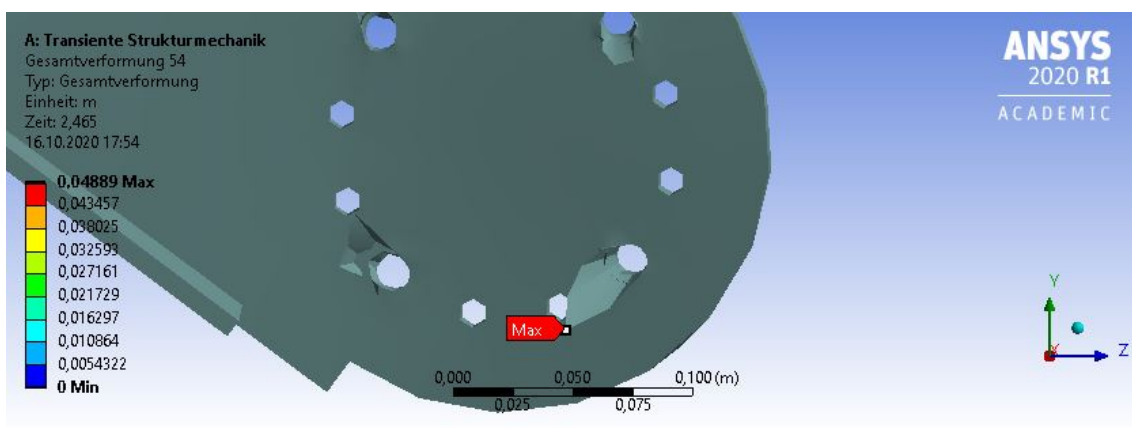


Figure 4.29: High deformation of the screws' holes, which causes the program to crash

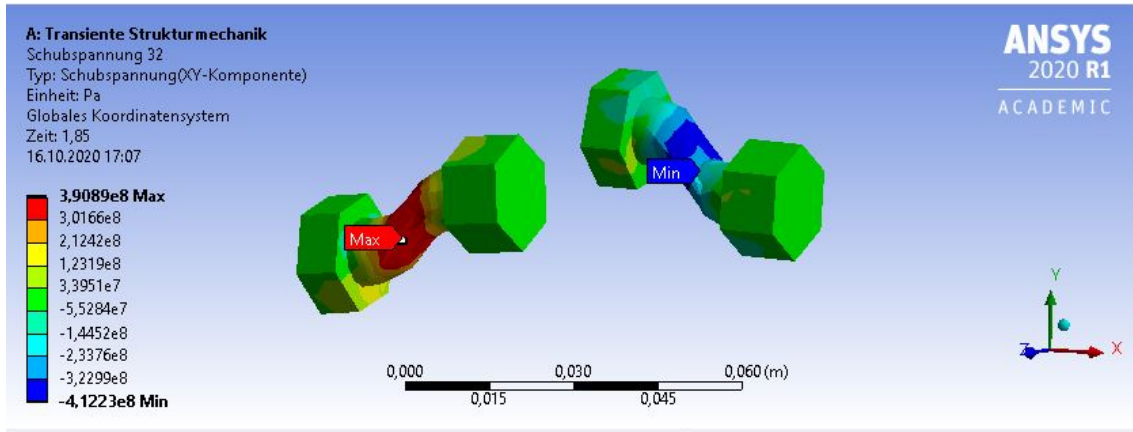


Figure 4.30: Concentration of the maximal shearing stress at the center of the screws

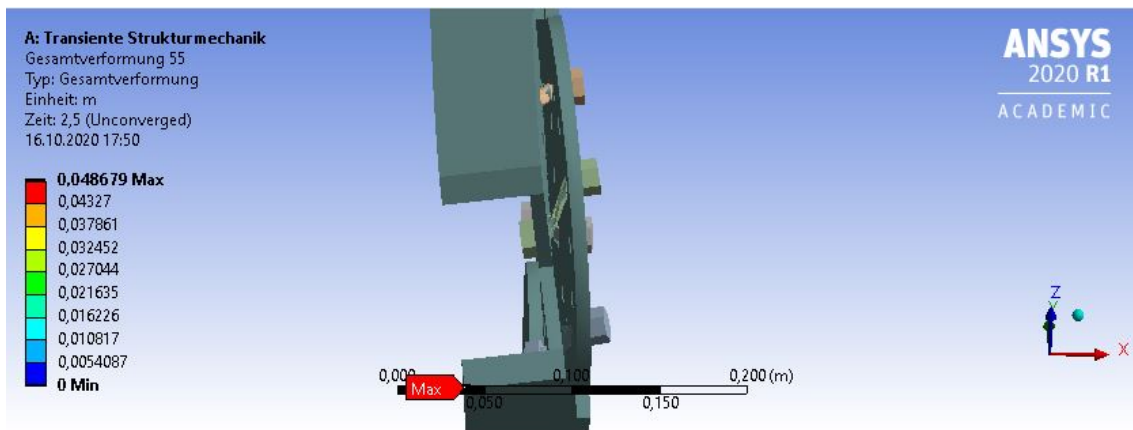


Figure 4.31: Separation of the plates due to lack of pretension

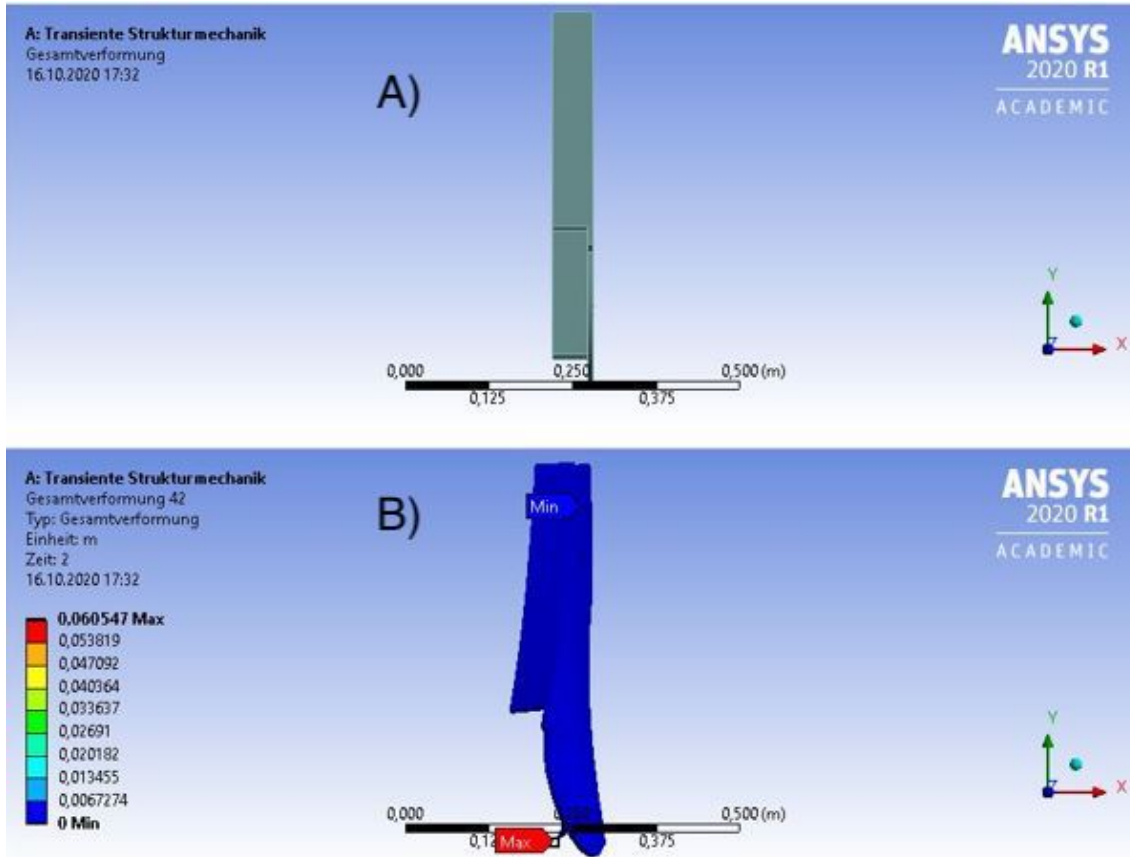


Figure 4.32: Support 2 in its A) neutral state and B) after the appliance of the load

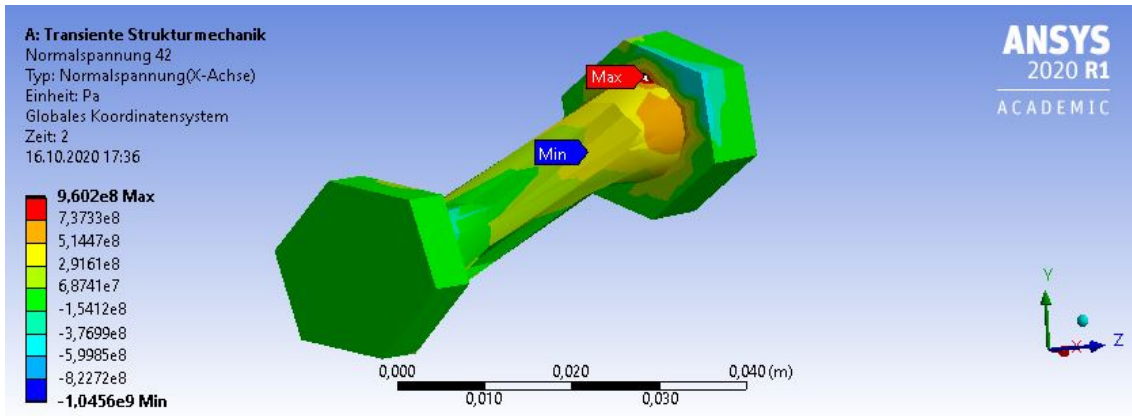


Figure 4.33: Maximal normal load in X-axis located at the head of the screw and the nut

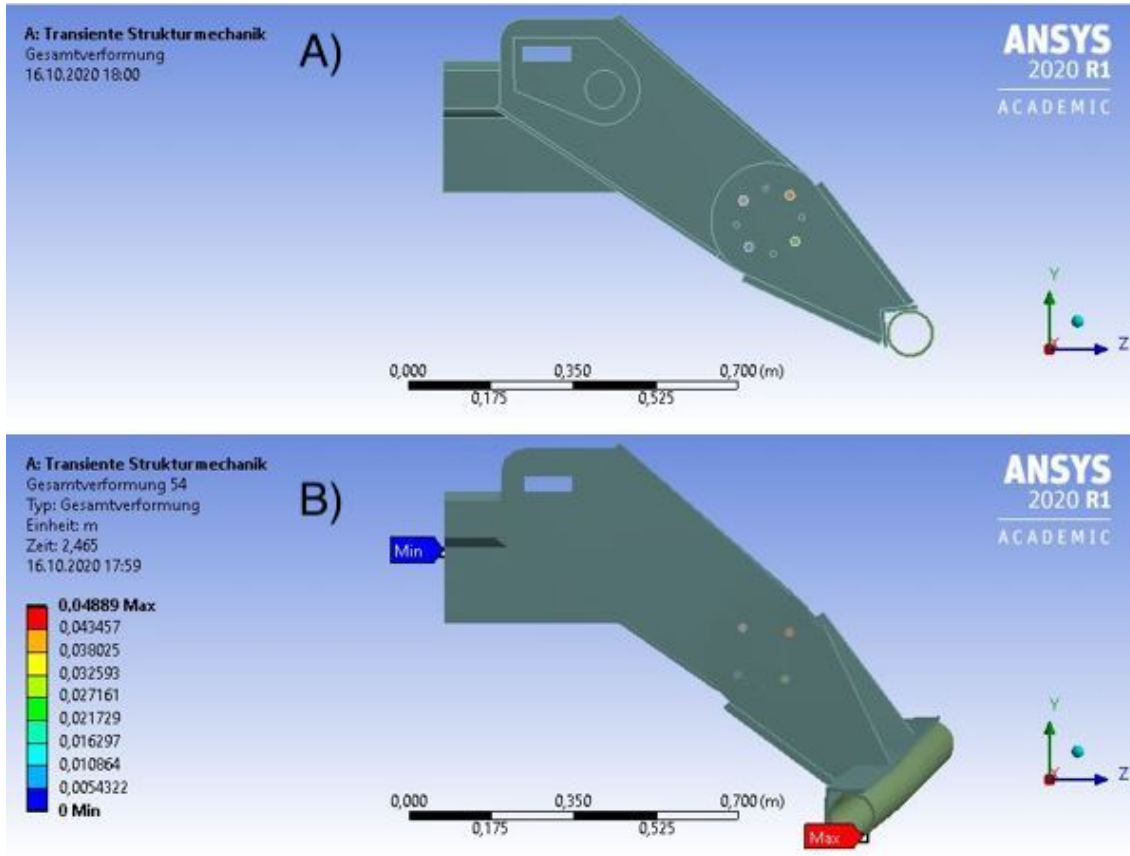


Figure 4.34: Results of the simulation: rear underrun protection A) in its neutral state and B) in its deformed state

As for the other components, their stress distribution remains relatively low in all sub-steps. This is indicative of the concentration of the load at the screws area, due to the fact that this union is specified as frictional. We expected the bolt to also suffer because of this, but it seems that the shearing and maximum distortion stress don't even reach this component fully. Figure 4.34 serves as a validation that the components representing the frame of the vehicle suffer the less from the applying loads.

4.6.3 Results of case study two: inclusion of pretension

For the second case study the pretensions of the bolts of the screws have to be taken into consideration: an extra step has to be added in order to tighten the screws with the adequate installation torque forces. ANSYS possesses an automatic

command for the necessary pretensions, in which the necessary cylindrical faces to be pretensioned have to be selected. The respective axial loads will afterwards be applied in the normal direction of the face (see Figure 4.35 for the direction of the pretension). The first step will then be set for load appliance. For the additional steps where the test force is being incremented and afterwards reduced, the bolts need to be locked in their constrained state. The pretension force was calculated using the formula 1.3 and a value of 28 kN was obtained (see Figure 4.36 to observe how the load is inputted). However, after launching the program, the calculation came to a sudden stop due to problems in the pretension. The face of the bolt has to be split in order to determine the area where the pretension can be applied: the shaft between the head of the screw and the nut (Figure 4.35). This pretension section must also include a structural element type. In order to create an appropriate mesh for the area, a further explanation of the concepts of the bolts' pre-load will be presented. As a first step the software divides the body using a PSMESH command. In order to successfully do this, the regions of the model where the pretension is applied must have identical meshes and nodes which coincide with each other, creating a coincident and connected area. This is where the error was presented: the mesh possesses varying nodes with different sizes, so the screws, mainly the shaft, is not being sliced regularly [30]. In order to solve this without disrupting the quality of the mesh a "Multizone" mesh is applied to all bodies coincident to the screws. This mesh provides automatic decomposition of geometry into structured regions, where it automatically creates a pure hexahedral mesh where possible. These meshed regions tend to be more similar and less complex (see Figure 4.37 for the obtained mesh) [33]. However the sizing of the mesh was not modified from the first case study. The second step for the pre-load concepts includes the definition of a constraint equation by means of a pretension element (command PRETS179) into a specific node which then transfer the displacement or force equation to the adjacent nodes. This is repeated until the nodes of the selected face obtain all respective equations [32]. The simulation didn't present any failures afterwards.

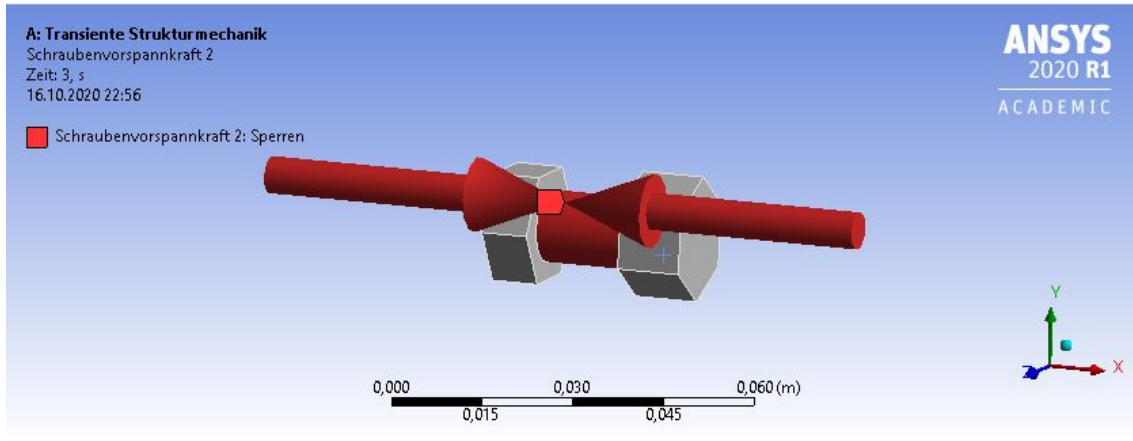


Figure 4.35: Selected area for the pretension and direction of the load. Pretension will only be applied to the shaft between head and nut

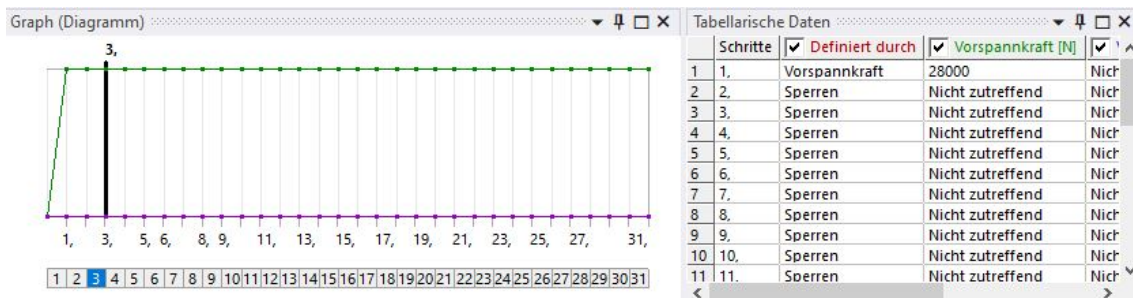


Figure 4.36: Technical data and details of pretension. Translation from German: step, defined by, pretension load

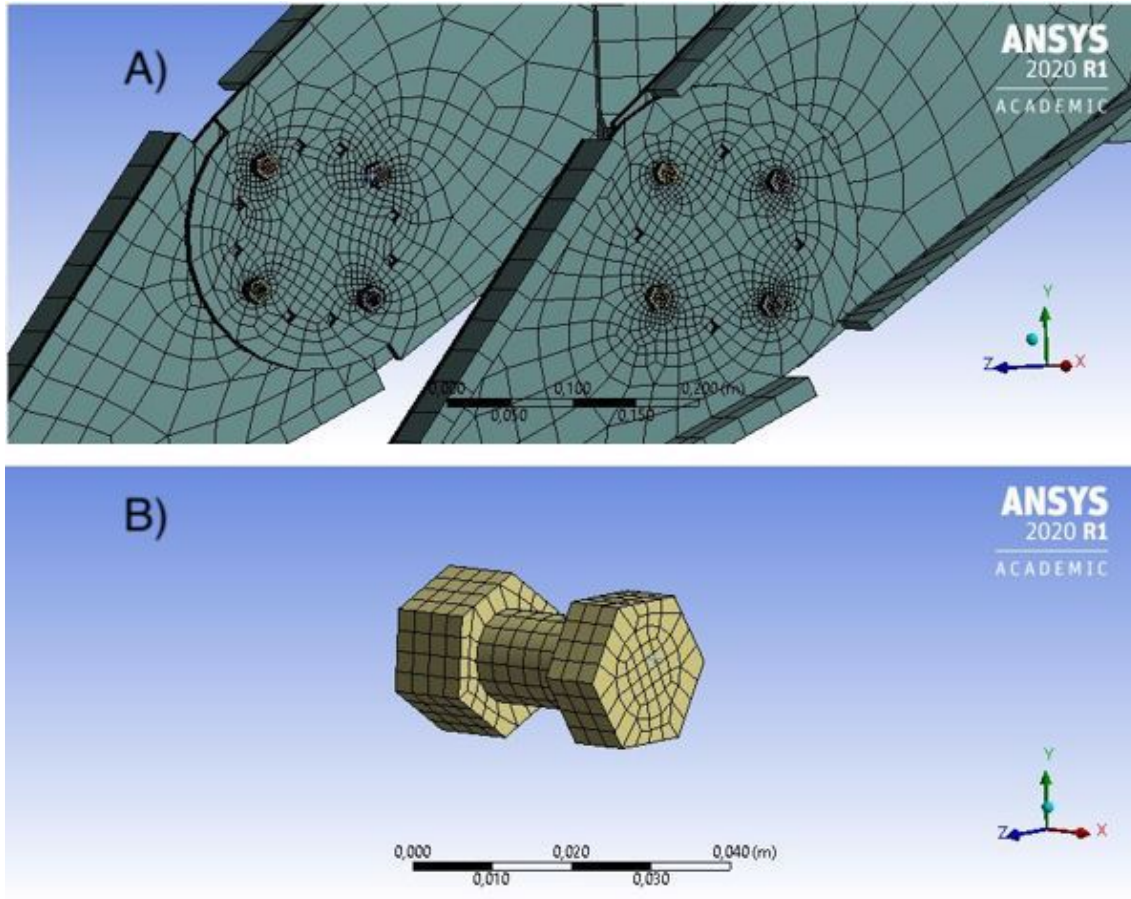


Figure 4.37: Modifications to the mesh with the command Multizone: only hexahedrons. A) Resulting mesh for the support 1 and 2 B) Mesh for the screw and nut

So in conclusion two steps have to be followed:

- I Input of pretension for the first step
- II Lock the screws in the desired place

After 30 hours of calculation the program crashes again because a convergent solution cannot be found. This is caused due to high deformations in some areas, before surpassing sub-step 21 and after reaching the peak load. By changing the deformation to a twice bigger factor than the original (to observe extreme conditions of the study case), it is possible to observe that the pretension works without problems: the supports 1 and 2 are fixed and not able to separate as easy (Figure

4.38). The drilled hole also don't suffer from such a high deformation. The applied force is transferred from the impact zone to the chassis. When observing all the results criteria, the normal stress shows reduced values in comparison to the first case study. However both the von Mises and the shearing stress show an increment of their values. The next Table 4.2 shows changes in the affecting- and the maximum allowed stresses. The maximum normal stress in case 1 exceeds the allowed one, thus the failure is caused by traction. Meanwhile the maximum shear stress in case 2 is over the maximum allowed one, corresponding to shear failure.

Table 4.2: Changes in maximal stresses between cases and ultimate allowed strength

	Max. normal stress	Max. shear stress	Max. von Mises stress
<i>Case 1</i>	960.2 MPa	392.44 MPa	788.98 MPa
<i>Case 2</i>	808.59 MPa	455.64 MPa	825.9 MPa
<i>Max. allowed</i>	800 MPa	400 MPa	840 MPa

Since movement in Y- and Z-direction is allowed and the device can rotate with reference to the X-axis, the device suffers from the highest stress in the last mentioned direction. It avoids displacements in this directions, which causes the loading to be so high. Maximum loading is still observed at the fasteners of the structure: location of the maximal normal stress in X-axis changes in each sub-step. All screws from the left side possess the maximal stress sequentially, which indicates that the majority of the loading is concentrated in just 1 screw (Figure 4.39). When the maximum allowed load is surpassed, the max. normal stress changes its location to the other screw. This may be because the screw fractures or fails and the load has to be resisted from another component. Maximal shearing stress is observed in specific screws: the two located nearest to the cross-member (Figure 4.40). Maximum shearing stress depends highly to distance from the neutral axis. This is why maximum shearing stress is maximal in the center of the shaft of the screw, where the distance to the neutral axis equals 0 and is minimal at the bottom and top of the head's surface. The screws nearest to the cross member are close to the neutral axis, which explains the high values of the stresses.

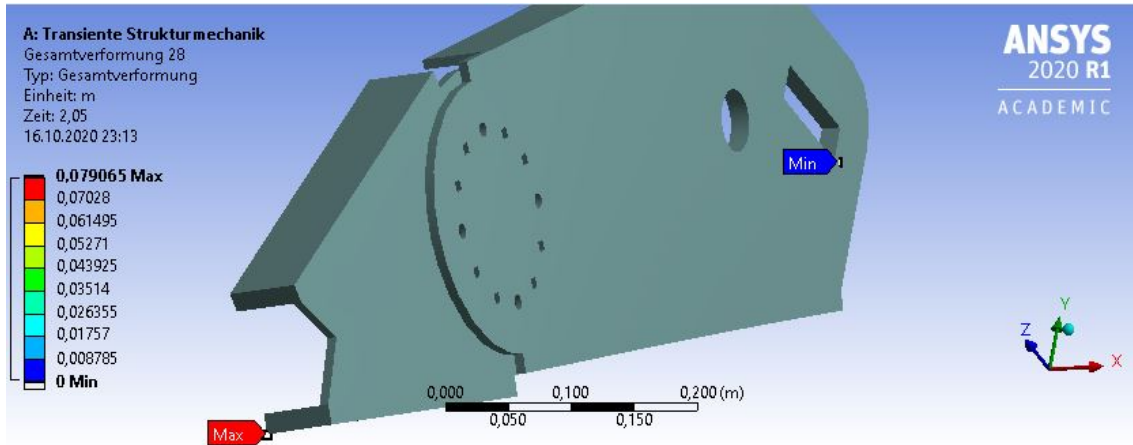


Figure 4.38: Reduced separation between supports thanks to pretension of the screws

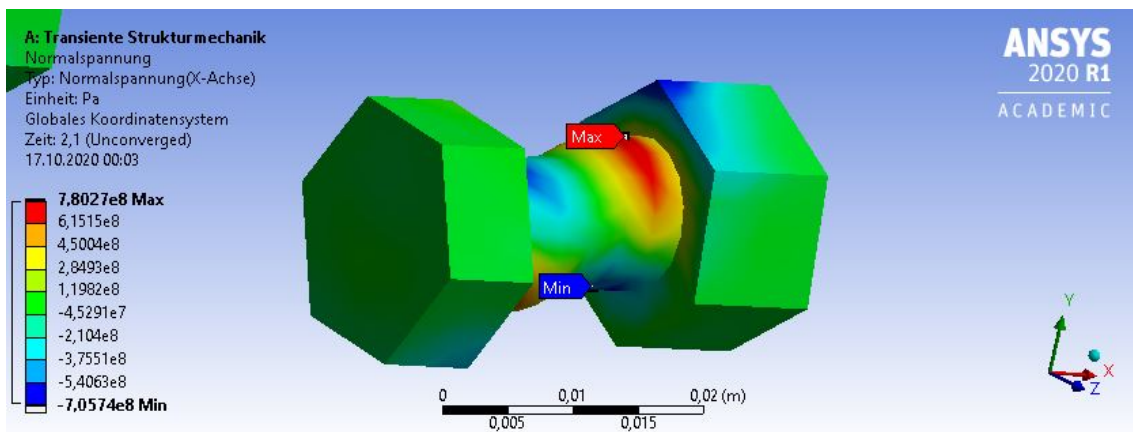


Figure 4.39: Location of the max. normal stress: head of the screw

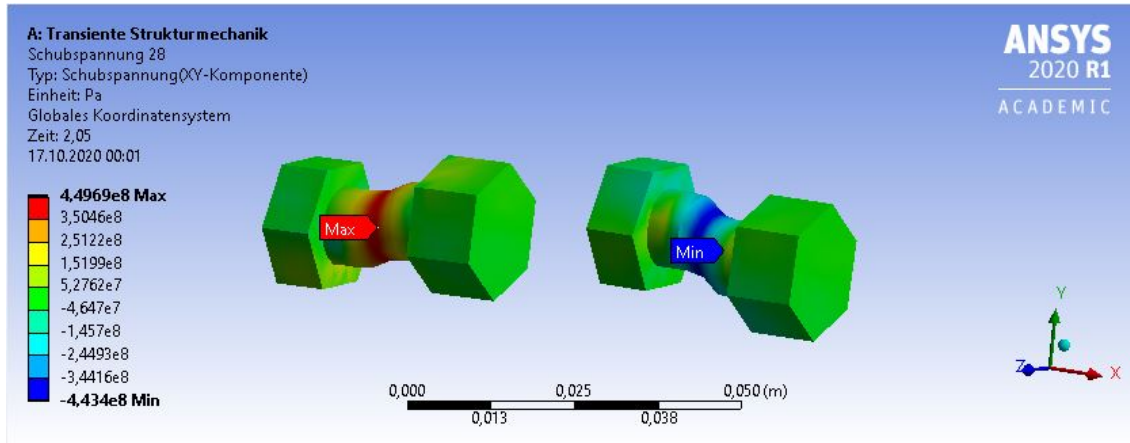


Figure 4.40: Decrease of shearing stress at the center of the shaft and reduced of deformation

The tube now suffers from the highest displacement, which is the target of this component: to dissipate all applying forces. It again deforms in direction to the ground and closer to the frame of the vehicle, which is the intended purpose. All the displacements of the RUP are shown in the Figures 4.41 and 4.42. However this time the deformation is less prominent, thanks to the compression of the supports. The RUP is able to maintain the allowed ground clearance in this case. The screws also don't suffer from the highest deformation and the holes at both supports don't grow in size (Figure 4.43) because of this (which caused the simulation to stop in the first study case). The plastic behavior of the bolts is still however reached, which makes the simulation crash. If this limit is surpassed, additional forces just cause irreversible damage to the bolts. All in all this case study is more representative of reality than the other one, in spite of some higher stresses, which don't destroy the RUP in its totality. However both RUP from both situations share the same problems. The material of the screws and the design of the RUP are not optimal to withstand the high forces of neither revision 2 and 3. The screws fracture after surpassing the yield stress limit and deform with irreversible consequences until finally they break. The maximal ultimate strength of the screws of 800 MPa (see chapter 1.2.6 for better understanding) is surpassed in both cases, which obliges a revision of the RUP.

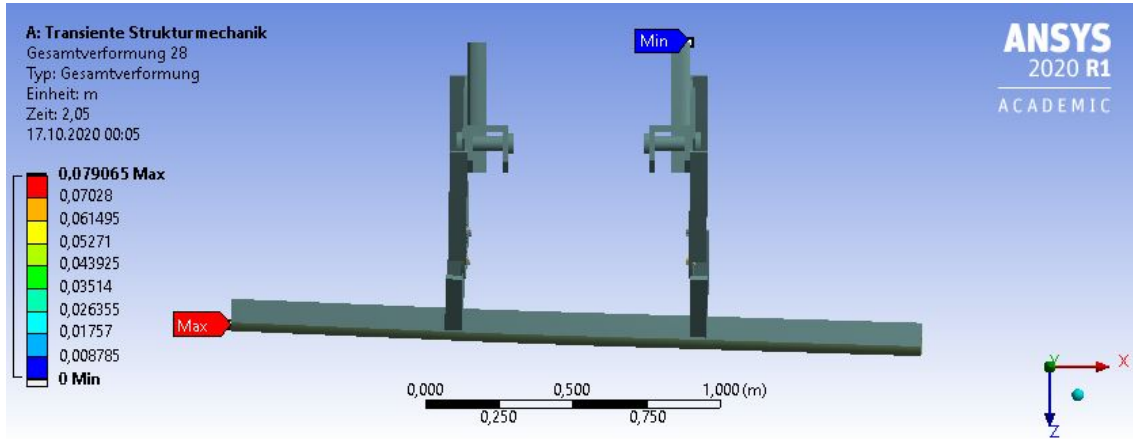


Figure 4.41: Displacements of the rear underrun protection observed from the Y-Axis

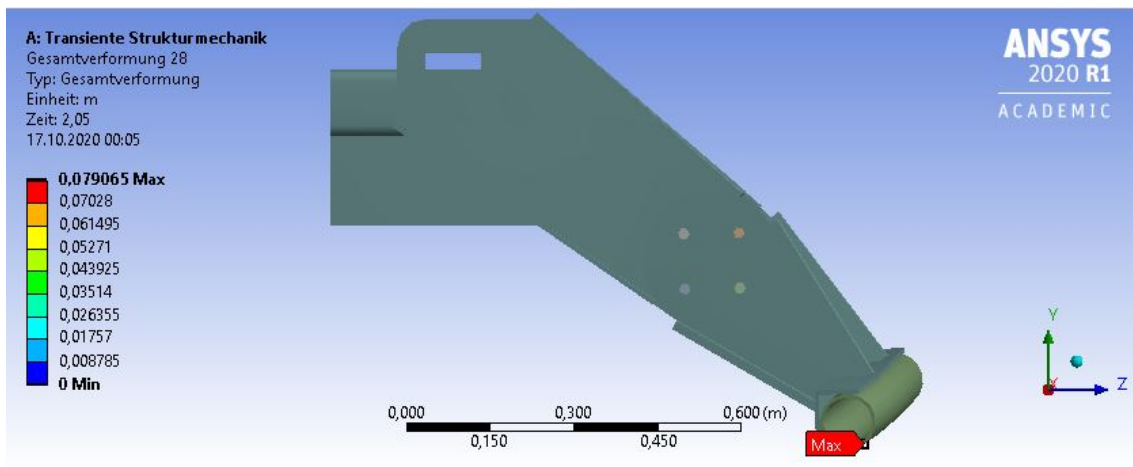


Figure 4.42: Displacements of the rear underrun protection observed from the X-Axis

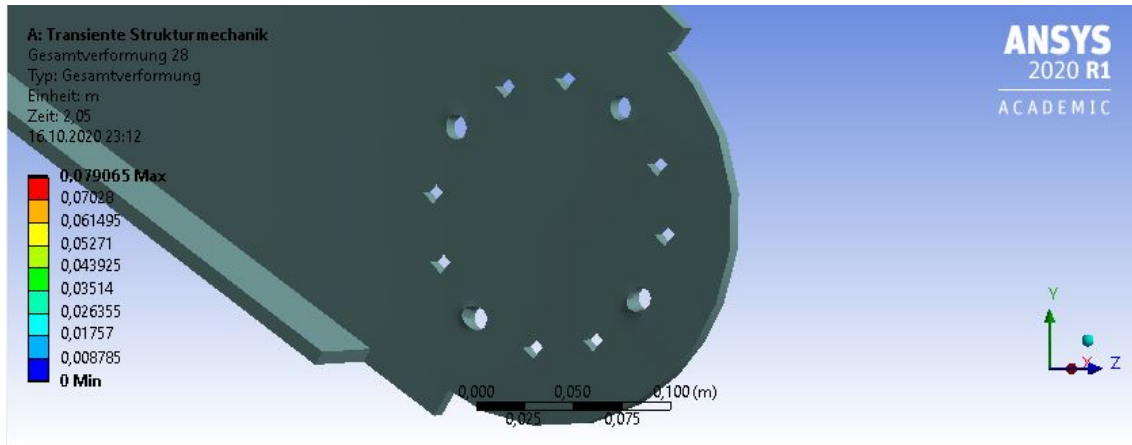


Figure 4.43: Reduction of the drilled holes' deformation

4.6.4 Calculations with LS-Dyna

Workbench allows for an easy integration with LS-Dyna. The project of transient structural can be directly linked to a new explicit calculation project supported by ANSYS. The model, materials and components can be directly imported to LS-Dyna without any additional process, as observed in Figure 4.44. Loading and boundaries must still be defined. LS-Dyna shares the same interface as mechanical so the commands are not new to the user. Some variations can still be observed: LS-Dyna supports the calculations of dynamic, non-linear projects. Input of sub-steps is not needed. Instead the user is only able to simulate a crash or impact per calculation. So the ramping and alternation of loads is not supported. Moreover in contacts there is a special command named interactions. This is used for specifying rigid or flexible bodies and their relationships with other components. In addition LS-Dyna doesn't support bonded contacts, rendering our specified contact conditions as useless. Initial conditions such as velocity and impedance are also available with the software. So acceleration of the vehicle or the testing machine can also be taken into consideration during testing [51].

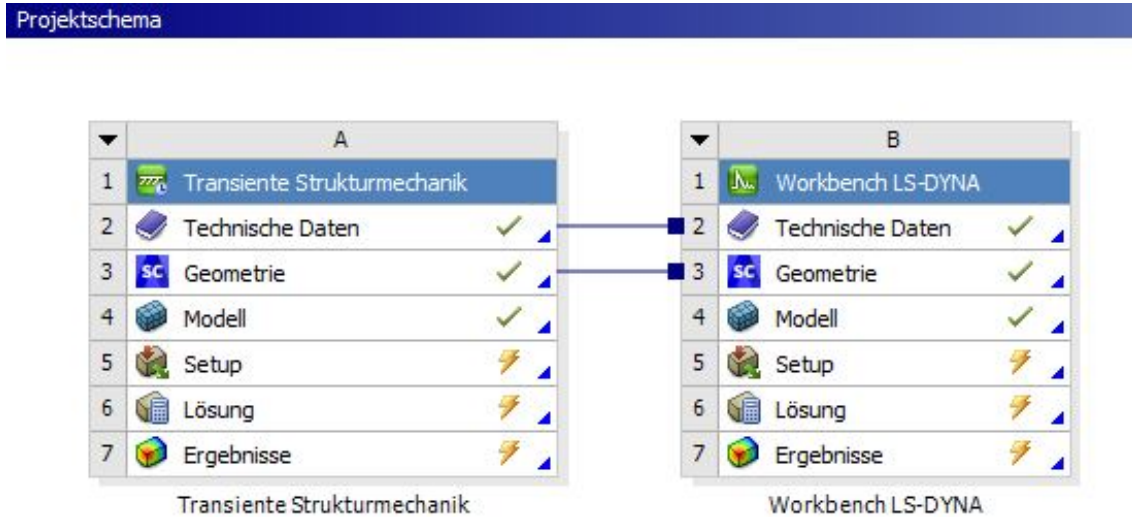


Figure 4.44: Workflow of ANSYS Workbench to interconnect with LS-Dyna

For the analysis setting only an end time is needed to start the calculation. We set all needed supports specified in chapter. For the loads, since only one can be applied, we decided to concentrate ourselves on the highest one of 100 kN. It will be applied 300 mm far away from the center of the cross-member, to the right. A ramping will be applied by setting the ending time of calculation to 3 s. The load will therefore be increased by a factor of 1/3 of its total. Afterwards we decided to test the software. The contacts presented some errors, because the cross-member was penetrating the supports and the L shaped metal support. Additional interactions and conditions still need to be specified. The ones we were able to input in past case studies, weren't valid for this new explicit calculation. So in order to make it more similar to the implicit calculation, additional constraints were specified: a master rigid body was set for the frame, in order to avoid movements in these areas. New contacts were specified to avoid penetrations: rigid contacts were needed. A new calculation was started with lesser problems. The results were totally different to the ones from the implicit calculation. In this case the cross-member suffers the highest deformity in the whole device (Figure 4.45). It compresses and deforms in positive direction of the Y-axis. The maximum von Mises' and shearing stresses are located near this last component, which causes its destruction. The cross-member partially separates from the L-support, which is an indication that the load is being increased too quickly. The stress field cannot be transported uniformly through the

whole RUP. The screws still suffer from high normal-stresses (Figure 4.46), however the value is much less than both of the prior study cases, only 400 MPa. Additional configurations or settings still have to be input, in order to obtain more similar results to the implicit calculation. Constrains still need to be detailed and the pretension of the bolts is still lacking. There is still the fear of making the RUP more resisting as it actually is or that the simulation is not being fully calculated to its whole capacity. So further studies on LS-Dyna still have to be performed. LS-Dyna and explicit calculations may be more adequate for crash tests, due to the lack of time dependency.

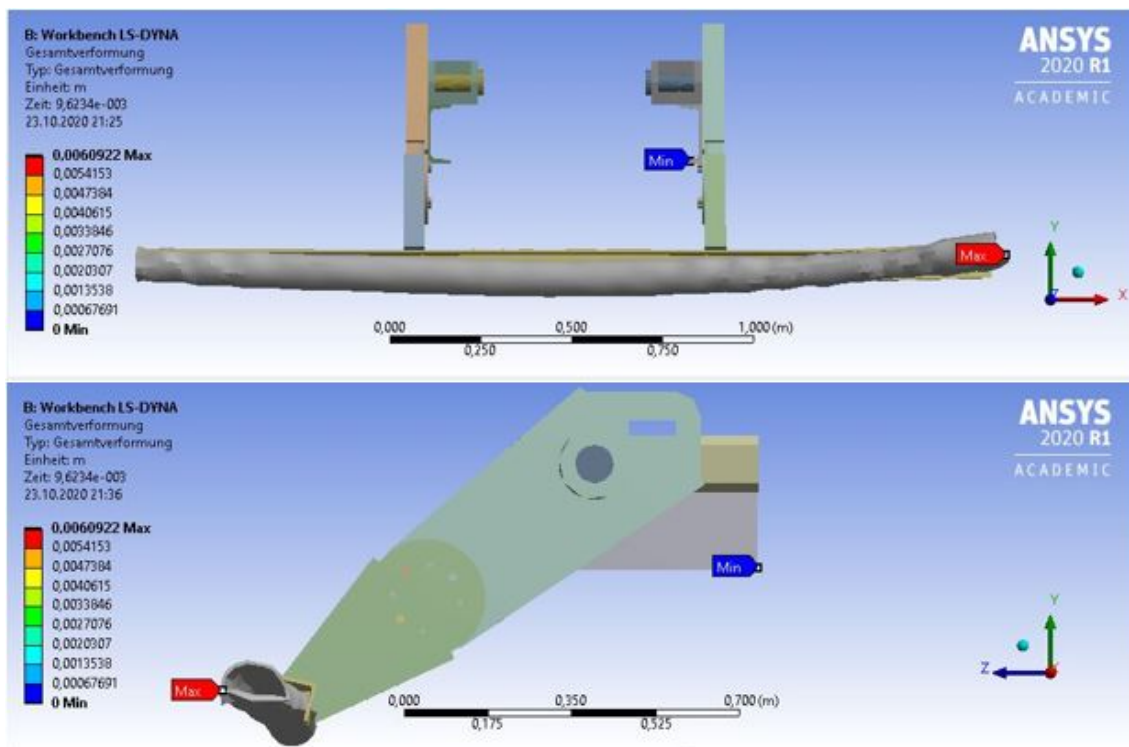


Figure 4.45: Explicit calculation: deformation of the RUP a) in Z-axis and b) in X-axis

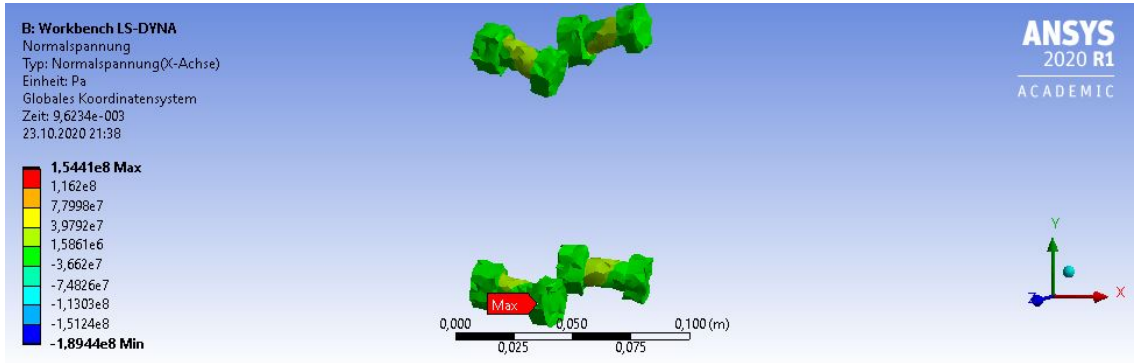


Figure 4.46: Explicit calculation: deformation of the screws due to the normal-stress

Chapter 5

Results and discussion

In the presented thesis some specific objectives were highlighted: discuss the role of the regulation CEPE ONU 58 revision 2 and 3 and its evolution within the years. The necessity of rear underrun protections as devices for ensuring passive security. Some computational methods for controlling the requirements of RUP, based on finite elements, were presented. And finally our new proposition for simulation the test conditions of the regulation CEPE ONU 58 was presented.

Important evolution have been made in relation to the advancement of the requirements and designs of rear protection devices, due to their high demand as a safety element. In order to reduce fatalities and ensure the condition of passengers, high resisting capabilities regulated by the CEPE 58 are expected. The evolution of RUP is due to constant adaptability of vehicle's designs. Newer vehicles are expected to be quicker and lighter, which cause more unfavorable situations during a crash: higher speeds, more offset crashes, alternative materials. That is why the regulation is regularly modified (the last revision entered in force in 2017). There is an exponential increase in the importance of transport (an additional 50 % is estimated for the year 2030) and consequently the number of vehicles in transit. In general, changes to the regulations increase the severity of the requirements of testing: RUPs are expected to withstand higher forces and their deformity has to be reduced to the lowest possible value. The test forces increased by almost 100 % from revision 2 to 3 (from 50 kN to 100 kN or from 100 kN to 180 kN), reducing existing and new possible devices that can withstand these loads. The modifications force changes in the designs of the RUP with respect to their weight and dimensions. Therefore, it is analyzed that the construction materials of the RUPs should be chosen with

caution. With regard to the geometrical requirements, the values of the regulation are highly flexible. This opens up the possibility for new possible designs by the manufacturers. Future revisions are expected with additional considerations come into effect in the next few years.

Calculations using Finite Elements are computer-aided processes used to solve complex physical tests. As observed there are a lot of existing works regarding explicit simulations of rear underrun protections. This work was centered on an implicit methodology used as an alternative for all existing studies. We propose a new analysis methodology based on transient calculations and steps for increasing or decreasing the loads. A new proposed design was modelled in both Solidworks and Workbench and latter simulated to the testing conditions of the UN regulation no. 58. Three important cases were studied: with general bonded conditions, without pretension and frictional conditions and finally, with the implementation of pretension. During the specification of properties, the pretension and the definition of contacts presented the most hardship. The first due to problems in the mesh and the latter due to high displacements of the components. Nevertheless the proposed programmed showed promising results in the end, even though the simulation was not able to be fully completed in 2 of the study cases. With bonded contacts, we were able to obtain results in lesser time. This showed that the geometry doesn't present any problems, such as unwanted gaps or penetration of components. Furthermore the applied conditions of materials, fixtures and loading are correct. However bonded contacts are not a representation of reality, as the components are all not welded together. Friction of the screws has to be taken into consideration. The simulation crashes in both study cases: after observing the results, the high deformation of the screws is what causes this to happen. The shearing and von-Mises stresses are on the edge of surpassing the allowed values, while the normal stress in X-direction exceeds the ultimate tensile strength of the screws' material. The proposed design cannot withstand the requirement loads and after further physical tests performed by the manufacturer, the results were validated. Changes in the material of the screws have to be made or additional screws must be implemented, so that the RUP doesn't collapses.

In order to become a homologation of the simulation software, the ENAC further requires the numerical calculation of additional 10 rear underrun protection devices. The devices are provided by the homologation entity and have to be calculated in

a period of 3 days to 1 week. This ensures that the software doesn't present any further problems and a margin of error can also be calculated. Not all results will be 100% representative of real destructive tests, however percentages variance or deviance based on the numbers of tests can be calculated. On account of privacy policies of the company and the ENAC, we cannot show the obtained RUPs' designs nor the results of the calculation. The software was able to simulate all 10 cases without problems, however in 1 case the deformation of the RUP deviated a lot from the physical test. All in all the software shows promising and accurate results, by also reducing economical costs. The LTR will begin the homologative procedure in brief, when the purchase of the complete ANSYS license is finished.

Further work on this topic will deal with study of explicit calculations with LS-DYNA. We showed the calculation properties of the software and the differences to an implicit analysis. The capabilities and differences regarding the accuracy of the results and time consumption of simulation must still be investigated. Due to the shifting nature of the transport sector, additional modifications on the testing methodology of RUP should also be implemented in the software.

Appendix A

Import Solidworks geometry into ANSYS Workbench

I Draw the desired component in Solidworks with all the respective conditions and geometric relationships. Smart parts like fasteners can also be added

II Afterwards export the file into an IGES format: File -> Save as -> Change the file type to "IGES (*.igs)" -> Click "Options" -> Change the "Surface representation/System preference" from "Standard" to "ANSYS" (see Figure A.1) -> Click "ok" to close "Export Options" -> Choose the folder and the name the file is saved -> Click "ok" (Choose "All bodies" if the dialog box "Export" popped up)

III Open ANSYS Workbench and import the file in the Geometry tab: Open a project -> Right Click on Geometry -> "Select Import Geometry" (Figure A.2 shows the process with more detail) -> Look for the IGES file and open it -> Open SpaceClaim

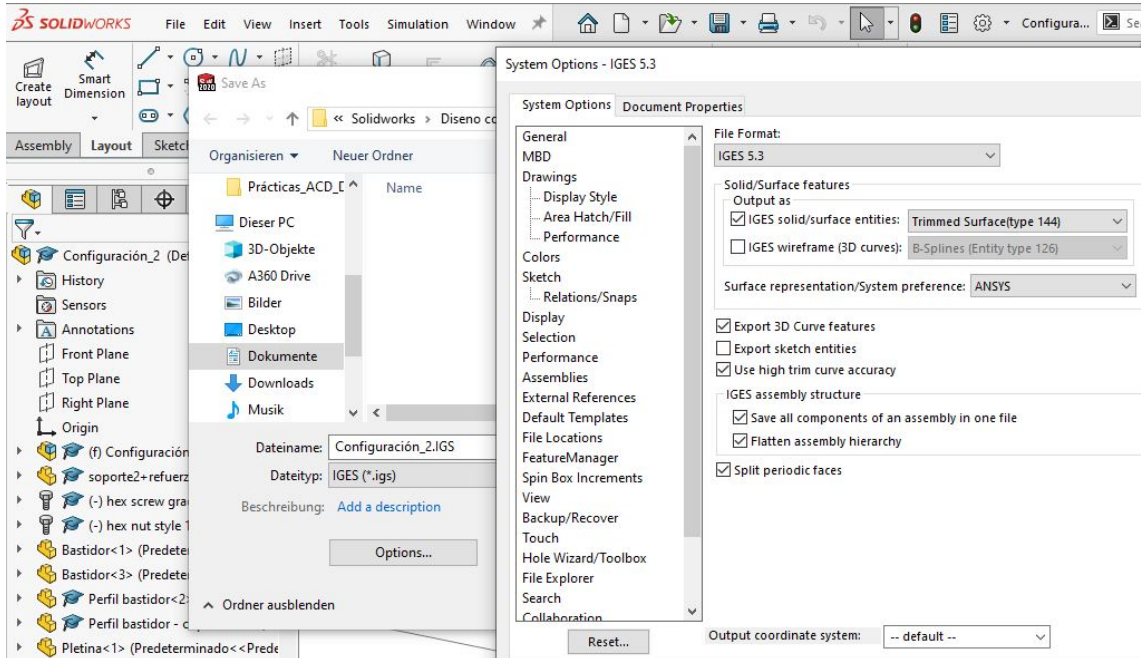


Figure A.1: Exportation of Solidworks file as IGES with ANSYS specifications

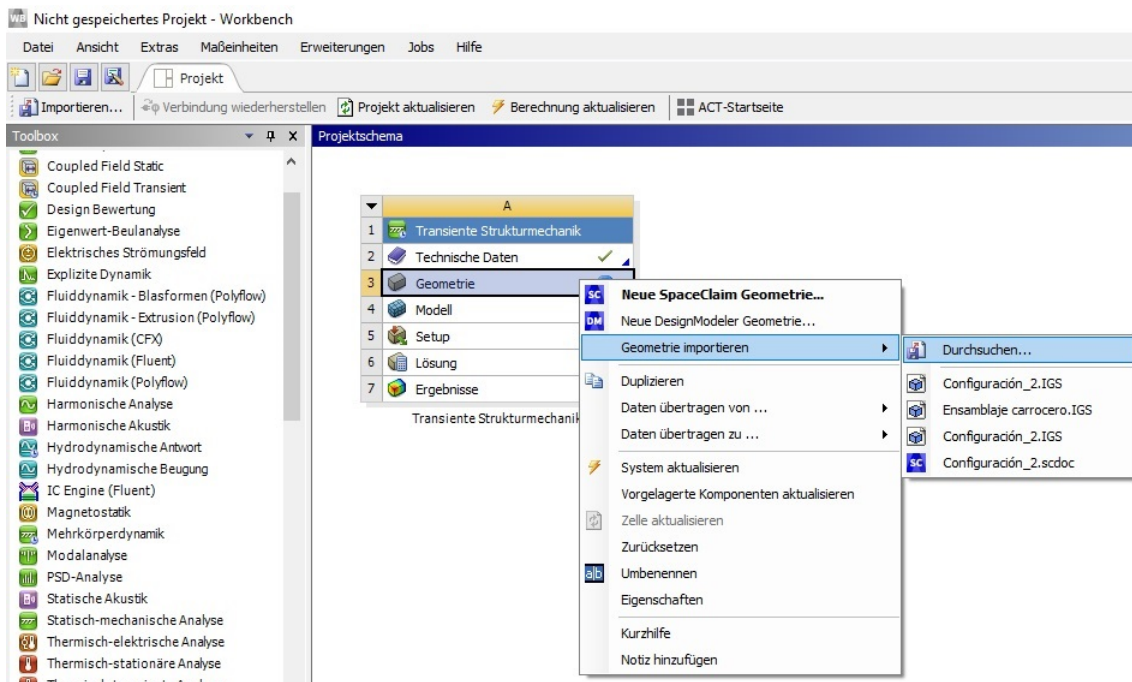


Figure A.2: Importation of the IGES file into Workbench

Appendix B

Creating a finer and isolated mesh

A good way of creating isolated mesh is by using the sphere of influence command available in ANSYS. This will target specific areas of the mesh only and refinements on the size can be made. In contrast to other commands, the sphere is also able to override pre-existing sizing information, which makes for a more gradient mesh without the need of more resources. Three important steps are needed for creating a sphere of influence:

- I Create a new coordinate system by selecting the command with the same name. In the yellow "geometry" space, insert the component where the coordinate system should be created, for example an edge, a surface or a face. Define the directions of the axis or input additional desires. In Figure B.1 the results of this step are presented.

- II In "Meshing" insert a new "Element Sizing". In the Details tab, change the type from "Element Sizing" to "Sphere of Influence". For the center of the sphere select the newly created coordinate system. In addition, define the sphere's radius, which will be the area where the new sizing will be applied. Also define the new size of the mesh and the parts, where the sizing will be considered (see Figure B.2).

- III Update mesh to the new size. The effects of the sphere of influence can be observed in Figure B.3.

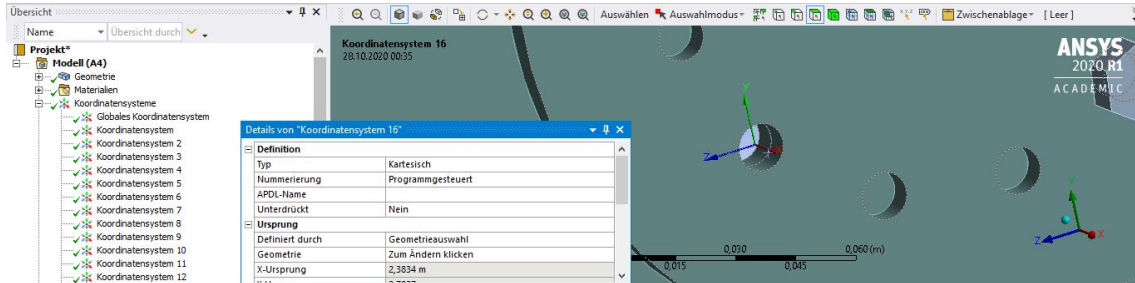


Figure B.1: Creation of a new coordinate system for the sphere of influence

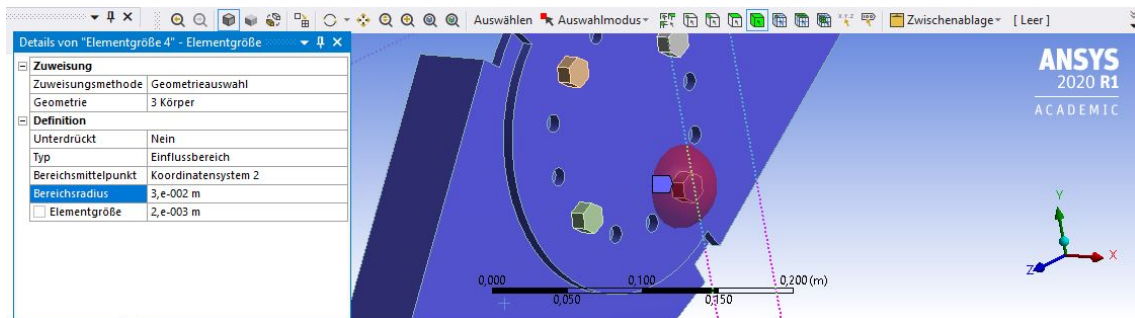


Figure B.2: Properties of sphere of influence

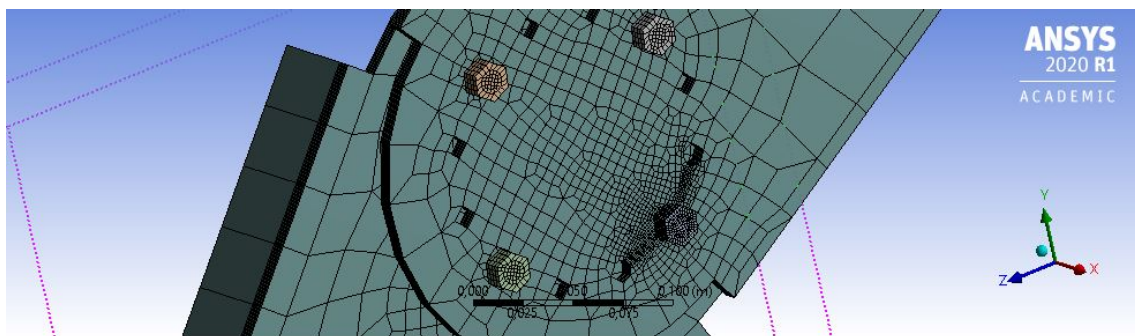


Figure B.3: Resulting mesh thanks to the sphere of influence

Symbols and abbreviations

<i>CAD</i>	Computer-aided design	
<i>CAE</i>	Computer-aided engineering	
<i>d</i>	Bolt nominal shank diameter	mm
<i>EEE</i>	European Economic Space	
<i>ENAC</i>	Entidad Nacional de Acreditación	
<i>F_{MAX}</i>	Force of friction, parallel to the surface	N
<i>F_N</i>	Normal force, perpendicular to the surface	N
<i>F_{PRE}</i>	Ideal pretension force	N
<i>FE</i>	Finite elements	
<i>HGV</i>	Heavy goods vehicle	
<i>HWV</i>	Heavy weight vehicle	
<i>K</i>	Torque coefficient constant	-
<i>LTR</i>	Laboratorio Técnico de Reformas	
<i>M_t</i>	Bolt installation torque	Nmm
<i>R58</i>	Regulation No. 58	
<i>RUPD</i>	Rear underrun protection device	
<i>S</i>	Cohesion sliding resistance coefficient	N
<i>StVZO</i>	Straßenverkehrs-Zulassungs-Ordnung	

Table Index

1.1	Contact types and characteristics	13
1.2	Contact types and characteristics	14
1.3	Contact types and characteristics	30
4.1	Physical properties of the selected materials	71
4.2	Changes in maximal stresses between cases and ultimate allowed strength	98

Figure Index

1.1	Sliding of smaller vehicle under the frame of the heavy weight vehicle	2
1.2	Relevant components of a RUP	3
1.3	Different configurations for RUPs	4
1.4	Vehicle components susceptible to homologation procedures	6
1.5	Example of a homologation mark for a vehicle approved in the Netherlands	10
1.6	Example of a testing bench for separated parts	16
1.7	Location of forces for a RUP with a width less than the distance between tires	17
1.8	Application of forces for a RUP with greater width than the tire distance	17
1.9	Annex 2: communicative paper for the participating parties	19
1.10	Discretization of a subject are with triangular elements	20
1.11	Application fields for implicit or explicit analysis	23
1.12	Dynamic analysis cases.	25
1.13	Dynamic analysis parameters	26
1.14	Steps and examples of contact definition in ANSYS	27
1.15	Example for contact definition	28
1.16	Information tool for verification of specified contacts	30
1.17	Typical low carbon steel stress-strain curve	33
1.18	Application of pretension in ANSYS for a bolt between two metal plates	33
1.19	Additional appendix with general dimensions of parts	35
1.20	Spreadsheet with calculations performed by the manufacturer and technical information of the device	36
3.1	Number of road accident fatalities from the year 2008 to 2018	44
3.2	Road accident fatalities separated by categories, year 2018	45

3.3	Number of road accident fatalities separated by categories, years 2008 to 2018	46
3.4	Comparison between types of accidents involving a heavy weight vehicle	47
3.5	Crash tests for the same vehicle with varying collision speeds	50
3.6	Results of full width tests for a standard RUP and for the new proposed design	51
3.7	Proposed design with an additional gusset member (d)	52
3.8	Von-Mises stress distribution for a simple RUP with positive results regarding CEPE 58	53
3.9	Stress application points and load application table on the rear protection device for a multi-point test assuming regulation 58	54
3.10	Results of the LS-DYNA simulation. Highest levels of stress where observed in the bolts and the connecting areas.	55
3.11	Comparison of deformation for the virtual and physical test with the proposed new requirements	56
3.12	Proposed test method with simultaneous loading at three zones . . .	57
3.13	Minimum required angle for trucks in specific operations	58
4.1	Technical drawing of the support 1 and the cross-member	63
4.2	Dimensions of the bolt ISO-4018-M12	64
4.3	Dimensions of the nut ISO-8673-M12	65
4.4	Technical drawing of the support 2 and the reinforcement plate . . .	66
4.5	Technical drawing for the complete rear underrun protection installed at the frame of the vehicle	67
4.6	Interface and commands of SpaceClaim with our proposed design . .	68
4.7	Reparation commands in SpaceClaim	68
4.8	Proposed simplified design for the screw and the nut	69
4.9	Overview and insertion of material properties in Workbench	71
4.10	Definition of plasticity and fracture behavior	72
4.11	Bonded contacts for the RUP	74
4.12	Bonded contacts for the vehicle's frame	75
4.13	Frictional contact between the faces of the support 1 and support 2 .	76
4.14	Frictional contact between the frame of the vehicle and the support 2	76
4.15	Frictional contacts for the screws and nuts. From up left to bottom right	78
4.16	Interface window for details and conditions of contacts	79

4.17	Mesh quality for the components of the rear underrun device	80
4.18	Mesh for the cross member and the L union	81
4.19	Mesh for the screw and nut	82
4.20	Contact meshing of 3 mm for the bolt and it's contacting areas	82
4.21	Resulting mesh with sphere of influence with a sizing of 3 mm	83
4.22	Details of time conditions and graph of the forces divided by the respective steps	85
4.23	Selected nodes representing the area where the load is applied	86
4.24	Input of loads by means of tabular data	86
4.25	Fixed support for the faces of the frame of the vehicle	87
4.26	Input of displacement of 0 for the Y-axis	87
4.27	Total applied commands for the simulation	88
4.28	Total applied commands for the simulation present at the RUP	89
4.29	Deformation of the screw holes	90
4.30	Concentration of the maximal shearing stress at the center of the screws	91
4.31	Separation of the plates due to lack of pretension	91
4.32	Support 2 in its neutral state and after the appliance of the load	92
4.33	Maximal normal load in X-axis located at the head of the screw and the nut	93
4.34	Rear underrun protection in its neutral state and in its deformed state	94
4.35	Selected area for the pretension and direction of the load	96
4.36	Technical data and details of pretension	96
4.37	Modifications to the mesh with the command Multizone	97
4.38	Reduced separation between supports thanks to pretension of the screws	99
4.39	Location of the max. normal stress: head of the screw	99
4.40	Decrease of shearing stress at the center of the shaft and reduced of deformation	100
4.41	Displacements of the rear underrun protection observed from the Y-Axis	101
4.42	Displacements of the rear underrun protection observed from the X-Axis	101
4.43	Reduction of the drilled holes' deformation	102
4.44	Workflow of ANSYS Workbench to interconnect with LS-Dyna	103
4.45	Deformation of the RUP	104
4.46	Deformation of the screws due to the normal-stress	105
A.1	Exportortation of Solidworks file as IGES with ANSYS specifications	112
A.2	Importation of the IGES file innto Workbench	112

B.1	Creation of a new coordinate system for the sphere of influence	114
B.2	Properties of sphere of influence	114
B.3	Resulting mesh thanks to the sphere of influence	114

Bibliography

- [1] *Test report on rear impact with hgv*, retrieved from: www.adac.de/infotestrat/tests/crash-test/unterfahrschutz_lkw_2012/default.aspx, Allgemeine Deutsche Automobil-Club e.V. (2006).
- [2] E. C. for Europe, “Regulation no. 58 of the economic commission for europe of the united nations (un/ece)-uniform provisions concerning the approval of: 1. rear underrun protection devices (rupds), 2. vehicles with regard to the installation of an rupd of an approved type, 3. vehicles with regard to their rear underrun protection (rup)”, Official Journal of the European Union (Issue 83, 2017).
- [3] S. Gogte and N. Vijendran, *Conceptual design and development of movable rear underrun protection*, Master’s thesis in Product Development, 2014.
- [4] A. Sobhani, W. Young, D. Logan, and S. Bahrololoom, “A kinetic energy model of two-vehicle crash injury severity”, *Accident Analysis and Prevention* **43**, 741–754 (2011).
- [5] H. M. Abid and R. I. B. A. Roslin Eida Nadirah an Jalal, “Performance of rear under-ride protection device (rupd) during car to heavy truck rear impact”, *International Journal of Engineering and Advanced Technology* **8**, 3367–3375 (2019).
- [6] S. Pooudom, S. Chanthanumataporn, S. Koetnियom, and J. Carmai, “Design and development of truck rear underrun protection device”, *IOP Conference Series: Materials Science and Engineering* **501** (2019).
- [7] M. Barreira Lamas, J. A. Vilán, A. Vilán, and D. D. Segade Robleda, “Dispositivos de protección trasera. aportaciones al reglamento cepe/onu 58”, PhD thesis (Universidad de Vigo, 2015).

-
- [8] E. C. for Europe, “Directive 2007/46/ec of the european parliament and of the council of 5 september 2007 establishing a framework for the approval of motor vehicles and their trailers, and of systems, components and separate technical units intended for such vehicles”, Official Journal of the European Union, 48–119 (Issue 68, 2019).
- [9] B. für Verkehrsentwicklung, “Straßenverkehrs-zulassungs-ordnung vom 26. april 2012 (bgbl. i s. 679), die zuletzt durch artikel 1 der verordnung vom 26. november 2019 (bgbl. i s. 2015) geändert worden ist”, Journal from the Bundesministerium für Verkehr, Bau und Stadtentwicklung (Issue 4, 2019).
- [10] *Manual de reformas de vehículos*, retrieved from: publicacionesoficiales.boe.es/, Ministerio de industria turismo y comercio (2019).
- [11] U. N. E. C. for Europe, *Establishment of relationships between the united nations and the universal post union*, retrieved from: unece.org, 2020.
- [12] E. C. for Europe, “On the approximation of the laws of the member states relating to liquid fuel tanks and rear protective devices for motor vehicles and their trailers”, Official Journal of the European Union, 192–193 (1970).
- [13] *Praktische einföhrung in die finite-elemente-methode (fem) mit dem programm abaqus/cae*, Institut für Materialprüfung, Werkstoffkunde und Festigkeitslehre, Universität Stuttgart ().
- [14] K.-J. Bathe, *Finite element procedures* (Englewood Cliffs New Jersey, 1996).
- [15] S. E. Benzley, K. Merkley, T. D. Blacker, and L. Schoof, “Pre- and post-processing for the finite element method”, 243–260 (1995).
- [16] R. Rossetti, *Machine tools simulation in the ansys*, CADFEM (Suisse) AG. (2002), pp. 1–50.
- [17] A. Harish, *Implicit vs explicit finite element method (fem): what is the difference?*, Simescale (2020).
- [18] M. Y. Ding, *Shock analysis*, presentation retrieved ANSYS Inc. ().
- [19] I. ANSYS, *Ansys mechanical apdl structural analysis guide*, Release 15, retrieved from: ansys.com (2013 SAS IP, Inc., 2013).
- [20] I. ANSYS, *Comparisson of implicit and explicit methods*, retrieved from: ansys.com ().
-

-
- [21] A. Inc., *Ansys capabilities chart r1*, PDF table retrieved from ANSYS Inc. (2020).
- [22] I. ANSYS, *Workbench user's guide*, Release 15, retrieved from: ansys.com (2013 SAS IP, Inc., 2013).
- [23] I. ANSYS, *Ansys explicit dynamics analysis guide*, Release 18.1, retrieved from: ansys.com (2017 ANSYS, Inc., 2017).
- [24] I. ANSYS, *Ansys contact technology guide*, Release 9, retrieved from: ansys.com (2004 SAS IP, Inc., 2004).
- [25] Y. F. Liu, J. Li, Z. M. Zhang, X. H. Hu, and W. J. Zhang, "Experimental comparison of five friction models on the same test-bed of the micro stick-slip motion system", *Mechanical Science Journal* **6**, 15–28 (2015).
- [26] A. Inc., *Ansys mechanical ansys mechanical structural nonlinearities*, Customer training material (2010).
- [27] H. Cheda, *Estudio de análisis y uniones atornilladas de alta resistencia para su utilización en emparrillados metálicos*, Master's thesis in Industrial Engineering, 2019.
- [28] D. Roylance, S. Urata, R. Funahashi, T. Mihara, A. Kosuga, and N. Miyasou, "Mechanical properties of oxide materials", *International Conference on Thermoelectrics, ICT, Proceedings* (2007).
- [29] R. Budynas and K. Nisbett, "Mechanical engineering design", in, 9th ed. (The McGraw-Hill Companies, 2012) Chap. Chapter 8.
- [30] I. ANSYS, *Ansys mechanical apdl basic analysis guide*, Release 15, retrieved from: ansys.com (2013 SAS IP, Inc., 2013).
- [31] I. ANSYS, *Ansys mechanical apdl element reference*, Release 15, retrieved from: ansys.com (2013 SAS IP, Inc., 2013).
- [32] I. ANSYS, *Ansys mechanical apdl command reference*, Release 15, retrieved from: ansys.com (2013 SAS IP, Inc., 2013).
- [33] I. ANSYS, *Ansys modeling and meshing guide*, Release 9, retrieved from: ansys.com (2004 SAS IP, Inc., 2004).
- [34] T. Smith, C. Grover, T. Gibson, W. Donaldson, and I. L. Knight, "Development of test procedures, limit values, costs and benefits for proposals to improve the performance of rear underrun protection for trucks", *Project Report PPR 317* (2008).
-

-
- [35] E. C. EU, *Road accident fatalities - statistics by type of vehicle*, retrieved from ec.europa.eu/eurostat/ (2020).
- [36] S. Radke, *Verkehr in zahlen 2019/2020* (Kraftfahrt-Bundesamt, Flensburg, Sept. 2019).
- [37] M. Hamacher, J. Ludwig, and A. Malczyk, *Unfallgeschehen mit lkw-beteiligung unter beruecksichtigung von leicht-lkw-kombinationen* (Gesamtverband der Deutschen Versicherungswirtschaft e.V., 2016).
- [38] H. M. Abid, E. N. Roslin, and R. I. B. A. Jalal, "Development of test procedures, limit values, costs and benefits for proposals to improve the performance of rear underrun protection for trucks", *International Journal of Engineering and Advanced Technology* **8**, 3367–3375 (2019).
- [39] V. Gogate, V. Pachore, and A. Thorat, "A new approach for rear underrun protection systems – accident investigations cae based development", *IRCOBI Conference* (2014).
- [40] P. Sen, R. Jaiswal, S. Bohidar, R. Anant, and R. Bhardwaj, "Optimization development of vehicle rear under-run protection devices in heavy vehicle (rupd) for regulative load cases", *Int. J. Innov. Res. Sci. Technol.* **1**, 27–33 (2014).
- [41] S. Gombi, S. Mahendra, and H. Amithkumar, "Energy absorption analysis of rupd", *Int. J. Innov. Res. Sci. Technol.* **4**, 208–215 (2015).
- [42] R. U. P. T. (R. using CAE Simulation, "Energy absorption analysis of rupd", *SAE Int. J. Commer. Veh.* **9** (2016).
- [43] G. Joseph, S. Dhananjay, and P. Gajendra, "Design and optimization of the rear under-run protection device using ls-dyna", *International Journal Of Engineering Research And Applications* **3**, 152–162 (2013).
- [44] P. Xiao-Ping, H. Ying, T. Sheng-Lin, X. Zheng, W. Guilin, X. Tanchumin, and W. Xing-Qiang, "Physical properties of high-strength bolt materials at elevated temperatures", *Results in Physics* **13** (2019).
- [45] I. Dzioba and S. Lipiec, "Microstructure, strength properties and fracture toughness of s355jr steel", *AIP Conference Proceedings* **1780**, 179–186 (2016).
- [46] D. I. Normierung, *Din en 1993-1-10:2010-12, eurocode 3: bemessung und konstruktion von stahlbauten* (2012).
- [47] Steel, *Steel material properties*, retrieved from Steel construction info (2020).
-

-
- [48] Marochnik, *Characteristics for grade s255 (255)*, retrieved from Database of Steel and Alloy (Marochnik) (2020).
 - [49] T. Cities, *Contact analysis*, retrieved from: Twin Cities ANSYS User Meeting (2013).
 - [50] R. Damián Valerio, *Estudio del estado tensional en uniones atornilladas mediante solidworks*, Bachelor's thesis in Industrial Engineering, 2018.
 - [51] M. Hörmann, "Using ls-dyna from ansys workbench environment", 10th International LS-Dyna Users Conference, 39–48 (2008).
-

Expression of thanks

I want to acknowledge every person that helped me with the development con completion of this work. Thanks to the Universidad Politécnica de Cartagena for being great guests in spite of the circumstances. Thanks to the professor José Hernández Grau for helping me with all my problems during my stay and for allowing me to find a good internship. Special mention to Dokt. Ing. Miguel Jiménez Martínez for his time and patience, but also for coordinating all processes in regards to my double master program.

Special thanks to the International Zentrum for always asking for me and also resolving all my problems and doubts as quick as possible. Also to the University of Stuttgart for allowing me to be the pioneer of the double degree program and for all the licenses it has provided for my investigation.

To the Laboratorio Técnico de Reformas S.A. and all of his workers there, but mainly Antonio González Carpena, I want to express my sincere thanks for allowing me to be part of your team. Thank you for your patience and for making me feel like a family, especially Francisco and Miguel. Thanks for allowing me to develop as an engineer and sorry if everything couldn't go as planned due to the pandemic.

I want to also express my sincere thanks to José Andrés Moreno Nicolás, the assisting tutor of this work. I have the uttermost respect for your work ethic and your patience. Thanks for supporting me so much during this process, even though of the harsh circumstances. I have learnt some much from your advises and your guidance, which have all made me a harder-working and more analytical person.

Finally I want to express my sincere thanks to my family, specially my brother. This has all been possible thanks to you.

Eidesstattliche Erklärung

Hiermit versichere ich, die vorliegende Abschlussarbeit selbstständig und nur unter Verwendung der von mir angegebenen Quellen und Hilfsmittel verfasst zu haben. Sowohl inhaltlich als auch wörtlich entnommene Inhalte wurden als solche kenntlich gemacht. Die Arbeit hat in dieser oder vergleichbarer Form noch keinem anderem Prüfungsgremium vorgelegen.

Datum: _____ Unterschrift: _____